

GEOCHRONOLOGY OF METASEDIMENTARY
AND GRANITIC ROCKS IN THE
GRANITES–TANAMI OROGEN:
1885–1790 MA GEODYNAMIC EVOLUTION

by
DW Maidment, MTD Wingate, JC Claoué-Long,
S Bodorkos, D Huston, JA Whelan, L Bagas,
A Lambeck and Y Lu



Government of Western Australia
Department of Mines, Industry Regulation
and Safety

Geological Survey of
Western Australia





Government of **Western Australia**
Department of **Mines, Industry Regulation and Safety**

REPORT 196

GEOCHRONOLOGY OF METASEDIMENTARY AND GRANITIC ROCKS IN THE GRANITES–TANAMI OROGEN: 1885–1790 Ma GEODYNAMIC EVOLUTION

by

**DW Maidment¹*, MTD Wingate, JC Claoué-Long¹, S Bodorkos¹, D Huston¹,
JA Whelan², L Bagas³, A Lambeck⁴ and Y Lu**

1 Geoscience Australia, GPO Box 378, Canberra ACT 2601

2 Northern Territory Geological Survey, Smith Street Mall, Darwin NT 0801

3 The University of Western Australia, Stirling Highway, Crawley WA 6009

4 LamSil Geological Services, 1000 Cottonwood Canyon Road, Marysville Utah US 84750

* Present address Newmont Goldcorp, 3 Bellows Street, Welshpool WA 6106

PERTH 2020



**Geological Survey of
Western Australia**

MINISTER FOR MINES AND PETROLEUM
Hon Bill Johnston MLA

DIRECTOR GENERAL, DEPARTMENT OF MINES, INDUSTRY REGULATION AND SAFETY
David Smith

EXECUTIVE DIRECTOR, GEOLOGICAL SURVEY AND RESOURCE STRATEGY
Jeff Haworth

REFERENCE

The recommended reference for this publication is:

Maidment, DW, Wingate, MTD, Claoué-Long JC, Bodorkos, S, Huston, D, Whelan, JA, Bagas, L, Lambeck, A and Lu, Y 2020,
Geochronology of metasedimentary and granitic rocks in the Granites–Tanami Orogen: 1885–1790 Ma geodynamic evolution:
Geological Survey of Western Australia, Report 196, 50p.

ISBN 978-1-74168-877-1
ISSN 1834-2280



A catalogue record for this
book is available from the
National Library of Australia



U–Pb measurements on GSWA samples were conducted using the SHRIMP II ion microprobes at the John de Laeter Centre, Curtin University, with the financial support of the Australian Research Council and AuScope NCRIS. U–Pb analyses of Geoscience Australia samples were conducted using the SHRIMP instruments in the Research School of Earth Sciences at the Australian National University.

Grid references in this publication refer to the Geocentric Datum of Australia 1994 (GDA94). Locations mentioned in the text are referenced using Map Grid Australia (MGA) coordinates, Zone 52. All locations are quoted to at least the nearest 100 m.

Disclaimer

This product was produced using information from various sources. The Department of Mines, Industry Regulation and Safety (DMIRS) and the State cannot guarantee the accuracy, currency or completeness of the information. Neither the department nor the State of Western Australia nor any employee or agent of the department shall be responsible or liable for any loss, damage or injury arising from the use of or reliance on any information, data or advice (including incomplete, out of date, incorrect, inaccurate or misleading information, data or advice) expressed or implied in, or coming from, this publication or incorporated into it by reference, by any person whatsoever.

Published 2020 by the Geological Survey of Western Australia

This Report is published in digital format (PDF) and is available online at <www.dmirs.wa.gov.au/GSWApublications>.



© State of Western Australia (Department of Mines, Industry Regulation and Safety) 2020

With the exception of the Western Australian Coat of Arms and other logos, and where otherwise noted, these data are provided under a Creative Commons Attribution 4.0 International Licence. (<http://creativecommons.org/licenses/by/4.0/legalcode>)

Further details of geoscience products are available from:

Information Centre
Department of Mines, Industry Regulation and Safety
100 Plain Street
EAST PERTH WESTERN AUSTRALIA 6004
Telephone: +61 8 9222 3459
www.dmirs.wa.gov.au/GSWApublications

Cover image: Total magnetic intensity image (reduced to pole) of the Granites–Tanami Orogen. Data from the Geoscience Australia sixth edition Total Magnetic Intensity (TMI) Grid of Australia 2015

Contents

Abstract.....	1
Introduction	1
Geological overview	2
Neoproterozoic rocks.....	3
Paleoproterozoic metasedimentary and meta-igneous rocks	5
Tanami Group stratigraphy.....	5
Tanami Group age constraints.....	5
Ware Group.....	8
Granitic rocks	8
Paleoproterozoic to Phanerozoic cover successions.....	8
Deformation and metamorphism.....	9
Analytical methods.....	11
U–Pb zircon geochronology	11
Metasedimentary rocks.....	12
GA 2004085006: metasandstone — Ferdies Member, Dead Bullock Formation	12
GSWA 177279: metasandstone — Stubbins Formation.....	12
GSWA 178809: metasandstone — Stubbins Formation.....	12
GA 2004085001: metasandstone — Killi Killi Formation	14
GA 2001082009: metasandstone — Killi Killi Formation	15
GA 2001082010: sandstone — Gardiner Sandstone.....	15
GA 2001082516: sandstone — Gardiner Sandstone.....	15
Igneous rocks.....	15
GSWA 178801: felsic igneous rock in Stubbins Formation	15
GA 2001082002: biotite monzogranite — Lewis Granite	18
GA 2001082005: biotite monzogranite — Lewis Granite.....	18
GA 72495003: muscovite monzogranite — Lewis Granite.....	18
GSWA 189942: muscovite–biotite syenogranite — Lewis Granite.....	18
GSWA 189936: biotite–hornblende granodiorite — Lewis Granite.....	20
GSWA 189937: biotite monzogranite — Lewis Granite.....	20
GA 2001082003: monzogranite — Balwina Granite	20
GA 72490306: biotite granodiorite — Balwina Granite.....	20
GA 2003082001: biotite monzogranite — Balwina Granite.....	21
GA 2001082004: aplitic muscovite syenogranite dyke in Balwina Granite.....	21
Discussion.....	22
Depositional age and provenance of the Tanami Group	22
Dead Bullock Formation	22
Stubbins Formation.....	22
Killi Killi Formation.....	23
Changes in provenance within the Tanami Group.....	23
Possible correlations with the Halls Creek Group, Kimberley region.....	24
Stratigraphic correlations within the Granites–Tanami Orogen	28
Stubbins Formation.....	28
Mount Charles Formation	28
Browns Range Metamorphics.....	29
Age and provenance of the Gardiner Sandstone.....	30
Timing of the Tanami Event	30
Regional correlations and sedimentary provenance: 1880–1835 Ma	31
Basal units dominated by Archean detritus (Detrital A provenance).....	31
Turbidites dominated by 1870–1865 Ma detritus (Detrital P provenance).....	31
Source of Detrital P detritus	34
Evolution of the North Australian Craton: 1885–1830 Ma.....	36
Proto-craton assembly before c. 1885 Ma.....	36
Back-arc development from c. 1885 Ma?	37
Crustal shortening in the northeastern North Australian Craton at 1870–1860 Ma.....	37
Basin disruption at c. 1835 Ma	38
Granitic rocks and the Stafford Event: 1825–1790 Ma	38
Ages and compositions of granitic rocks in the Granites–Tanami Orogen	38
1825–1790 Ma belt of magmatism and tectonism.....	40
Geodynamic setting of the Stafford Event	40
Neoproterozoic–Paleozoic isotopic disturbance.....	43
Conclusions	43
References	44

Figures

1. Location of the Granites–Tanami Orogen in the North Australian Craton	2
2. Simplified basement geology of the Granites–Tanami Orogen	3
3. Seismic reflection profile across the Granites–Tanami Orogen and Aileron Province	4
4. Stratigraphy and tectonism of the Granites–Tanami Orogen	7
5. Total magnetic intensity (reduced to pole) image of the Granites–Tanami Orogen	9
6. Concordia plots and probability density diagrams for the Ferdies Member and Stubbins Formation	14
7. Concordia plots and probability density diagrams for the Killi Killi Formation and Gardiner Sandstone	16
8. Cathodoluminescence image of zircons from the Stubbins Formation and Ferdies Member	17
9. Concordia plots for a felsic unit in the Stubbins Formation and the Lewis Granite	19
10. Concordia plots for the Balwina Granite and a felsic dyke in the Balwina Granite	21
11. Composite Th/Sc and Cr/Th for metasedimentary rocks in the lower Tanami Group	24
12. Th/Sc vs Cr/Th for regional samples of the Tanami Group and correlatives	25
13. Comparison of the stratigraphy of the Tanami and Halls Creek Groups	26
14. Detrital zircon age spectra for the Tanami and Halls Creek Groups	27
15. Time–space plot for the North Australian Craton between 1885 and 1815 Ma	32
16. Distribution of sedimentation, magmatism and tectonism in the North Australian Craton at 1870–1850 Ma	33
17. Composite detrital zircon probability density plots for 1885–1835 Ma units in the Granites–Tanami Orogen, Lamboo Province and Pine Creek Orogen	34
18. Composite detrital zircon probability density plots for 1870–1835 Ma units with the ‘Detrital P’ signature in the North Australian Craton	35
19. Possible geodynamic setting of the North Australian Craton at 1885–1855 Ma	39
20. Histogram of ages for granitic rocks in the Granites–Tanami Orogen	40
21. Distribution of sedimentation, magmatism and tectonism in the North Australian Craton at 1820–1790 Ma	41

Tables

1. Summary of stratigraphic units in the Granites–Tanami Orogen	6
2. Comparison of structural frameworks for the Granites–Tanami Orogen	10
3. Summary of isotopic ages obtained for metasedimentary and igneous rocks	13

Appendices

Available with the PDF online as an accompanying digital resource

1. SHRIMP analytical session parameters
2. SHRIMP U–Pb data tables

Geochronology of metasedimentary and granitic rocks in the Granites–Tanami Orogen: 1885–1790 Ma geodynamic evolution

by

DW Maidment¹*, MTD Wingate, JC Claoué-Long¹, S Bodorkos¹, D Huston¹,
JA Whelan², L Bagas³, A Lambeck⁴ and Y Lu

Abstract

Dating of detrital zircons from the Paleoproterozoic Tanami Group shows that Archean detritus dominates the lower part of the succession, and c. 1865 Ma detritus with a minor c. 2500 Ma component dominates the upper part. Detrital zircon ages for the upper Stubbins Formation in Western Australia are consistent with a correlation with the upper Dead Bullock Formation in the Northern Territory, whereas previously collected data for the Mount Charles Formation are consistent with a correlation with the lower Dead Bullock Formation. Metasedimentary rocks with a dominant c. 1865 Ma detrital zircon age component were deposited over much of the North Australian Craton between c. 1865 and 1840 Ma, possibly within a back-arc setting related to a plate margin north of the currently preserved craton. Tectonism at c. 1865 Ma in the northeastern part of the craton may represent remnants of a larger orogen that acted as the dominant source of sediment. The widespread occurrence of metasedimentary rocks with this distinctive provenance signature suggests craton assembly was largely complete prior to deposition. Dates of 1807–1800 Ma for granitic rocks in the western part of the orogen confirm that they were emplaced during the 1810–1790 Ma Stafford Event. These granitic rocks form part of an >800 km-long west-northwesterly trending magmatic belt, the development of which was coeval with bimodal magmatism, extension and sedimentation in other parts of the craton. This magmatism may have been a consequence of intraplate extension, possibly driven by processes along the southern craton margin. Folding and orogenic Au mineralization in the Granites–Tanami Orogen during the Stafford Event may reflect transient compression punctuating a more prolonged period of extension.

KEYWORDS: Birrindudu Basin, detrital zircon geochronology, geodynamics, intraplate, magmatism, Tanami Event, Tanami Group, Stafford Event

Introduction

The Granites–Tanami Orogen in the Northern Territory and Western Australia (Figs 1, 2) preserves a complex record of Paleoproterozoic basin development, deformation and magmatism in the west–central part of the North Australian Craton (Crispe et al., 2007; Lambeck et al., 2012; Bagas et al., 2014). The orogen provides an important source of information about the assembly and development of the North Australian Craton, and hosts numerous orogenic Au deposits, including the world-class Callie deposit in the Dead Bullock Soak goldfield (Huston et al., 2007; Pendergast et al., 2017; Wygralak et al., 2017).

Geological study of the Granites–Tanami Orogen is hampered by extensive Mesoproterozoic to Cenozoic sedimentary cover, with most information derived from widely spaced areas of weathered, low outcrop, and drillcore. Geological event frameworks have been constructed (e.g. Crispe et al., 2007; Bagas et al., 2008, 2014; Ahmad et al., 2013b), although significant differences exist between aspects of these models, including the timing and correlation of sedimentary packages and the number, timing and character of tectonic events. Most published geochronological data have been obtained from the Northern Territory (Smith, 2001; Cross and Crispe, 2007; Worden et al., 2008b; Iaccheri, 2018), with fewer data obtained for rocks in Western Australia (Wingate et al., 2009; Kirkland and Wingate, 2010; Bagas et al., 2010; Iaccheri, 2018).

In this Report, we compile SHRIMP U–Pb zircon dating of metasedimentary and igneous rocks in the Granites–Tanami Orogen, carried out as part of collaborative research between Geoscience Australia (GA), the Geological Survey of Western Australia (GSWA) and the Northern Territory Geological Survey (NTGS) in the middle to late 2000s. Samples were collected to provide constraints on the timing and provenance of sedimentation,

1 Geoscience Australia, GPO Box 378, Canberra ACT 2601

2 Northern Territory Geological Survey, Smith Street Mall, Darwin NT 0801

3 The University of Western Australia, Stirling Highway, Crawley WA 6009

4 LamSil Geological Services, 1000 Cottonwood Canyon Road, Marysvale Utah US 84750

* Present address Newmont Goldcorp, 3 Bellows Street, Welshpool WA 6106

stratigraphic correlations and the ages of magmatic suites. Preliminary dates for some of these samples have been cited in earlier publications (e.g. Bagas et al., 2008; Lambeck et al., 2008), but the data are recalculated and fully documented here. The geochronological framework for the orogen is then assessed within the broader context of the North Australian Craton, to evaluate the potential geodynamic settings of basin formation, magmatism and deformation.

Geological overview

The Granites–Tanami Orogen forms part of the North Australian Craton, an assemblage of Archean to Mesoproterozoic orogens and basins that form the basement of much of northern Australia (Fig. 1; Myers et al., 1996;

Betts and Giles, 2006; Huston et al., 2012). The geological evolution of the Granites–Tanami Orogen (Tanami Region in NTGS terminology) spans the development of Neoproterozoic basement inliers, the formation of Paleoproterozoic (meta)sedimentary and igneous rocks, and an extended record of tectonic, magmatic and basin-forming events that extends into the Phanerozoic (Crispe et al., 2007; Ahmad et al., 2013b). The orogen adjoins the Aileron Province to the southeast, which includes metasedimentary successions and magmatic rocks of comparable age (Scrimgeour, 2013). In near-surface geology, the boundary between the two domains is indistinct and possibly transitional, but a major crustal boundary is inferred at depth from seismic data, which is coincident with the southern margin of the east-northeast-trending Willowra Gravity Ridge (Fig. 3; Goleby et al., 2009). The Paleoproterozoic Lamboo Province, exposed in the

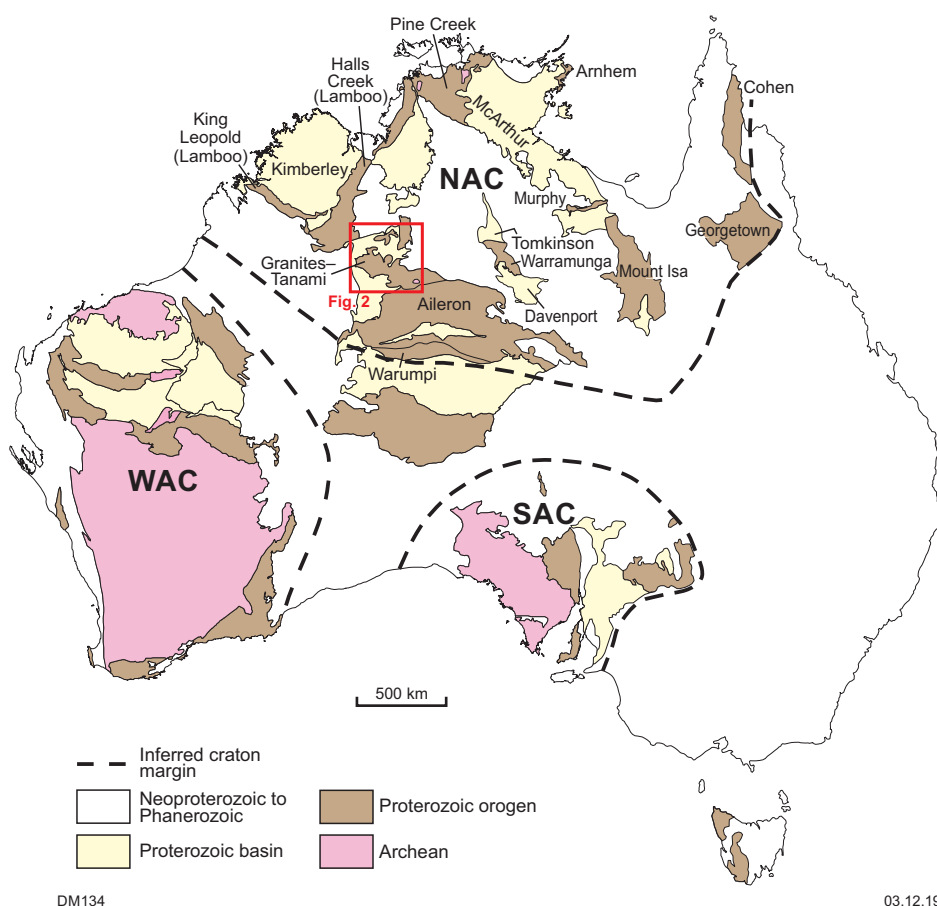


Figure 1. Location of the Granites–Tanami Orogen within the North Australian Craton. Note that the King Leopold and Halls Creek Orogens comprise the Lamboo Province, and the Tomkinson, Warramunga and Davenport Provinces comprise the Tennant Region. Abbreviations: NAC, North Australian Craton; SAC, South Australian Craton; WAC, West Australian Craton

Halls Creek and King Leopold Orogens, crops out to the northwest of the Granites–Tanami Orogen (Fig. 1). The Lamboo Province also contains Paleoproterozoic metasedimentary successions of a similar age to those in the Granites–Tanami Orogen, but it experienced a somewhat different tectonothermal evolution, interpreted to reflect plate margin interactions along the northwestern edge of the North Australian Craton (Griffin et al., 2000; Sheppard et al., 2001; Tyler et al., 2012). The boundary between the Granites–Tanami Orogen and the Lamboo Province is obscured by younger sedimentary basins, including the Birrindudu, Murraba, Wolfe, Ord and

Canning Basins, as are basement rocks to the northeast and southwest of the Granites–Tanami Orogen, about which little is known.

Neoproterozoic rocks

The Billabong Complex is a poorly exposed domain of quartzofeldspathic gneiss in the southeastern Granites–Tanami Orogen (Fig. 2), which forms a rare inlier of Neoproterozoic basement rocks. U–Pb zircon dating of quartzofeldspathic gneiss from the complex yielded a date of

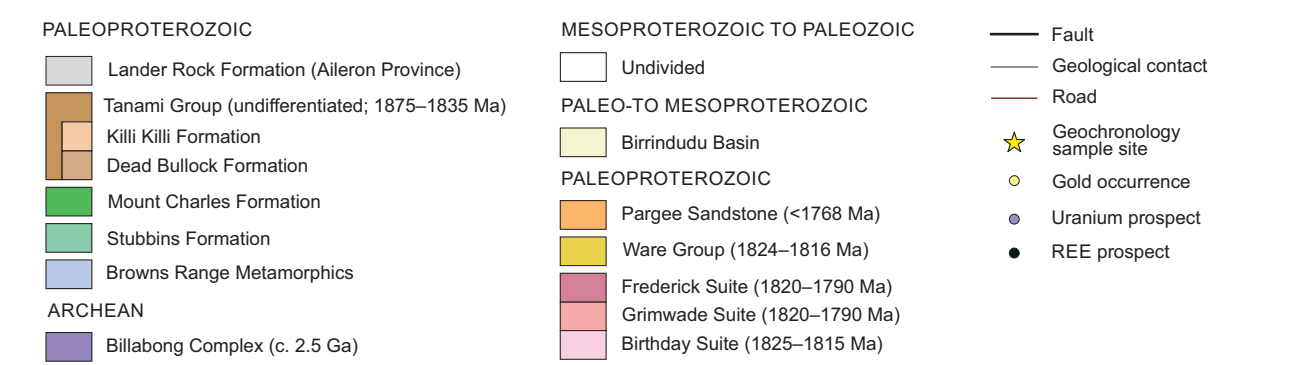
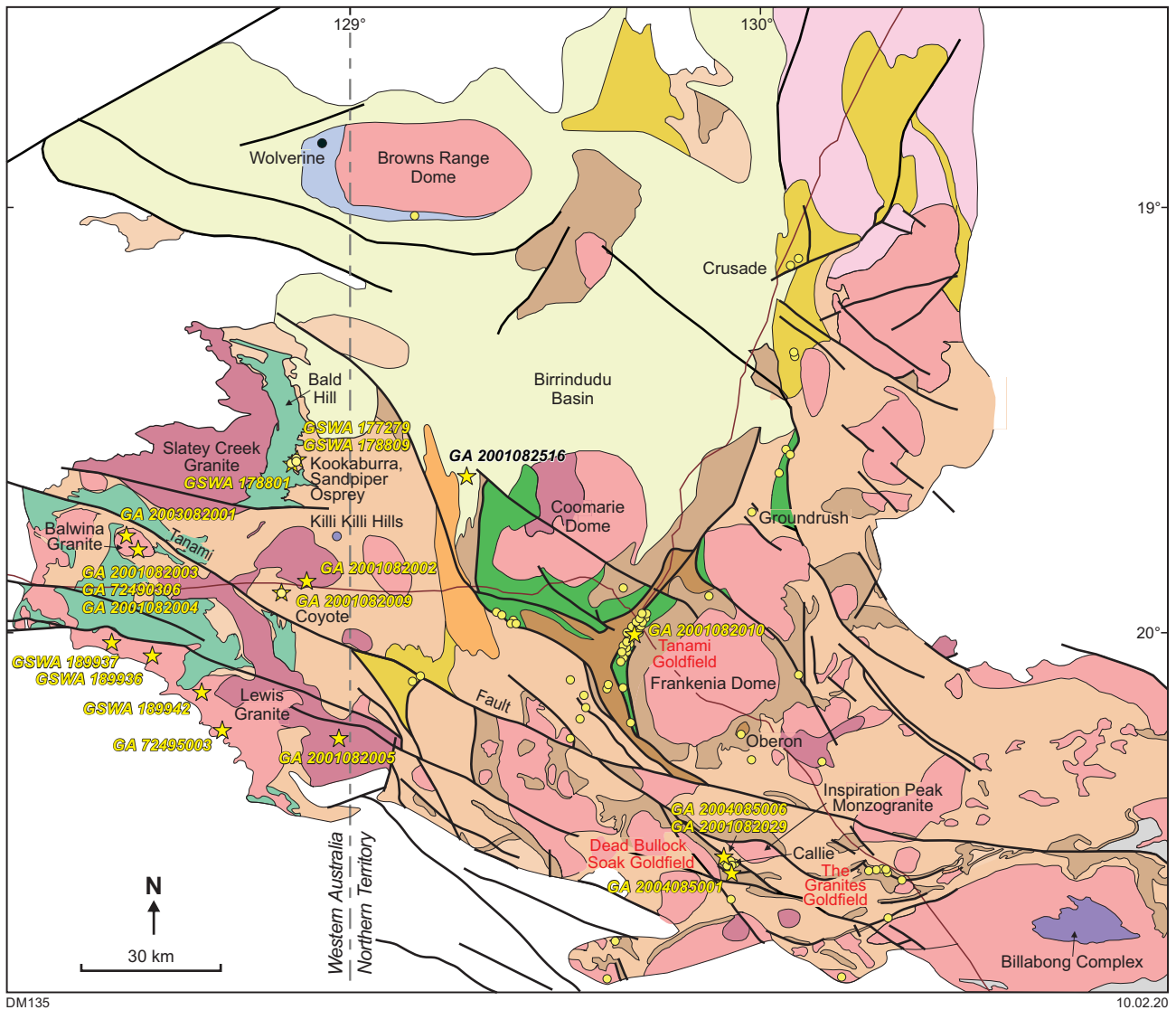


Figure 2. Simplified basement geology of the Granites–Tanami Orogen, after Bagas et al. (2010), Ahmad and Scrimgeour (2006) and GSWA (2016a)

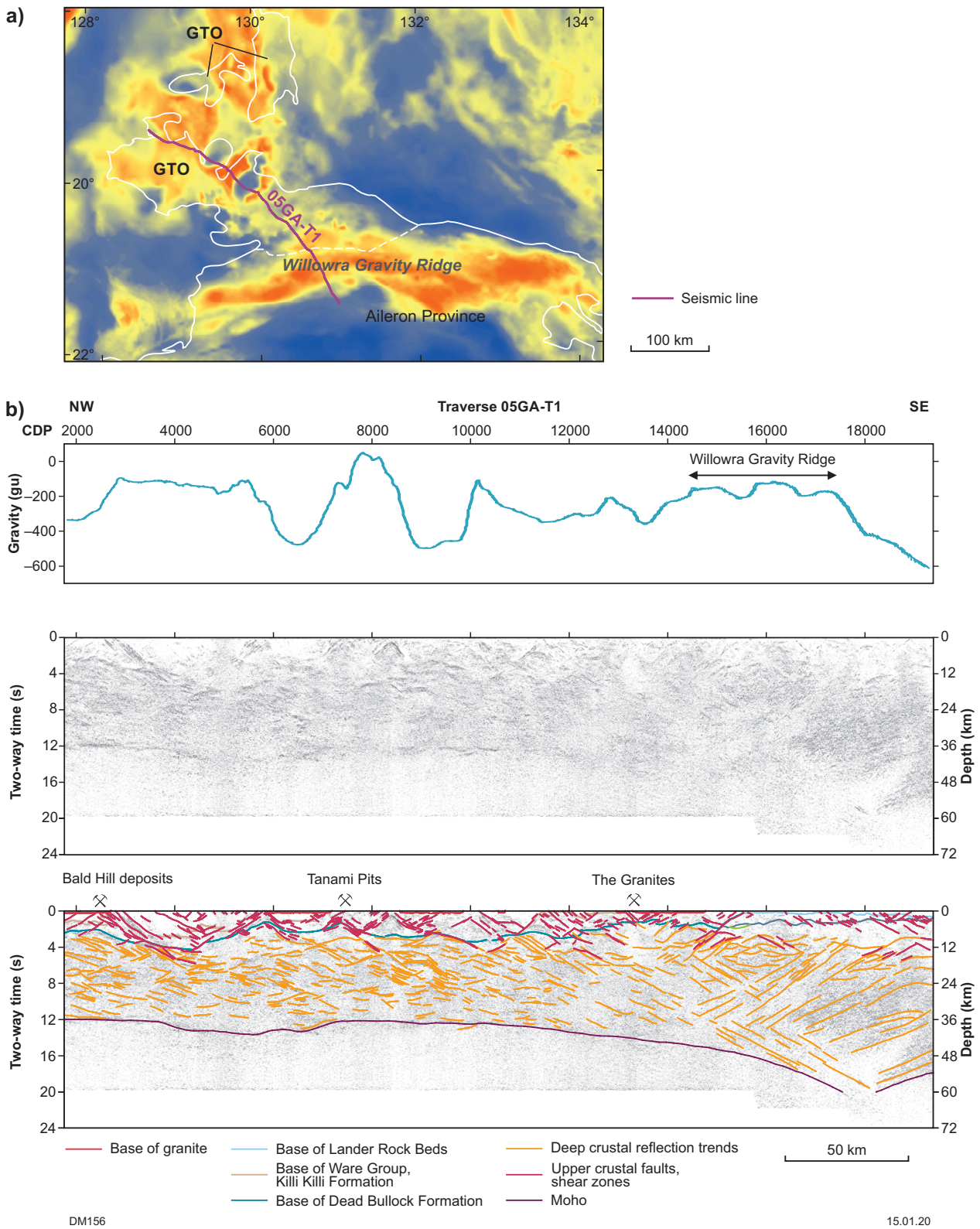


Figure 3. Seismic reflection profile across the Granites–Tanami Orogen (GTO) and Aileron Province: a) location of seismic line on gravity image; b) raw and interpreted migrated seismic section, with gravity data collected along traverse shown at top, simplified from Goleby et al. (2009). $V/H = 1$ at 6 km s^{-1} . Abbreviation: CDP, common depth point

2513 ± 3 Ma, interpreted to record magmatic crystallization and inherited age components at c. 2550 and 2530 ± 4 Ma (Page et al., 1995b). Similar age components were obtained from granitic orthogneiss in a more recent study, which yielded a U–Pb zircon date of 2510 ± 4 Ma, interpreted as a magmatic age and a large inherited age component at 2532 ± 3 Ma (Kositsin et al., 2013a; Whelan et al., 2014).

The Browns Range Metamorphics, which are exposed in the western and southern margins of the granite-cored Browns Range Dome (Fig. 2), have also been proposed as an inlier of Neoproterozoic basement. These rocks consist of feldspathic metasandstone, metaconglomerate and muscovite schist, with less common calc-silicate rock and banded iron-formation, and are unconformably overlain by sedimentary rocks of the Paleoproterozoic to Mesoproterozoic Birrindudu Basin (Blake et al., 2000). The interpretation of zircon dates obtained from the Browns Range Metamorphics remains the subject of debate, with inferred depositional ages ranging from Mesoarchean to Neoproterozoic (Page et al., 1995b; Nazari-Dehkordi et al., 2017) to Paleoproterozoic (Cross and Crispe, 2007; Ahmad et al., 2013b; Lu et al., 2017i,j).

Paleoproterozoic metasedimentary and meta-igneous rocks

Tanami Group stratigraphy

The Billabong Complex is overlain by the Paleoproterozoic Tanami Group, a package of dominantly siliciclastic metasedimentary and lesser volcanic and chemical metasedimentary rocks metamorphosed under greenschist to locally amphibolite facies conditions (Blake et al., 1979; Hendrickx et al., 2000; Vandenberg et al., 2001; Crispe et al., 2007; Lambeck et al., 2012; Ahmad et al., 2013b; Bagas et al., 2014). In the Northern Territory, the Tanami Group consists of the basal Dead Bullock Formation and the overlying Killi Killi Formation (Fig. 4; Table 1). The Dead Bullock Formation is >1.3 km thick (Bagas et al., 2014) and is divided into the Ferdies and Callie Members (Crispe et al., 2007). Bagas et al. (2014) proposed a modification of the boundary between the two members, and defined a third unit, the Kairos member (currently informal), beneath the Ferdies Member. The base of the Dead Bullock Formation has not been observed and the transitions between its constituent members are considered to be conformable and locally gradational. The Dead Bullock Formation has been divided into numerous informal subunits by mine geologists at the Dead Bullock Soak goldfield, summarized in Pendergast et al. (2017). These include the Coora dolerite, a 200 m-thick sill that intrudes the Callie Member.

The Kairos member of the Dead Bullock Formation, as described by Bagas et al. (2014), comprises a >145 m-thick succession of very fine- to fine-grained lithic sandstone with minor siltstone and shale. The overlying ~450 m-thick Ferdies Member consists of banded graphitic and non-graphitic siltstone and claystone as well as iron-formation and chert. The Ferdies Member hosts the Auron orebody in the Dead Bullock Soak goldfield (Pendergast et al., 2017). The ~750-m thick Callie Member in the upper part of the formation hosts many of the Au deposits in the region, including the Callie orebody (Huston et al., 2007). The Callie Member consists of well-bedded to laminated siltstone,

chert, iron-rich siltstone, banded ironstone, carbonaceous siltstone, sandstone, minor calc-silicate rocks and chert, and rare volcanoclastic rocks (Crispe et al., 2007; Lambeck et al., 2008; Ahmad et al., 2013b; Bagas et al., 2014).

The Killi Killi Formation is a ~4 km-thick siliciclastic metasedimentary unit that conformably overlies the Dead Bullock Formation (Blake et al., 1975, 1979; Crispe et al., 2007; Lambeck et al., 2008, 2010; Bagas et al., 2009). It consists of a compositionally immature package of sandstone, siltstone and lesser mudstone, which is interpreted to have been deposited as part of an extensive turbidite system containing a relatively high proportion of sandy units deposited as channelized or sheet sand lobes (Crispe et al., 2007; Lambeck et al., 2012). The depositional setting of the Killi Killi Formation represents a significant change from that of the upper Dead Bullock Formation, which contains a high proportion of laminated, fine-grained siliciclastic and chemical sediments deposited in a deep water, sediment-starved setting (Crispe et al., 2007; Lambeck et al., 2008, 2012).

In the Western Australian part of the orogen, Bagas et al. (2008) defined the 2–3 km-thick Stubbins Formation as the oldest exposed part of the succession. The Stubbins Formation consists of sandstone, shale and pillow basalt, as well as rare metarhyolite and chert, and is intruded by numerous dolerite sills. Initial interpretations placed the Stubbins Formation stratigraphically below the Dead Bullock Formation (Bagas et al., 2008), with differences in geochemistry between the two packages interpreted to reflect deposition during different basin phases (Lambeck et al., 2008, 2010). Bagas et al. (2014) revised this interpretation, suggesting that the Stubbins Formation is a correlative of the Dead Bullock Formation, noting overall lithological similarities between the two packages and a transitional contact with the overlying Killi Killi Formation (Li et al., 2013).

The Mount Charles Formation* is a ~1 km-thick package of sandstone, siltstone and shale with interbedded basalt and rare chert that hosts orogenic Au deposits in the Tanami goldfield (Tunks, 1996; Crispe et al., 2007; Lambeck et al., 2010; Bagas et al., 2014). The relationship of this unit to others in the region is uncertain due to poor exposure, faulting and a lack of tight age constraints. Some workers (Crispe et al., 2007; Cross and Crispe, 2007; Ahmad et al., 2013b) considered the Mount Charles Formation to unconformably overlie the Tanami Group, noting a lack of field evidence for the earliest three regional deformation events. In contrast, Bagas et al. (2014) correlated the Mount Charles Formation with the Dead Bullock Formation on the basis of similar lithological transitions, a different structural interpretation and an unpublished date of c. 1825 Ma for a felsic intrusion obtained by these authors that would constrain deposition to be older than the c. 1800 Ma age inferred by Crispe et al. (2007).

Tanami Group age constraints

The depositional ages of units in the Tanami Group are constrained between maximum ages provided by detrital zircon geochronology and minimum ages provided by dating of felsic igneous rocks. The youngest detrital zircon age components in individual samples range between c. 2533

* Name currently superseded as the unit was amalgamated into the Dead Bullock Formation; however, this status is disputed by the authors

and 1864 Ma, with the oldest parts of the succession dominated by Neoproterozoic detritus (Cross and Crispe, 2007; Bagas et al., 2009). An 1838 ± 6 Ma zircon U–Pb date for a felsic unit assigned to the Callie Member has been interpreted to date volcanism (Cross and Crispe, 2007), while a date of 1844 ± 4 Ma for a granitic rock intruding the Dead Bullock Formation (Smith, 2001) has been taken as a minimum age constraint for at least part of the unit. Bagas et al. (2014) questioned the interpretation of the c. 1838 Ma felsic unit as a tuff, and raised the possibility that this rock may in fact be an intrusive rock, providing only a minimum age for the Dead Bullock Formation. Bagas et al. (2008) cited an unpublished

1864 ± 3 Ma date for a felsic rock interpreted as a rhyolite within the Stubbins Formation, and considered this to date deposition of the host unit. A revised date for this sample is presented in this Report, as is a discussion of other possible geological interpretations.

Samples of the Killi Killi Formation have yielded dominant c. 1865 Ma detrital zircon age components (Cross and Crispe, 2007; Bagas et al., 2009). Cross and Crispe (2007) inferred deposition of the Killi Killi Formation at 1840–1820 Ma on the basis of the interpreted c. 1838 Ma age of volcanism in the underlying Dead Bullock Formation and the (imprecise)

Table 1. Summary of stratigraphic units in the Granites–Tanami Orogen

<i>Unit</i>	<i>Age (Ma)</i>	<i>Location</i>	<i>Lithologies</i>	<i>Estimated thickness (m)</i>	<i>Depositional setting</i>
Gardiner Sandstone (Birringdudu Basin)	1768–1632	Northern Territory and Western Australia	Cross-bedded, thinly to thickly bedded sublithic arenite, quartz arenite, conglomerate, shale, siltstone, glauconitic sandstone	3000	Shallow marine to emergent
Pargee Sandstone	<c.1768	Restricted area west of Coomarie Dome (Northern Territory)	Thickly bedded quartz arenite, lithic arenite, conglomerate, minor siltstone	≤1300	High-energy shallow marine to fluvial
Ware Group	1824–1816	Mostly in northeast of orogen, restricted area in west (Northern Territory)	Felsic volcanic rocks, coarse-grained lithic sandstone, minor siltstone and basalt	≤5500	Subaerial to marine, possibly fluvial and lacustrine
Stubbins Formation	1885–1865	Western part of orogen (Western Australia)	2–3 km-thick lower succession of sandstone, siltstone, shale, rare rhyolite; upper 200 m-thick package of Fe-rich siltstone and shale, graphitic and carbonaceous shale, chert, basalt, rare turbiditic sandstone	2000–3000	Turbidity currents, low-energy marine
Killi Killi Formation	1865–1840	Widespread in Northern Territory and Western Australia	Micaceous greywacke, quartz wacke, lithic greywacke, quartz and lithic arenite, siltstone and mudstone	4000	Turbidity currents, proximal to mid-fan
Mount Charles Formation	1885–1865	Tanami Goldfield (Northern Territory)	Basalt, basaltic breccia, sandstone, mudstone, carbonaceous mudstone, intraclast conglomerate, rare chert	<3000	Turbidity currents, below storm wave base
Callie Member (Dead Bullock Formation)	1875–1865	Dead Bullock Soak and surrounding region (Northern Territory)	Siltstone, chert, Fe-rich siltstone, banded ironstone, carbonaceous siltstone, minor calc-silicate, rare volcanoclastic rock	>730	Low-energy marine, below storm wave base, low sedimentation rate
Ferdies Member (Dead Bullock Formation)	1885–1865	Dead Bullock Soak and surrounding region (Northern Territory)	Siltstone, carbonaceous siltstone, lesser sandstone	435	Low-energy marine, below storm wave base
Kairos member (Dead Bullock Formation)	1885–1865	Dead Bullock Soak (Northern Territory)	Cross-laminated and slump-structured, very fine- to fine-grained lithic sandstone, minor siltstone and shale	>135	Marine, moderate water depths?
Browns Range Metamorphics	1885–1865? 3000–2500?	Browns Range Dome (Western Australia)	Quartzofeldspathic gneiss, muscovite schist, metamorphosed arkosic sandstone	1000–3000	Uncertain

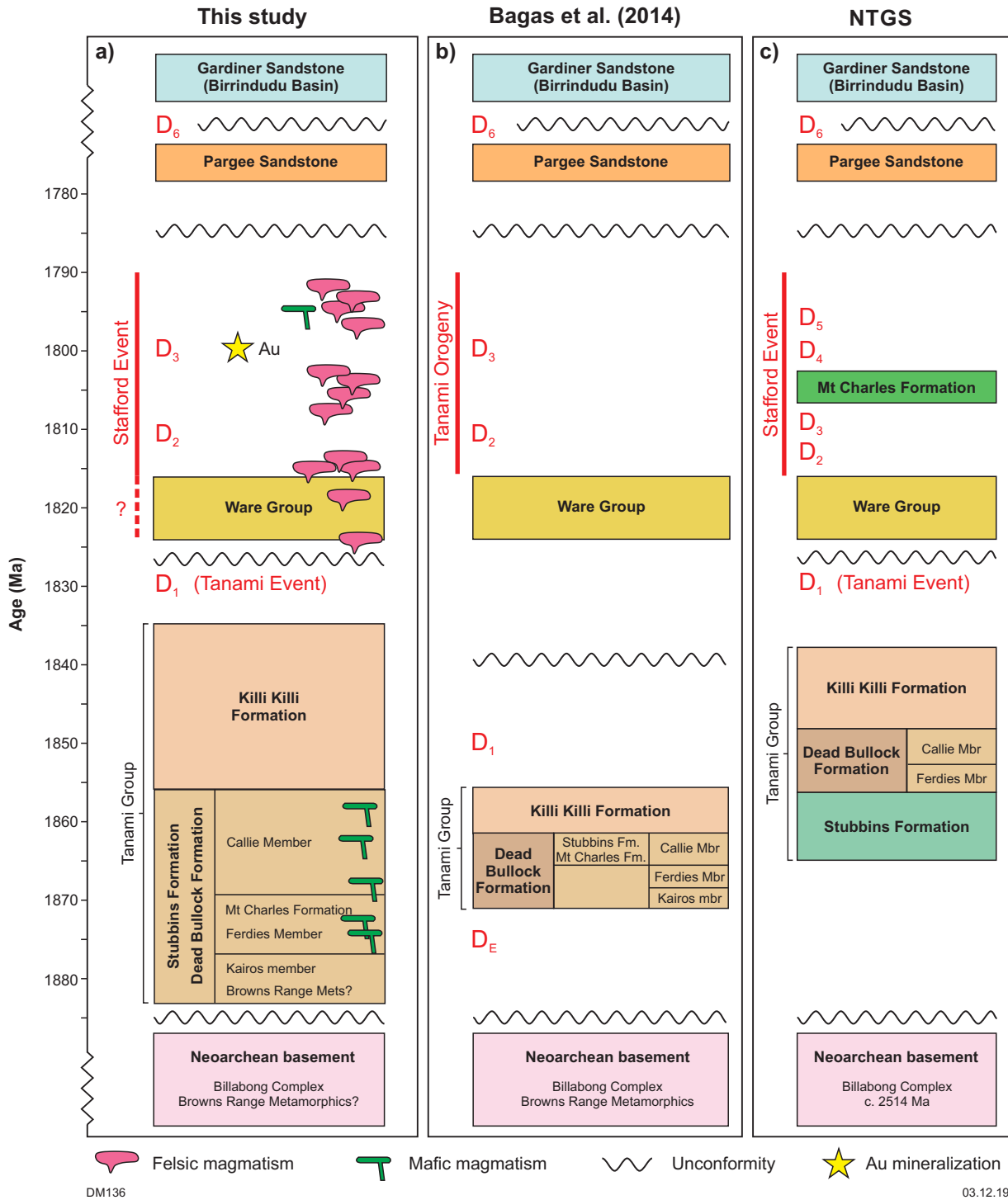


Figure 4. Stratigraphy and tectonism of the Granites–Tanami Orogen: a) inferred ages and relationships adopted in this study. This event framework is a modification of previous syntheses, including those produced by workers from b) UWA — Bagas et al. (2008, 2009, 2010, 2014), Joly et al. (2010) and Li et al. (2013, 2014); and c) the NTGS — Crispe et al. (2007) and Ahmad et al. (2013b). Magmatic events are not depicted in b) and c). The age of the Browns Range Metamorphics is the subject of debate, and different possible ages are noted. The Stafford Event is interpreted here as a prolonged period of extension punctuated by short-lived compressional events, which possibly also encompasses felsic magmatism of the Ware Group

dates of the youngest individual zircons. In contrast, Bagas et al. (2014) suggested that the Killi Killi Formation and all other units of the Tanami Group were deposited before c. 1850 Ma, an age inferred by these authors for the first major deformation event to affect these rocks.

Ware Group

The Ware Group is considered to unconformably overlie the Tanami Group on the basis of structural interpretations, though the contact is not exposed (Crispe et al., 2007). It consists mainly of felsic volcanic rocks, with lesser coarse-grained lithic sandstone and minor siltstone and basalt (Blake et al., 1979; Orth, 2007; Ahmad et al., 2013b). The Ware Group comprises the Mount Winnecke Formation, Nanny Goat Volcanics, Wilson Formation and Century Formation, and felsic volcanic rocks have been dated at 1824–1816 Ma (Page, 1996b,d; Smith, 2001; Worden et al., 2008b). The 1815 ± 5 Ma Winnecke Granophyre (Page, 1996a) intrudes the Mount Winnecke Formation and is considered to be part of the same magmatic event that produced the felsic volcanic rocks. The depositional setting of the volcanic rocks is interpreted to be subaerial, with sedimentary units deposited in a fluvial to lacustrine, or shallow-marine setting, though a deeper water setting has been suggested for the Wilson Formation (Crispe et al., 2007; Orth, 2007).

Granitic rocks

Voluminous granitic intrusions in the Granites–Tanami Orogen comprise about 50% of the near-surface by area (Fig. 2; Bagas et al., 2010). These granitic rocks intrude the Tanami and Ware Groups and are unconformably overlain by sedimentary rocks of the Paleoproterozoic to Mesoproterozoic Birrindudu Basin (Blake et al., 1979; Crispe et al., 2007; Ahmad et al., 2013b). The granitic rocks consist of I-type granodiorite to monzogranite, and are generally calcic to calc-alkalic, peraluminous and magnesian at lower SiO₂, trending to ferroan at higher SiO₂ (Dean, 2001; Bagas et al., 2010; Ahmad et al., 2013b). The granitic rocks are biotite-bearing, with hornblende in rocks with the lowest SiO₂, and contain minor magnetite, ilmenite, titanite and zircon. Muscovite is present in the most peraluminous granitic rocks and is more abundant than biotite in some intrusions in Western Australia, where Bagas et al. (2010) noted compositions generally more peraluminous than those recorded in the Northern Territory. The aluminium saturation index (ASI) increases with increasing SiO₂ (Ahmad et al., 2013b).

The granitic rocks of the Granites–Tanami Orogen have been divided into different magmatic suites, which are broadly coeval, but are distinguished by differences in their magnetic character, composition and age (Dean, 2001; Crispe et al., 2007; Bagas et al., 2010; Ahmad et al., 2013b; Iaccheri, 2018). The nomenclature and grouping of these suites has evolved over time, and this study uses the terminology adopted by Ahmad et al. (2013b).

The Birthday Suite is restricted to the northeastern part of the orogen and has not been recognized in Western Australia. It includes the Winnecke Granophyre and felsic volcanic rocks of a similar age in the Mount Winnecke Formation. The suite is alkali-calcic, highly

potassic and silica-rich (>70.7 wt% SiO₂), and forms areas of strong magnetization on aeromagnetic images (Ahmad et al., 2013b). U–Pb zircon dates from the Birthday Suite range between c. 1825 and 1815 Ma, slightly older than most of the other granitic rocks in the region (Smith, 2001).

The Grimwade Suite was emplaced across the Granites–Tanami Orogen and extends into the northwestern Aileron Province. It comprises monzogranite to syenogranite with generally weak magnetization, forming small to very large intrusive bodies. It has the broadest range of SiO₂ of the three suites, is calcic (Crispe et al., 2007), and yields U–Pb zircon dates of 1821–1791 Ma (Smith, 2001; Worden et al., 2004; Cross et al., 2005a; Bagas et al., 2010; Iaccheri, 2018). A date of 1785 ± 4 Ma (Cross et al., 2005a) for a granite in the Aileron Province might represent a younger component of this magmatic suite (Scrimgeour, 2013).

The Frederick Suite comprises medium- to fine-grained, equigranular, biotite monzogranite to syenogranite characterized by relatively strong magnetization. It is distributed across the Granites–Tanami Orogen, but has not been identified in the Aileron Province. The Frederick Suite is calc-alkaline, with SiO₂ contents of 63–72 wt% (Ahmad et al., 2013b), and has yielded U–Pb zircon dates of 1815–1778 Ma (Smith, 2001; Bagas et al., 2010).

Granitic units in Western Australia dated in this study (Fig. 5) include the Lewis Granite, a large composite body comprising magnetic and non-magnetic phases assigned to the Frederick and Grimwade Suites, and the Balwina Granite, which is assigned to the Frederick Suite (Huston et al., 2007). Geochemical data reported by Bagas et al. (2010) indicate that the monzogranites to granodiorites comprising the Lewis and Balwina Granites, and the Slaty Creek Granite to the north, have an SiO₂ content of 69–76 wt%, are calc-alkaline to alkali-calcic, and range from magnesian to ferroan with increasing SiO₂, using the scheme of Frost et al. (2001). They contain 2.36 – 5.44 wt% K₂O, 2.58 – 4.89 wt% Na₂O and a broad range of K₂O/Na₂O ratios (0.48 – 1.87). The sampled rocks are peraluminous, with ASI values of 1.03 – 1.31. The most aluminous compositions possibly reflect the effects of fractionation of I-type magma, rather than indicating an S-type affinity (Bagas et al., 2010). Mantle-normalized trace element patterns show a negative slope, with relative positive anomalies of U and Pb and a negative Ti anomaly. For samples with rare earth element (REE) data, chondrite-normalized plots show enrichment in light rare earth elements (LREE) and a gentle listric profile. The overall geochemical character of the granitic rocks from Western Australia is comparable to that of granitic rocks elsewhere in the orogen (Dean, 2001), and is consistent with derivation from crustal sources (Bagas et al., 2010).

Paleoproterozoic to Phanerozoic cover successions

The Pargee Sandstone unconformably overlies the Killi Killi Formation west of the Coomarie dome (Fig. 2) and consists of a >1.5 km-thick succession of interbedded

quartz-rich to lithic sandstone, conglomerate and minor siltstone (Blake et al., 1975, 1979; Crispe et al., 2007). The succession broadly coarsens up sequence and is interpreted to have been deposited in a shallow-marine to fluvial environment. Detrital zircon dating indicates a maximum depositional age of 1768 ± 14 Ma (Cross and Crispe, 2007), post-dating the period of granitic magmatism.

Sedimentary rocks of the Paleoproterozoic to Mesoproterozoic Birrindudu Basin unconformably overlie the Pargee Sandstone and older rocks of the Granites–Tanami Orogen (Fig. 2). The c. 1768 Ma maximum depositional age of the underlying Pargee Sandstone defines a maximum age for the basin, while a minimum age for the lowermost unit of the basin (the Gardiner Sandstone) is provided by a 1632 ± 3 Ma U–Pb date from secondary xenotime (Vallini et al., 2007), which is similar in age to 1639–1635 Ma felsic tuffs stratigraphically higher in the basin (Fanning, 1991; Smith, 2001; Cutovinos et al., 2002). The Birrindudu Basin is, in turn, overlain by Neoproterozoic sedimentary rocks of the Murraba, Wolfe and Victoria Basins. Cambrian mafic volcanic rocks and subordinate siliciclastic sedimentary rocks of the Antrim Plateau Volcanics are widespread in the region and form part of the Kalkarindji Large Igneous Province, which is preserved across a broad area of northwestern Australia (Hanley and Wingate, 2000; Glass and Phillips, 2006; Glass et al., 2013; Jourdan et al., 2014). $^{40}\text{Ar}/^{39}\text{Ar}$ dating of K-feldspar from basalt yields dates between c. 508 and 498 Ma (Glass and Phillips, 2006; Marshall et al., 2018).

Phanerozoic sedimentary rocks of the Canning Basin unconformably overlie Proterozoic units in the western part of the region.

Deformation and metamorphism

Various studies of the structural history of the Granites–Tanami Orogen have been carried out, including deposit-to goldfield-scale studies (Ireland and Mayer, 1984; Nicholson, 1990; Mayer, 1990; Adams, 1991; Lovett et al., 1993; Scott, 1993; Tunks, 1996; Smith et al., 1998; Tunks and Cooke, 2007; Adams et al., 2007) and regional syntheses (Blake et al., 1979; Cooper and Ding, 1997; Vandenberg et al., 2001; Crispe et al., 2007; Bagas et al., 2008, 2009, 2010; Ahmad et al., 2013b). There are significant differences between the structural schemes established by the NTGS (Vandenberg et al., 2001; Crispe et al., 2007; Ahmad et al., 2013b) and those adopted by researchers from The University of Western Australia (UWA), who studied areas in Western Australia and the Northern Territory (Bagas et al., 2008, 2009, 2010, 2014; Joly et al., 2010; Li et al., 2013, 2014). The differences between these schemes in part reflect the complex deformation history, the paucity of outcrop and differences in the inferred depositional ages of sedimentary units.

The regional structural frameworks established by the NTGS and UWA researchers are summarized in Table 2. Both schemes recognize deformation of the Tanami

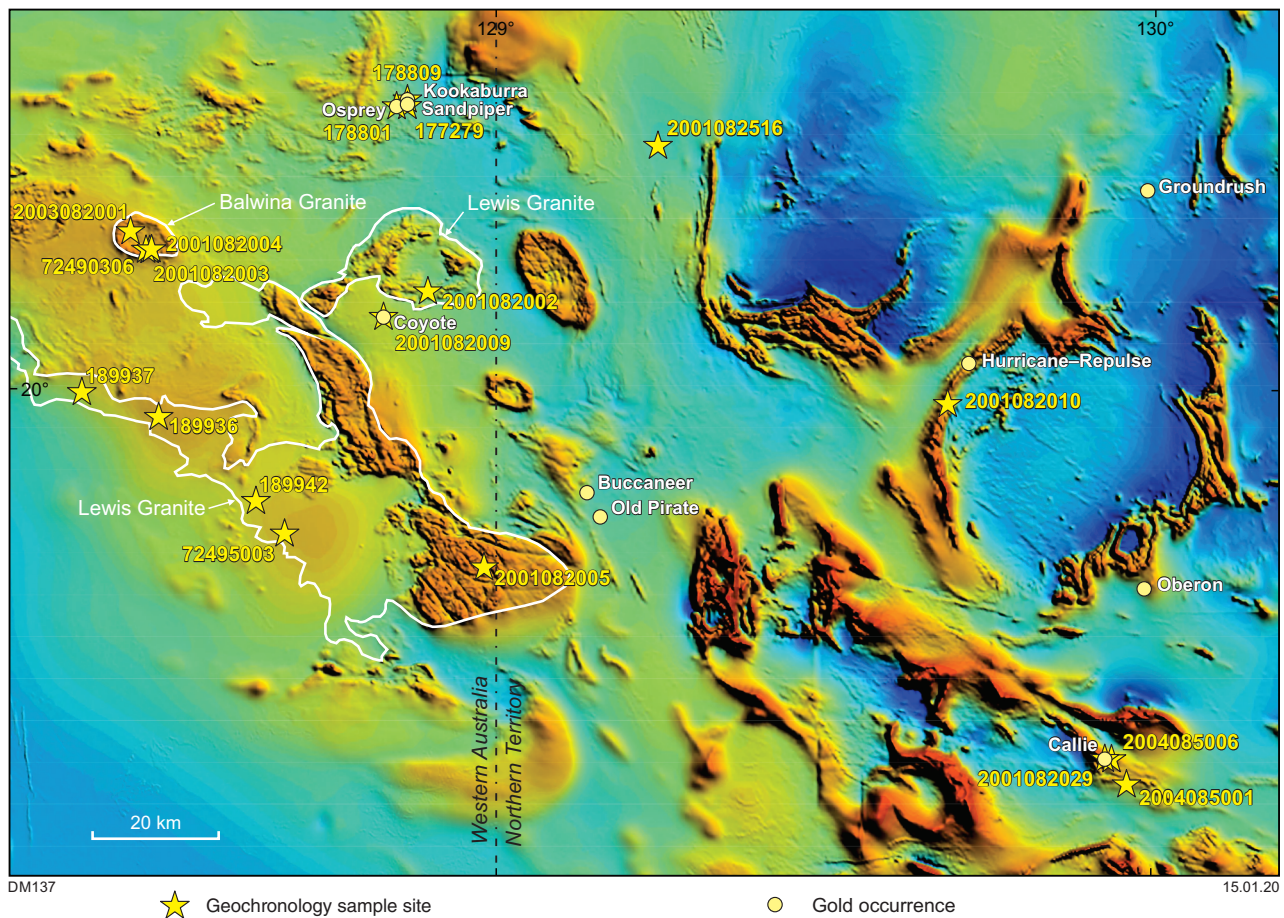


Figure 5. Total magnetic intensity (reduced to pole) aeromagnetic image of the Granites–Tanami Orogen, showing locations of geochronology samples. Subset of data from the Geoscience Australia sixth edition Total Magnetic Intensity (TMI) anomaly grid of Australia (Nakamura and Milligan, 2015)

Group pre-dating deposition of the 1824–1816 Ma Ware Group, and both interpret deformation events that are broadly coeval with granite emplacement at c. 1800 Ma. The schemes differ in the interpreted number of deformation events between c. 1850 and 1790 Ma, with the NTGS scheme interpreting several compressional events in the period 1815–1790 Ma, as well as an extensional event in this period to account for an interpreted post-Ware Group depositional age for the Mount Charles Formation. The schemes also differ in terminology, with the term Tanami Event assigned by the NTGS to deformation and metamorphism that pre-dated deposition of the Ware Group, whereas the UWA scheme assigns the term Tanami Orogeny to the c. 1800 Ma deformation and magmatism that post-dates deposition of the Ware Group. In this Report, the term Tanami Event is used in accordance with the NTGS scheme, recognizing the precedence of terminology introduced by NTGS workers (Vandenberg et al., 2001; Crispe et al., 2007). Similarly, the tectonism at 1810–1790 Ma is here referred to as the Stafford Event, rather than the Tanami Orogeny.

Tanami Group metamorphism during the Tanami Event ranges from greenschist facies to locally low-pressure, high-temperature middle amphibolite facies, with peak metamorphic conditions of about 600°C and 3.5 kbar at The Granites goldfield (Scrimgeour and Sandiford, 1993). An 1839 ± 9 Ma date for monazite from metasiltstone of the Ferdies Member at the Dead Bullock Soak goldfield is interpreted as the age of peak metamorphism (Petrella et al., 2019). $^{40}\text{Ar}/^{39}\text{Ar}$ dating of metamorphic hornblende from dolerite sills in the Dead Bullock Formation that were folded during the Tanami Event yielded dates of 1840 ± 14 and 1840 ± 19 Ma, which are also considered to constrain the age of this metamorphism (Li et al., 2014). Regional metamorphic conditions during younger events such as the Stafford Event were generally lower grade, typically greenschist facies or lower, though locally higher grades were established in the contact metamorphic aureoles of larger granitic bodies. $^{40}\text{Ar}/^{39}\text{Ar}$ biotite cooling dates for metasedimentary rocks in the Dead Bullock Soak and The Granites goldfields range between c. 1760 and 1710 Ma (Fraser, 2002; Li et al., 2014) and 1820–1755 Ma for

Table 2. Comparison of published structural frameworks for the Granites–Tanami Orogen. Event names are those used in sources

<i>Deformation event</i>	<i>Structural scheme, UWA*</i>	<i>Structural scheme, NTGS†</i>
D ₆₊		D₆₊ faulting: Late thrust, oblique-slip and normal faults cutting earlier structures. Likely multiple events <1700 Ma
D ₅		Stafford Event: Shear zones, thrusts and oblique-slip faults pre-dating deposition of Pargee Sandstone; southeast-, east- to northeast-, and west- to southwest-dipping thrust fault networks; likely multiple events; orogenic Au mineralization; 1815–1790 Ma?
D ₄		Stafford Event: East-northeasterly to locally east-trending, upright, chevron folds, crenulation of D ₃ structures in Tanami and Ware Groups; north-northwest – south-southeast shortening; limited overprinting evidence indicates D ₄ closely followed emplacement of many 1815–1790 Ma granitic intrusions
Post-D ₃		Rift event leading to deposition of sedimentary and mafic volcanic rocks of the Mount Charles Formation; 1810–1790 Ma (broadly syn-Stafford Event)
D ₃	Tanami Orogeny: Locally developed open folds plunging moderately north-northeast; rare subvertical cleavage; greenschist facies; D ₁ –D ₃ interpreted to post-date Mount Charles Formation; ~northwest–southeast shortening c. 1800 Ma	Stafford Event: Open, upright, angular, northwest- to north-trending folds, local crenulation of D ₁ fabrics; dominant structures in Ware Group; D ₁ –D ₃ interpreted to pre-date Mount Charles Formation; F ₃ folds pre-date c. 1791 Ma granite; 1815–1800 Ma
D ₂	Tanami Orogeny: Tight to isoclinal refolding of D ₁ structures by asymmetrical, angular folds of ~1 km wavelength; greenschist facies; north-northeast–south-southwest shortening at c. 1800 Ma post-dates deposition of Ware Group; D ₂ –D ₃ associated with Au mineralization	Stafford Event: Local, open, angular northeast- to north-northeast-striking folds; crenulation of D ₁ fabrics; oldest structures in Ware Group; northwest–southeast to west-northwest – east-southeast shortening at 1815–1800 Ma
D ₁	D_{GTO1}: Isoclinal folds in Tanami Group with well-developed axial planar cleavage; common layer-parallel faults; greenschist facies; east–west compression c. 1850 Ma, pre-dates deposition of Ware Group	Tanami Event: Asymmetric disharmonic folds in Tanami Group with axial planar slaty cleavage; F ₁ folds trend northwest–southeast to east–west, with variations due to younger deformation; pre-dates deposition of Ware Group; greenschist to middle amphibolite facies, low-pressure, high-temperature metamorphism; c. 1830 Ma
Pre-D ₁	D_{GTOE}: Faulting during north–south extension; amphibolite-facies metamorphism of Billabong Complex pre-dating deposition of Tanami Group	Upper amphibolite facies metamorphism of the Neoproterozoic Billabong Complex and development of gneissosity; pre-dates deposition of Tanami Group

* Bagas et al. (2008, 2009, 2010, 2014), Joly et al. (2010), Li et al. (2013, 2014), Stevenson et al. (2013)

† Vandenberg et al. (2001), Crispe et al. (2007), Ahmad et al. (2013b)

granitic rocks (Fraser, 2002). These dates appear to reflect relatively slow cooling following deformation and granite emplacement during the Stafford Event.

The Granites–Tanami Orogen contains multiple orogenic Au deposits in several goldfields, including the world-class Callie deposit in the Dead Bullock Soak goldfield (Huston et al., 2007; Bagas et al., 2007b; Ahmad et al., 2013b; Pendergast et al., 2017; Wygralak et al., 2017). Although most mineralization is hosted within Fe-rich, cherty, carbonaceous or mafic metasedimentary and meta-igneous rocks of the Dead Bullock Formation, or possible correlatives (Stubbins and Mount Charles Formations), some Au is also hosted by the Killi Killi Formation, and locally by felsic porphyry at Twin Bonanza. Syn-mineralization xenotime at the Callie deposit has been dated at 1803 ± 19 Ma (Cross et al., 2005d), 1805 ± 11 and 1805 ± 20 Ma (Petrella et al., 2019). A similar, unpublished, xenotime date of 1791 ± 8 Ma for the Coyote deposit was noted in Bagas et al. (2007a). These dates are similar to a $^{40}\text{Ar}/^{39}\text{Ar}$ sericite date of 1794 ± 12 Ma for the Sandpiper deposit (Fraser et al., 2012) and an unpublished 1778 ± 12 Ma Re–Os date for Au-associated pyrite and arsenopyrite in the Bald Hill/Coyote area cited by Bagas et al. (2014). Together, these dates indicate that Au mineralization, at least in these deposits, was associated with the Stafford Event.

Analytical methods

Samples were crushed and milled at the GA Mineral Separation Laboratory and the GSWA Carlisle laboratory. Mineral density separation at GA was undertaken using a Wilfley table, using multiple iterations to reduce the sample to about 1–2% of its post-milling weight, and high-density liquids. Mineral separation at the Carlisle laboratory involved removal of very fine particles by elutriation in a custom glass funnel apparatus, followed by high-density liquids. Highly magnetic minerals were removed by hand magnet prior to magnetic separation using a Frantz isodynamic separator. Handpicking of zircons from igneous samples focused on non-fractured grains from the fraction with the weakest paramagnetism. For metasedimentary samples, a random selection of zircon grains was separated from the least paramagnetic fraction, with the aim of sampling a representative spread of the detrital source regions, while minimizing the proportion of metamict grains. Zircons were cast with zircon standards QGNG and SL13 in GA mounts, and with Temora 2 and CZ3 in GSWA mounts, in epoxy resin disks and polished to expose grain interiors. Mounts were documented prior to analysis with reflected- and transmitted-light photomicroscopy and cathodoluminescence (CL) imaging.

U–Pb analyses were conducted between 2001 and 2005 using the SHRIMP I, SHRIMP II and SHRIMP RG instruments at the Research School of Earth Sciences at the Australian National University, and in 2008 using the SHRIMP-A and SHRIMP-B instruments at the John De Laeter Centre of Isotope Research at Curtin University. Analytical procedures adopted are similar to those of Compston et al. (1984), Clauoué-Long et al. (1995) and Wingate and Lu (2017). Data were reduced using SQUID 1 (for older SHRIMP 1 data) or SQUID 2 (Ludwig, 2009) and Isoplot 3.71 (Ludwig, 2003) add-ins for Microsoft

Excel 2003, with decay constants recommended by Steiger and Jäger (1977). Corrections for common Pb used measured $^{204}\text{Pb}/^{206}\text{Pb}$ and compositions based on the crustal common-Pb model of Stacey and Kramers (1975). Calibration of U/Pb ratios assumed a $^{238}\text{U}/^{206}\text{Pb}$ age of 1842 Ma for zircon standard QGNG and 416.8 Ma for Temora 2 (Black et al., 2003, 2004). Calibration and external spot-to-spot (reproducibility) uncertainties are included in the errors of $^{238}\text{U}/^{206}\text{Pb}$ ratios and dates listed in Appendix 1. Measured $^{207}\text{Pb}^*/^{206}\text{Pb}^*$ ratios in QGNG are used to monitor the accuracy of measured $^{207}\text{Pb}^*/^{206}\text{Pb}^*$ in grains of unknown age ($\text{Pb}^* = \text{radiogenic Pb}$). For each analytical session, the weighted mean $^{207}\text{Pb}^*/^{206}\text{Pb}^*$ age for QGNG is slightly younger than the reference $^{207}\text{Pb}^*/^{206}\text{Pb}^*$ age of 1851.6 Ma, and adjustments for this instrumental mass fractionation (IMF) (Appendix 1) are applied to increase the $^{207}\text{Pb}^*/^{206}\text{Pb}^*$ ratios measured in zircons of unknown age (Appendix 2). Uncertainties associated with this correction are added in quadrature to the uncertainties of $^{207}\text{Pb}^*/^{206}\text{Pb}^*$ ratios and resulting dates. Discordance of 204-corrected dates is calculated as $100 \times [1 - (^{238}\text{U}/^{206}\text{Pb}^* \text{ date}) / (^{207}\text{Pb}^*/^{206}\text{Pb}^* \text{ date}^*)]$. Analyses used for assessment of detrital zircon and magmatic ages are those that are <5% discordant and indicate low common Pb ($f_{204} < 1\%$; f_{204} is the proportion of common ^{206}Pb in total ^{206}Pb , as calculated from measured $^{204}\text{Pb}/^{206}\text{Pb}$ ratios).

U–Pb zircon geochronology

This Report presents data for 18 metasedimentary and felsic igneous rocks, of which 14 were collected in Western Australia as part of collaborative work between GA and GSWA, and four from the Northern Territory in conjunction with NTGS. Samples were collected from both drillcore and outcrop, focusing on metasedimentary rocks of the Tanami Group and the large granitic bodies that intrude the succession. Two samples of the Gardiner Sandstone were studied to provide data for the lowermost Birrindudu Basin, the age of which is not tightly constrained. The data are fully documented here for the first time, superseding informal dates based on preliminary processing that were cited in Bagas et al. (2008) and Lambeck et al. (2008).

In this Report, samples of metasedimentary rocks of the lowermost Tanami Group in Western Australia are referred to as the Stubbins Formation, rather than their inferred correlative, the Dead Bullock Formation as adopted by Bagas et al. (2014), for convenience when discussing the potential stratigraphic correlations.

Isotope data are summarized in Table 3, tabulated in detail in Appendix 2, and interpreted below. For purposes of discussion, individual zircon analyses are placed into interpretive groups: Group I indicates analyses interpreted to record primary igneous crystallization ages; Group X indicates analyses interpreted to represent xenocrystic grains; Group Y identifies the youngest single detrital zircon in a metasedimentary rock; Group S denotes older detrital zircons in a metasedimentary rocks; Group P denotes concordant data younger than a rock's interpreted emplacement age, possibly due to loss of radiogenic Pb; and Group D indicates zircon compositions that are >5% discordant or that have high common Pb ($f_{204} > 1\%$).

Detrital zircon dates for each sample are interpreted as the ages of zircon-crystallizing rocks in the detrital source region(s), or the ages of detrital components derived from reworked sedimentary rocks. For each sedimentary sample, we report the age of the youngest individual grain with a U–Pb date $\leq 5\%$ discordant (Group Y), and the youngest statistically coherent group of three or more concordant dates that agree to within 2.5 sigma as a conservative estimate of the youngest age component in the detritus — the maximum age of sediment deposition. Significant age components quoted below are those that comprise age-probability contributions (at 2 sigma) from three or more analyses, and the number of analyses reported for an age component are those that contribute age probability to that component (Gehrels, 2009).

Most dates discussed in this Report are based on $^{207}\text{Pb}^*/^{206}\text{Pb}^*$ ratios. Ratios and dates for individual analyses are quoted with 1 sigma uncertainties in data tables and in the text. Mean values for grouped data are quoted with 95% confidence intervals calculated as $t\sigma\sqrt{\text{MSWD}}$, where MSWD is >1 , and 1.96σ where MSWD is <1 ; t is Student's t ; MSWD is mean square of weighted deviates. A concordia age is calculated for one sample, based on both $^{238}\text{U}/^{206}\text{Pb}^*$ and $^{207}\text{Pb}^*/^{206}\text{Pb}^*$ ratios, and is quoted with a value for MSWD for combined concordance and equivalence (Ludwig, 1998). Uncertainties on concordia intercept dates produced by discordia regression are calculated following Ludwig (2003).

Discrepancies between the dates documented in this Report, and informal preliminary dates cited in Bagas et al. (2008) and Lambeck et al. (2008) are largely due to the application here of IMF corrections, on the basis of data obtained from zircon standards.

Metasedimentary rocks

GA 2004085006: metasandstone — Ferdies Member, Dead Bullock Formation

Fine-grained sandstone of the informal lower Blake beds within the Ferdies Member was sampled from drillcore at the Callie Au deposit (Figs 2, 5; DBD378: 828.2 – 829.0 m). The sampled interval consists of thin-bedded turbidites with micro-flame structures (<5 mm), rip-up mud clasts and convolute laminations. It was studied in an attempt to place tighter constraints on its depositional age, because previous samples of the Ferdies Member from other parts of the orogen had yielded mainly Archean detrital zircon ages (Cross and Crispe, 2007). The sample yielded relatively few (30) zircons, which are colourless to dark brown, anhedral to subhedral, and variably rounded. The zircons are up to 200 μm long, and equant to slightly elongate, with aspect ratios up to 4:1. All exhibit concentric zoning and some contain high-U, metamict zones.

Thirty analyses of 30 zircons are concordant to strongly discordant (Fig. 6a, Appendix 2). Fifteen analyses with discordance $>5\%$ and/or high common Pb (Group D) are not considered to provide reliable age information. The youngest analysis (Group Y) yields a $^{207}\text{Pb}^*/^{206}\text{Pb}^*$ date of 1884 ± 8 Ma (1σ), and the remaining 14 analyses (Group S)

yield $^{207}\text{Pb}^*/^{206}\text{Pb}^*$ dates of 2539–2456 Ma. Provided all analyses are of unmodified detrital zircons, the date of 1884 ± 8 Ma (1σ) for the youngest analysis represents a maximum depositional age for the sandstone. A more conservative estimate of the maximum depositional age can be based on the weighted mean $^{207}\text{Pb}^*/^{206}\text{Pb}^*$ date of 2519 ± 6 Ma (MSWD = 1.9) for the youngest coherent group of 10 analyses in Group S. The data indicate a significant age component at c. 2530 Ma, based on contributions from approximately 10 analyses (Fig. 6b).

GSWA 177279: metasandstone — Stubbins Formation

Fine-grained sandstone from the Stubbins Formation was sampled from drillcore at the Kookaburra prospect (LKD100: 133.4 – 134.6 m) (Figs 2, 5). The sandstone is massive, framework to matrix supported, with a maximum grain size of 2 mm. It consists of quartz, feldspar, muscovite, tourmaline, zircon, rare biotite and very rare pelitic clasts in a fine-grained recrystallized matrix consisting of quartz, sericite, biotite, chlorite and rare rutile. Zircons from this sample are colourless to dark brown or opaque, anhedral to subhedral, and subspherical to slightly rounded. The crystals are up to 250 μm long, and equant to elongate, with aspect ratios up to 4:1.

Eighty-seven analyses of 86 zircons are concordant to strongly discordant (Appendix 2), and the pattern of discordance suggests that Pb loss was mainly geologically recent (Fig. 6c). Fifty-two analyses with discordance $>5\%$ or high common Pb (Group D) are excluded. The youngest analysis (Group Y) yields a $^{207}\text{Pb}^*/^{206}\text{Pb}^*$ date of 1863 ± 9 Ma (1σ). The remaining 34 analyses (Group S) yield $^{207}\text{Pb}^*/^{206}\text{Pb}^*$ dates of 3422–1863 Ma. The date of 1863 ± 9 Ma (1σ) for the youngest analysis may represent a maximum depositional age for the sandstone, although a more conservative estimate can be based on the weighted mean $^{207}\text{Pb}^*/^{206}\text{Pb}^*$ date of 1874 ± 5 Ma (MSWD = 0.63) for the youngest 17 analyses in Groups Y and S. The data indicate significant age components at c. 2521, 2476 and 1872 Ma, based on contributions from approximately 4, 4 and 17 analyses, respectively (Fig. 6d).

GSWA 178809: metasandstone — Stubbins Formation

Poorly sorted metasandstone from the Stubbins Formation was collected from drillcore at the Sandpiper prospect (BLRCD001, 166.5 – 166.7 m), about 400 m to the northeast of the Kookaburra prospect (Figs 2, 5). The sandstone consists of quartz and less abundant feldspar in a matrix of sericite, chloritized biotite, quartz and feldspar, with minor tourmaline, zircon and rutile. Zircons from the metasandstone are colourless to dark brown, anhedral to euhedral, and variably rounded. The crystals are up to 250 μm long and equant to slightly elongate, with aspect ratios up to 4:1.

A total of 115 analyses of 114 zircons are concordant to strongly discordant (Appendix 2), and their distribution is consistent with the combined effects on some zircons of late Neoproterozoic and recent Pb loss (Fig. 6e). Fifty-seven analyses (Group D) are $>5\%$ discordant and/or indicate high common Pb, and analyses that yield the youngest U/Pb dates indicate high U contents (1000–4800 ppm). Excluding Group D, the youngest analysis

Table 3. Summary of isotopic ages obtained for metasedimentary and igneous rocks. All coordinates are in MGA zone 52. Abbreviations: IGN, igneous crystallization age; MAX, maximum igneous age; MDA, maximum depositional age; MIN, minimum igneous age; NT, Northern Territory; WA, Western Australia

Sample number	Longitude	Latitude	Easting	Northing	State	Lithology	Unit	Age (Ma)	n	MSWD	Interpretation	Approx. lower intercept (Ma)
GA 2004085006	129.92921	-20.53161	596873	7729413	NT	Metasandstone	Ferdies Member	2519.1 ± 6.4	10	1.9	MDA	0
GSWA 177279	128.86302	-19.59068	485634	7833807	WA	Metasandstone	Stubbins Formation	1873.5 ± 5.0	17	0.6	MDA	0
GSWA 178809	128.86537	-19.58632	485881	7834290	WA	Metasandstone	Stubbins Formation	1865.4 ± 3.1	30	0.8	MDA	700–600
GA 2004085001	129.96232	-20.56848	600301	7725313	NT	Metasandstone	Killi Killi Formation	1875.6 ± 3.5	42	1.2	MDA	0
GA 2001082009	128.82836	-19.89853	482034	7799738	WA	Metasandstone	Killi Killi Formation	1871.9 ± 5.6	16	0.8	MDA	none
GA 2001082010	129.68701	-20.02258	571856	7785872	NT	Sandstone	Gardiner Sandstone	1828 ± 19	7	1.4	MDA	0
GA 2001082516	129.24562	-19.65209	525749	7826999	NT	Sandstone	Gardiner Sandstone	1841 ± 16	9	2.5	MDA	0
GSWA 178801	128.84933	-19.59587	484199	7833232	WA	Quartzofeldspathic rock	In Stubbins Formation	1874.0 ± 2.4	35	1.1	MAX	none
GA 2001082002	128.89597	-19.86185	489108	7803803	WA	Biotite monzogranite	Lewis Granite	1807.4 ± 4.5	18	0.8	IGN	0
GA 2001082005	128.98146	-20.25877	498064	7759883	WA	Granitic rock	Lewis Granite	1802.8 ± 4.3	23	1.0	IGN	c. 400
GA 72495003	128.67768	-20.20970	466328	7765280	WA	Muscovite monzogranite	Lewis Granite	>1737 ± 11	3	0.4	MIN	600–500
GSWA 189942	128.6361	-20.12871	461965	7774234	WA	Biotite–muscovite syenogranite	Lewis Granite	<1865 ± 24	1	-	MAX	0
GSWA 189936	128.48891	-20.04286	446551	7783694	WA	Biotite–hornblende granodiorite	Lewis Granite	1800 ± 15	15	2.3	IGN	449 ± 100
GSWA 189937	128.36587	-20.01133	433670	7787139	WA	Biotite monzogranite	Lewis Granite	1788 ± 8	10	0.49	IGN	494 ± 50
GA 2001082003	128.47263	-19.79920	444764	7810653	WA	Monzogranite	Balwina Granite	<1866 ± 5	9	0.6	MAX	c. 600
GA 72490306	128.46798	-19.79860	444277	7810718	WA	Granodiorite	Balwina Granite	1804.4 ± 8.0	5	0.5	IGN	600–500
GA 2003082001	128.44402	-19.77189	441758	7813665	WA	Biotite monzogranite	Balwina Granite	1799.6 ± 5.6	6	0.4	IGN	450–350
GA 2001082004	128.47368	-19.79685	444873	7810913	WA	Granitic rock	Dyke in Balwina Granite	1794.7 ± 7.5	2	2.9	MAX	c. 650

(Group Y) yields a $^{207}\text{Pb}^*/^{206}\text{Pb}^*$ date of 1830 ± 7 Ma (1σ). The remaining 57 analyses (Group S) yield $^{207}\text{Pb}^*/^{206}\text{Pb}^*$ dates of 2876–1837 Ma. Provided all analyses are of unmodified detrital zircons, the date of 1830 ± 7 Ma (1σ) for the youngest analysis represents a maximum depositional age for the sandstone. A more conservative estimate of the maximum depositional age can be based on the weighted mean $^{207}\text{Pb}^*/^{206}\text{Pb}^*$ date of 1865 ± 3 Ma (MSWD = 0.81) for the youngest 30 analyses in Group S. The data indicate significant age components at c. 2503, 2481, 1866 and 1833 Ma, based on contributions from approximately 6, 6, 33 and 5 analyses, respectively (Fig. 6f).

GA 2004085001: metasandstone — Killi Killi Formation

A coarse-grained lithological variant of the Killi Killi Formation was sampled from outcrop in the Dead Cat Rock area, about 8 km southeast of the Callie Mine (Figs 2, 5). This sample was taken to complement a Killi Killi Formation sample studied by Cross and Crispe (2007) from the Callie Mine area, and to provide a reference with which sedimentary rocks from the western part of the orogen could be compared. The sampled rock is coarse-grained, poorly sorted metasandstone interbedded with mudstone.

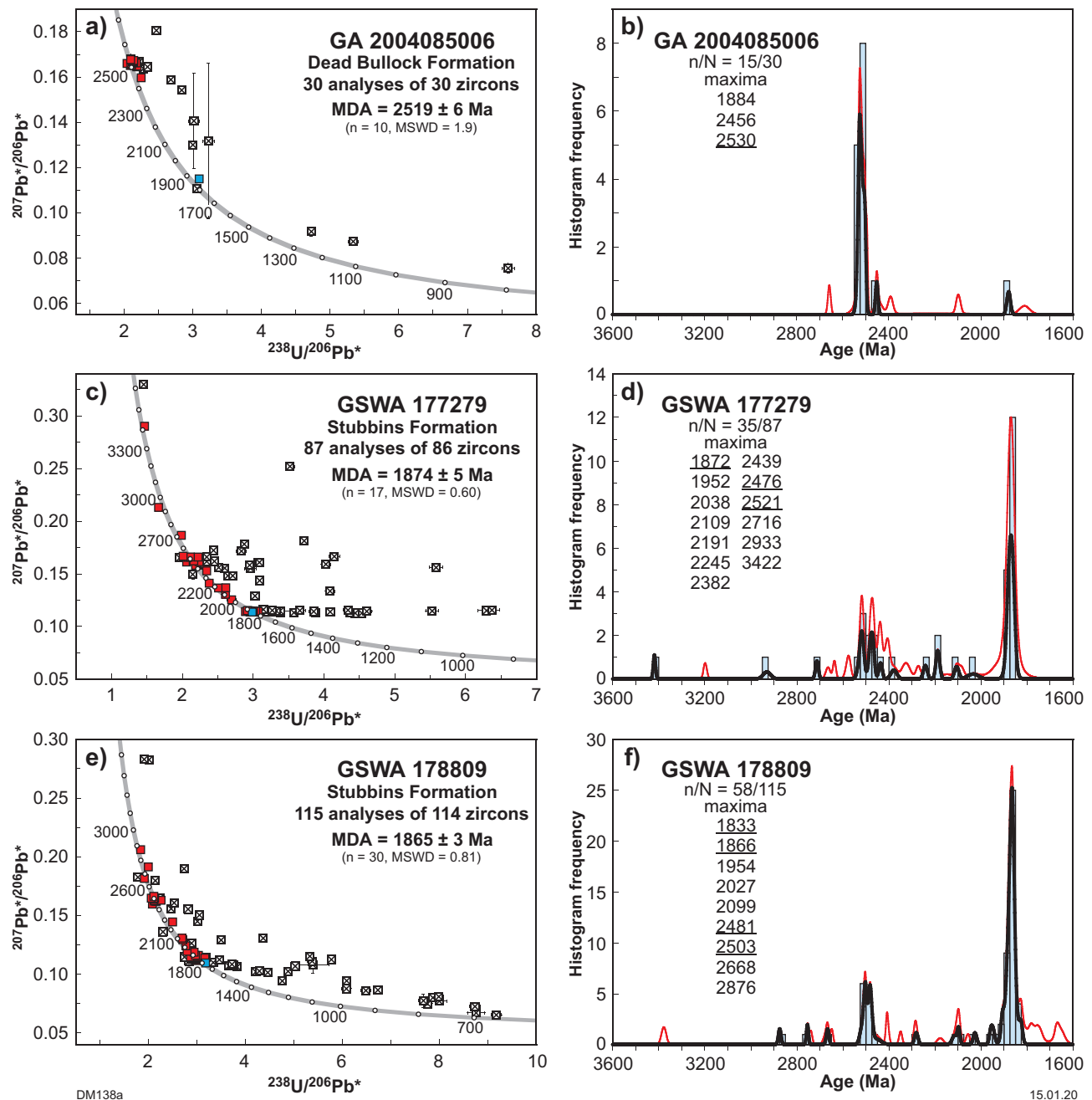


Figure 6. Concordia plots and probability density diagrams for metasedimentary rocks from the Ferdies Member of the Dead Bullock Formation (a, b) and the Stubbins Formation (c–f). Concordia plots — blue square, youngest concordant analysis; red squares, older concordant analyses; crossed squares, discordant or high common Pb analysis. Probability density plots — red line, all data; black line, accepted data; underlined maxima values are those based on three or more ages. Abbreviations: MDA, maximum depositional age; n/N, number of accepted data/total data

Zircons from this sample are pale yellow to dark brown or opaque, anhedral to euhedral, and variably rounded. The crystals are up to 250 µm long and equant to elongate, with aspect ratios up to 4:1.

Eighty-three analyses of 83 zircons are concordant to strongly discordant (Appendix 2), and the horizontal discordance trend (constant $^{207}\text{Pb}^*/^{206}\text{Pb}^*$, Fig. 7a) indicates that Pb loss was geologically recent. Excluding 32 analyses that indicate discordance >5% and/or high common Pb (Group D), the youngest (Group Y) yields a $^{207}\text{Pb}^*/^{206}\text{Pb}^*$ date of 1839 ± 9 Ma (1σ). The remaining 50 analyses (Group S) yield $^{207}\text{Pb}^*/^{206}\text{Pb}^*$ dates of 3359–1855 Ma. The date of 1839 ± 9 Ma (1σ) for the youngest analysis may represent a maximum depositional age for the sandstone, although a more conservative estimate of the maximum depositional age can be based on the weighted mean $^{207}\text{Pb}^*/^{206}\text{Pb}^*$ date of 1876 ± 4 Ma (MSWD = 1.2) for the youngest 42 analyses in Group S. The data indicate a significant age component at c. 1875 Ma, based on contributions from approximately 38 analyses (Fig. 7b).

GA 2001082009: metasandstone

— Killi Killi Formation

This sample is a metasandstone of the Killi Killi Formation, taken from drillcore at the Coyote Au deposit (CYDD15: 254.6 – 257.6 m) (Figs 2, 5). Zircons recovered from this sample are mainly colourless, anhedral to subhedral, and subspherical to slightly rounded. The crystals are up to 200 µm long and equant to elongate, with aspect ratios up to 4:1. Two splits of detrital zircons were mounted for analysis. Unsorted grains included an unacceptable number of highly metamict grains, so a split sorted for lower magnetic susceptibility (higher quality crystals) was analysed instead.

Sixty-four analyses of 64 zircons are concordant to strongly discordant (Fig. 7c, Appendix 2). Seventeen analyses are >5% discordant (Group D), and are not considered to provide reliable age information. Of the remaining 47 analyses, the youngest (Group Y) yields a $^{207}\text{Pb}^*/^{206}\text{Pb}^*$ date of 1841 ± 19 Ma (1σ), and 46 analyses (Group S) yield $^{207}\text{Pb}^*/^{206}\text{Pb}^*$ dates of 2926–1849 Ma. The date of 1841 ± 19 Ma (1σ) for the youngest analysis may represent a maximum depositional age for the sandstone, although a more conservative estimate of the maximum depositional age can be based on the weighted mean $^{207}\text{Pb}^*/^{206}\text{Pb}^*$ date of 1872 ± 6 Ma (MSWD = 0.83) for the youngest 16 analyses in Groups Y and S. The data indicate significant age components at c. 2500, 2488, 2177, 1969 and 1874 Ma, based on contributions from approximately 7, 8, 4, 3 and 16 analyses, respectively (Fig. 7d).

GA 2001082010: sandstone

— Gardiner Sandstone

The Gardiner Sandstone was sampled from the Money open pit in the Tanami Goldfield (Figs 2, 5). Zircons recovered from this sample are colourless to dark brown and Fe-staining is common. The crystals are anhedral to subhedral and variably rounded. The zircons are up to 200 µm long and equant to slightly elongate, with aspect ratios up to 4:1.

Ninety-four analyses of 89 zircons are concordant to strongly discordant (Appendix 2), and the pattern of discordance suggests that Pb loss was mainly geologically recent (Fig. 7e). Sixty-eight analyses indicate discordance >5% and/or high common Pb (Group D), and are not considered to provide reliable age information. The youngest analysis (Group Y) yields a $^{207}\text{Pb}^*/^{206}\text{Pb}^*$ date of 1727 ± 17 Ma (1σ). The remaining 25 analyses (Group S) yield $^{207}\text{Pb}^*/^{206}\text{Pb}^*$ dates of 2564–1752 Ma. Provided all analyses are of unmodified detrital zircons, the date of 1727 ± 17 Ma (1σ) for the youngest analysis represents a maximum depositional age for the sandstone. A more conservative estimate of the maximum depositional age can be based on the weighted mean $^{207}\text{Pb}^*/^{206}\text{Pb}^*$ date of 1829 ± 19 Ma (MSWD = 1.4) for the youngest coherent group of seven analyses in Group S. The data indicate significant age components at c. 2519, 1982, 1943 and 1838 Ma, based on contributions from approximately 4, 4, 3 and 6 analyses, respectively (Fig. 7f).

GA 2001082516: sandstone

— Gardiner Sandstone

The Gardiner Sandstone was sampled from the Pargee Range, about 3 km east-southeast of Mount Frederick (Figs 2, 5) where it unconformably overlies the Pargee Formation. The sample was taken about 300 m to the north-northeast of a sample of Pargee Formation reported by Cross and Crispe (2007). Zircons from the sandstone are colourless, anhedral to subhedral and mostly strongly rounded. The crystals are up to 200 µm long and mainly equant, with aspect ratios up to 3:1.

One hundred and twelve analyses of 112 zircons are concordant to strongly discordant (Appendix 2), and the pattern of discordance suggests that Pb loss was mainly geologically recent (Fig. 7g). Ninety-seven analyses indicate discordance >5% (Group D), and are not considered to provide reliable age information. Of the remaining 16 analyses, the youngest (Group Y) yields a $^{207}\text{Pb}^*/^{206}\text{Pb}^*$ date of 1811 ± 13 Ma (1σ), and 15 analyses (Group S) yield $^{207}\text{Pb}^*/^{206}\text{Pb}^*$ dates of 2530–1816 Ma. The date of 1811 ± 13 Ma (1σ) for the youngest analysis may represent a maximum depositional age for the sandstone, although a more conservative estimate of the maximum depositional age can be based on the weighted mean $^{207}\text{Pb}^*/^{206}\text{Pb}^*$ date of 1841 ± 16 Ma (MSWD = 2.5) for the youngest nine analyses in Groups Y and S. The data indicate a single significant age component at c. 1860 Ma, based on contributions from approximately eight analyses (Fig. 7h).

Igneous rocks

GSWA 178801: felsic igneous rock in Stubbins Formation

A fine-grained felsic igneous rock in the Stubbins Formation was sampled from drillcore at the Osprey prospect (LGD05: 242.2 – 242.6 m) (Figs 2, 5). The unit has sharp contacts with adjacent metasedimentary rocks and comprises quartz and feldspar phenocrysts in a weakly foliated, very fine-grained matrix consisting of intergrown quartz, feldspar and magnetite with accessory biotite, titanite and zircon.

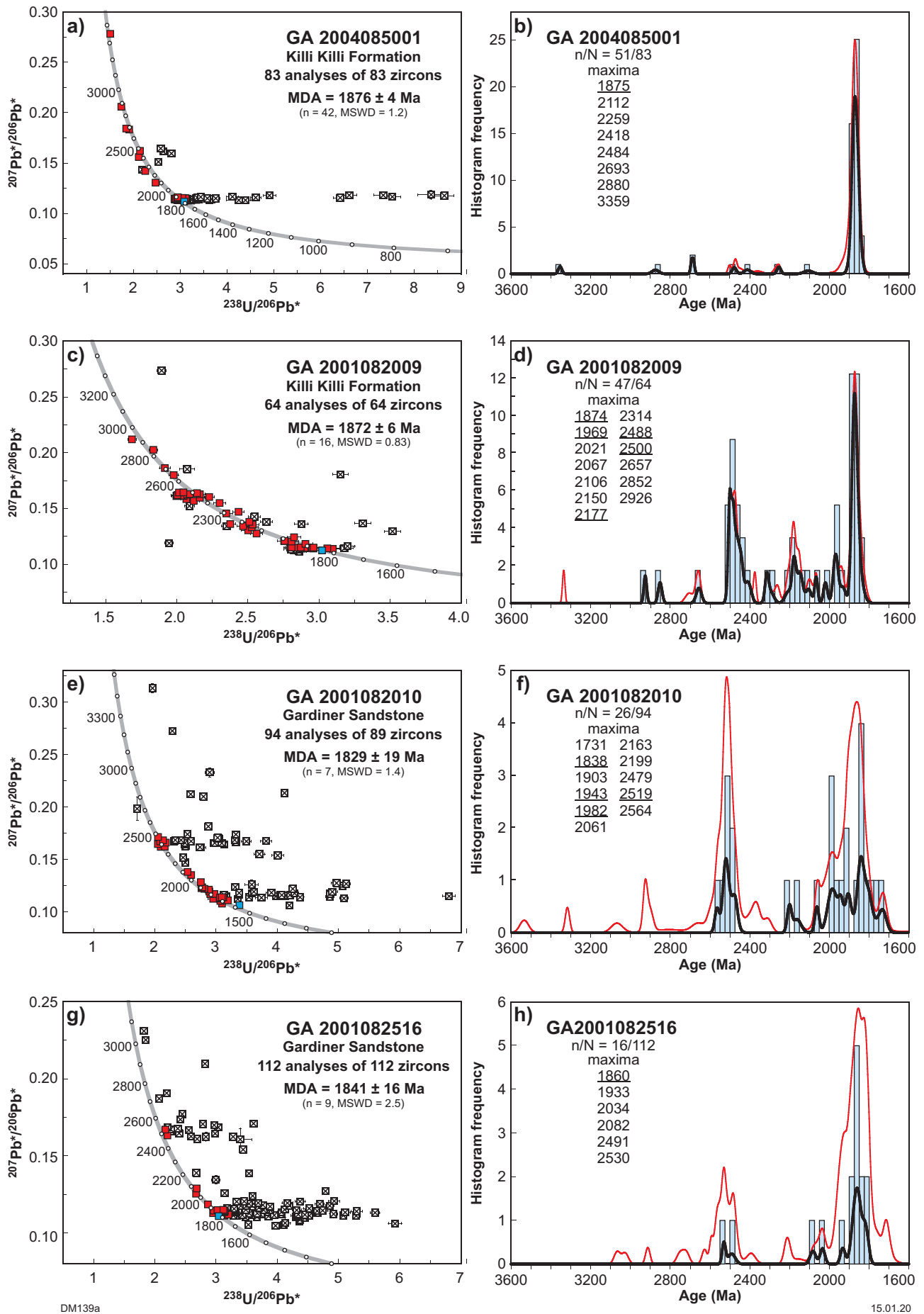
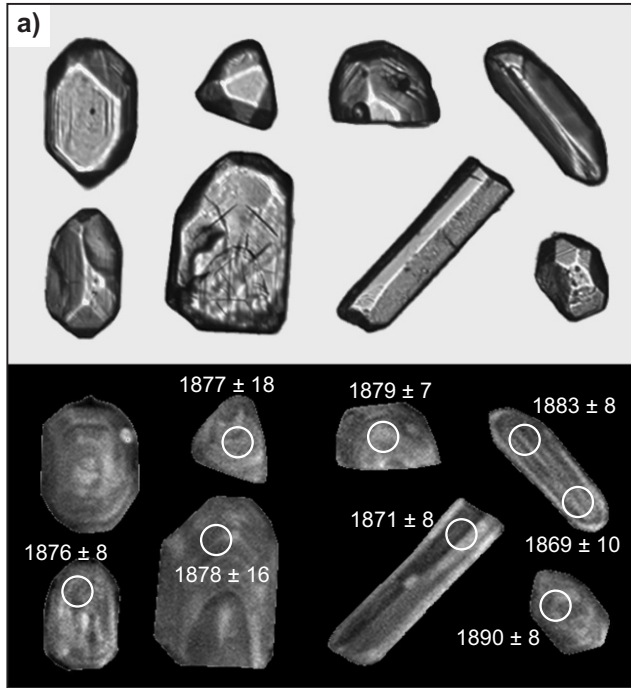


Figure 7. Concordia plots and probability density diagrams for metasedimentary rocks from the Killi Killi Formation (a–d) and Gardiner Sandstone (e–h). Other diagram features as described in Figure 6

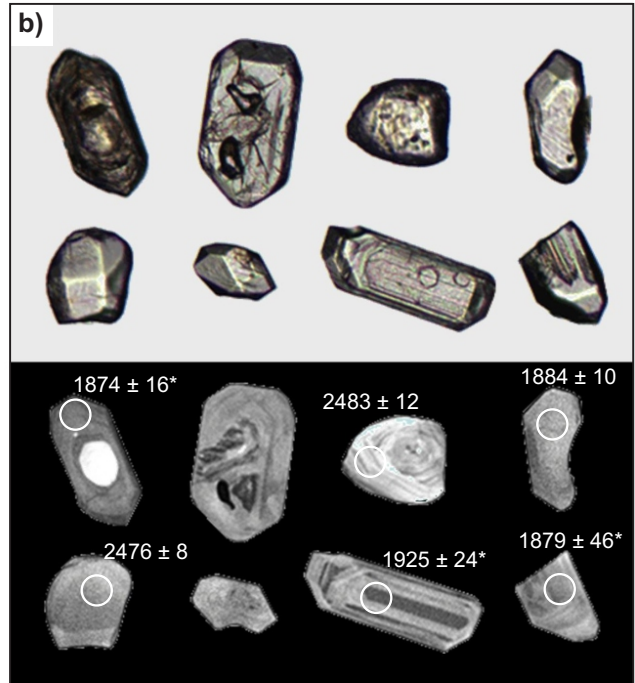
Feldspar has been altered to sericite, minor epidote, albite, calcite and Fe oxides. The rock contains a weak foliation and could be either a thin hypabyssal intrusion or a volcanic horizon. Zircons from this sample are colourless to dark brown, anhedral to euhedral and variably rounded. The crystals are up to 200 µm long and equant to elongate,

with aspect ratios up to 4:1 (Fig. 8a). Most zircons exhibit concentric zoning. The most rounded and abraded zircons were avoided during analysis, which focused on the more euhedral crystals in an attempt to define a magmatic crystallization age for this rock.

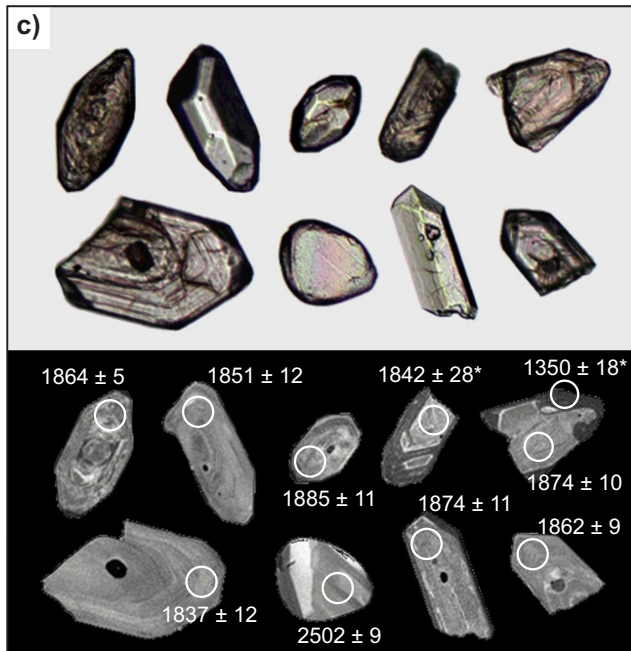
178801 felsic unit, Stubbins Formation



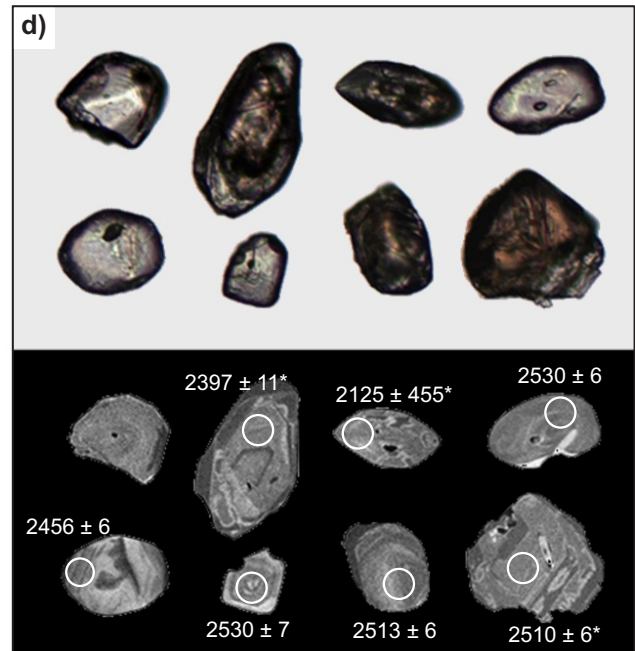
177279 sandstone, Stubbins Formation



178809 sandstone, Stubbins Formation



GA 2004085006 sandstone, Ferdies Member



DM141

50 µm

03.12.19

Figure 8. CL images of zircons, showing analysis locations and $^{207}\text{Pb}/^{206}\text{Pb}$ dates in Ma (1σ): a) euhedral to subhedral grains from felsic rock in the Stubbins Formation (GSWA 178801); b) and c) sandstones of the Stubbins Formation (GSWA 177279 and 178809); and d) sandstone from the Ferdies Member of the Dead Bullock Formation (GA 2004085006). The euhedral grains targeted in the felsic rock from the Stubbins Formation are of similar character and age (c. 1870 Ma) to the most euhedral grains in the sandstone units that host the felsic rock, and might represent xenocrysts. Detrital zircons in the Ferdies Member are considerably more rounded and yield dates of c. 2500 Ma. In most of the samples dated in this study, analyses of zircons with irregular dark-CL zones and embayments are affected by Pb loss; for example, c) and d). Asterisks indicate an analysis >5% discordant

Thirty-nine analyses of 36 zircons are concordant or only slightly discordant (Fig. 9a, Appendix 2). A dominant coherent group of 35 analyses yields a weighted mean $^{207}\text{Pb}^*/^{206}\text{Pb}^*$ date of 1874 ± 2 Ma (MSWD = 1.1). Two analyses (Group P) have $^{207}\text{Pb}^*/^{206}\text{Pb}^*$ dates of 1852 and 1835 Ma, and two analyses (Group X) have individual $^{207}\text{Pb}^*/^{206}\text{Pb}^*$ dates of c. 2302 and 2123 Ma. Interpretation of these data depends on whether the rock unit is considered to be extrusive or intrusive, and whether the zircons are considered to be inherited or magmatic. This is discussed in a later section, in context with wider considerations of Stubbins Formation correlations.

GA 2001082002: biotite monzogranite — Lewis Granite

The Lewis Granite intrudes sedimentary rocks assigned to the Killi Killi Formation and was sampled from outcrop about 8 km east-northeast of the Coyote deposit, where it forms part of a concentric zone of relatively strong magnetization (Figs 2, 5). At this locality, the Lewis Granite consists of foliated, medium-grained, equigranular to seriate quartz–K-feldspar–plagioclase–biotite monzogranite with rare mafic and fine-grained granitic xenoliths. This sample yielded zircons that are colourless and mainly euhedral. The crystals are up to 200 μm long, and mainly elongate, with aspect ratios up to 5:1. All zircons exhibit concentric zoning.

Forty analyses of 37 zircons are concordant to moderately discordant (Fig. 9b, Appendix 2). Fifteen analyses indicate discordance >5% or high common Pb (Group D), and are not considered to provide reliable age information, although the pattern of discordance indicates mainly minor recent Pb loss. Eighteen analyses (Group I) yield a weighted mean $^{207}\text{Pb}^*/^{206}\text{Pb}^*$ date of 1807 ± 5 Ma (MSWD = 0.84), interpreted as the age of igneous crystallization. Three analyses (Group X) yield $^{207}\text{Pb}^*/^{206}\text{Pb}^*$ dates of 2086–1841 Ma, interpreted as the ages of xenocrystic zircons. One analysis (Group P) indicates a $^{207}\text{Pb}^*/^{206}\text{Pb}^*$ date of 1778 ± 11 Ma, interpreted to reflect minor ancient loss of radiogenic Pb.

GA 2001082005: biotite monzogranite — Lewis Granite

A magnetic phase of the Lewis Granite was sampled in the southeastern part of the intrusive complex, about 25 km south-southeast of Coyote (Figs 2, 5). The sample consists of fine- to medium-grained, seriate, quartz–K-feldspar–plagioclase–biotite–hornblende monzogranite. The biotite grains are generally extensively chloritized, and both the K-feldspar and plagioclase grains are moderately sericitized, with the K-feldspar more intensely sericitized than the plagioclase grains. Zircons recovered from this sample are colourless and locally Fe stained. The crystals are subhedral to euhedral, and exhibit concentric zoning. The crystals are up to 250 μm long, and equant to slightly elongate, with aspect ratios up to 4:1.

Forty-one analyses of 28 zircons are concordant to strongly discordant (Fig. 9c, Appendix 2). The data suggest a poorly defined lower intercept of c. 400 Ma. Sixteen analyses indicate discordance >5% and/or

high common Pb (Group D), and are not considered to provide reliable age information. Twenty-three analyses (Group I) yield a weighted mean $^{207}\text{Pb}^*/^{206}\text{Pb}^*$ date of 1803 ± 4 Ma (MSWD = 0.96), interpreted as the age of igneous crystallization. Two analyses (Group X) yield $^{207}\text{Pb}^*/^{206}\text{Pb}^*$ dates of c. 1983 and 1839 Ma, interpreted as the ages of xenocrystic zircons.

GA 72495003: muscovite monzogranite — Lewis Granite

A large, irregularly shaped body of uniformly weak magnetization within the Lewis Granite was sampled to determine if there is a significant difference in age between this phase and a more strongly magnetized phase of this composite intrusive complex. On a magnetic image (Fig. 5), the weakly magnetized body appears to intrude the more highly magnetized phase, but there are no contact relationships exposed to confirm this. The weakly magnetized granitic phase intrudes both the Stubbins and Killi Killi Formations and gravity data suggest it extends farther to the southwest beneath the Neoproterozoic Murraba Basin.

The Lewis Granite was sampled from the Lewis Range, about 38 km west-southwest of Coyote (Figs 2, 5), where it consists of a medium-grained, unfoliated to foliated, seriate-textured quartz–K-feldspar–plagioclase–muscovite–biotite monzogranite. Zircons from the monzogranite are colourless to dark brown or opaque and subhedral to euhedral. The crystals are up to 200 μm long and mainly elongate, with aspect ratios up to 6:1. All zircons exhibit concentric zoning.

Thirty-five analyses of 32 zircons are concordant to strongly discordant (Fig. 9d, Appendix 2). Thirty analyses indicate discordance >5% or high common Pb (Group D), and are not considered to provide reliable age information. The pattern of discordance is consistent with Pb loss mainly between about 600 and 500 Ma. Of the five remaining analyses, three (Group I) yield a weighted mean $^{207}\text{Pb}^*/^{206}\text{Pb}^*$ date of 1737 ± 11 Ma (MSWD = 0.37), and two (Group X) yield a weighted mean $^{207}\text{Pb}^*/^{206}\text{Pb}^*$ date of 1884 ± 12 Ma (MSWD = 0.94). It is possible that the date of 1737 ± 11 Ma for the three younger analyses in Group I was affected by Pb loss or a younger tectonothermal event, and is thus interpreted as a minimum age for igneous crystallization. The date of 1884 ± 12 Ma for the two analyses in Group X is interpreted as the age of an inherited component.

GSA 189942: muscovite–biotite syenogranite — Lewis Granite

A sample of weakly magnetized Lewis Granite was collected from an outcrop about 27 km south of the Tanami Road and 4.0 km west of Schultz Cairn (Figs 2, 5). The sample consists of quartz, K-feldspar, plagioclase, muscovite and biotite, with minor tourmaline and apatite. Zircons from the sample are pale brown to dark brown or opaque, and subhedral to euhedral. The crystals are up to 300 μm long and equant to elongate, with aspect ratios up to 6:1. In CL images, most crystals consist of concentric zoned cores with high-U, zoned, metamict rims.

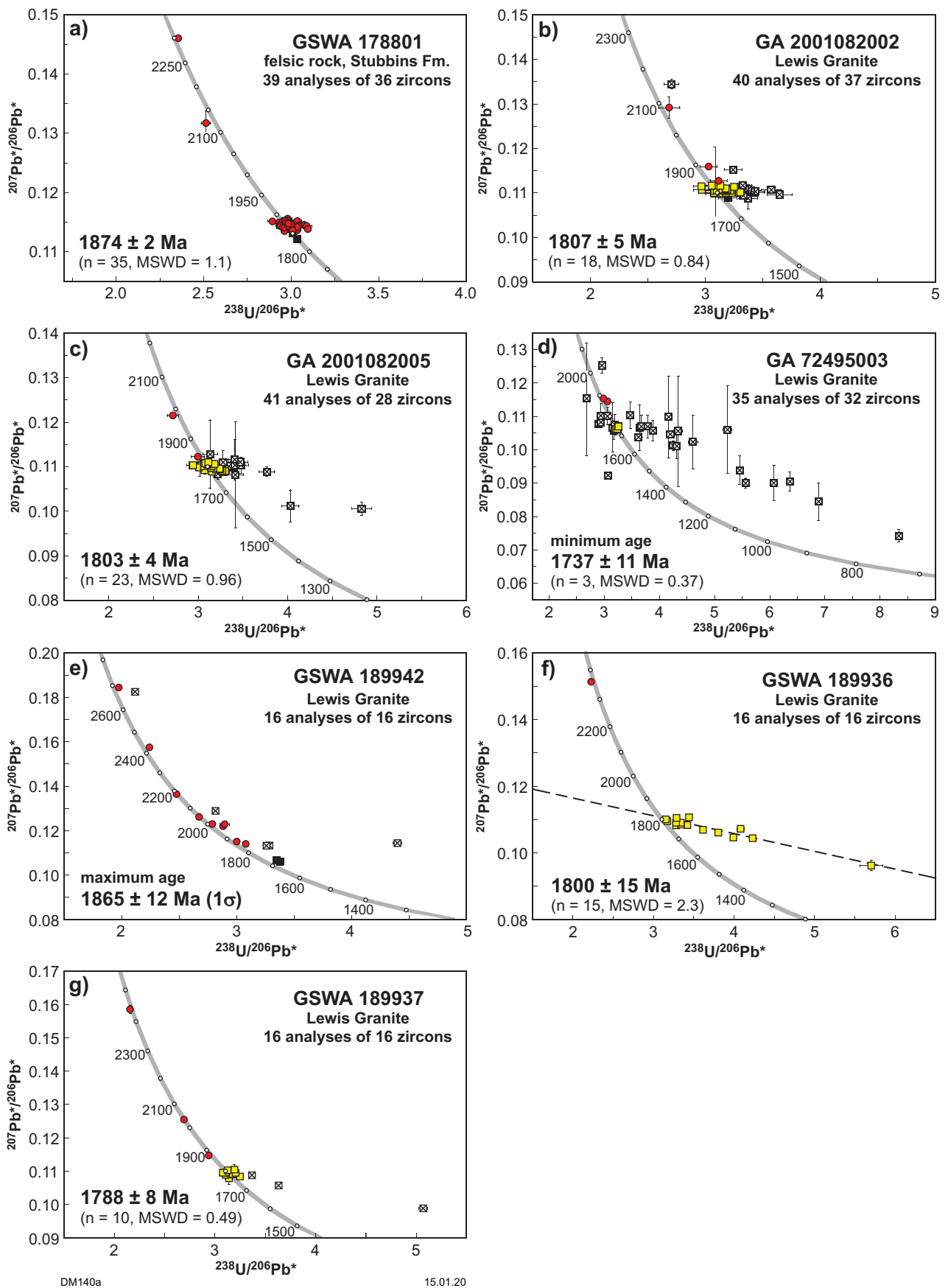


Figure 9. Concordia plots for a felsic igneous rock in the Stubbins Formation (a) and samples of the Lewis Granite (b–g). Yellow squares, analyses of igneous grains used to calculate the crystallization age; red circles, xenocrysts; black squares, radiogenic-Pb loss; crossed squares, discordance >5% or high common Pb

Sixteen analyses were obtained from 16 zircons (Fig. 9e, Appendix 2). Zircon rims could not be analysed successfully owing to their very high U and common Pb contents. Five analyses >5% discordant are not considered to be geologically significant. Nine analyses of zircon cores (Group X) yield $^{207}\text{Pb}^*/^{206}\text{Pb}^*$ dates of 2692–1865 Ma, which are interpreted to represent xenocrysts based in part on 1807–1788 Ma dates obtained for other samples of the Lewis Granite (this study; Bagas et al., 2010), with the youngest date of 1865 ± 12 Ma (1σ) representing a maximum age for the syenogranite. Two analyses of zircon cores (Group P) with dates of c. 1747 and 1735 Ma are interpreted to reflect minor ancient radiogenic-Pb loss, perhaps related to the effects of a younger tectonothermal event.

GSWA 189936: biotite–hornblende granodiorite — Lewis Granite

A sample of weakly magnetized Lewis Granite was collected from an outcrop northeast of the Lewis Range, about 21 km west-northwest of Schultz Cairn and 16.8 km south of the Tanami Road (Figs 2, 5). The sample is medium to coarse grained, consisting of plagioclase, quartz, biotite, K-feldspar, allanite, epidote and hornblende, with minor titanite, apatite and zircon. Some biotite is altered to chlorite or contains cleavage-parallel laminae of epidote or prehnite, consistent with low-temperature alteration. Zircons from the sample are pale to dark brown or opaque, and subhedral to euhedral. The crystals are up to 500 μm long and elongate, with aspect ratios up to 8:1. In CL images, concentric zoning is ubiquitous, and many crystals contain high-U, metamict domains.

Sixteen analyses were obtained from 16 zircons (Fig. 9f, Appendix 2). The analyses are concordant to highly discordant. One analysis indicates a date of c. 2361 Ma, interpreted as the age of an inherited zircon. Fifteen analyses (Group I) yield a discordia regression (MSWD = 2.3) with intercepts at 1800 ± 15 Ma and 449 ± 100 Ma. The upper intercept is interpreted as the magmatic age of the granite, whereas the lower intercept is interpreted to reflect the age of low-temperature radiogenic-Pb loss.

GSWA 189937: biotite monzogranite — Lewis Granite

A sample of weakly magnetized Lewis Granite was collected from an outcrop northeast of the Lewis Range, about 35 km west-northwest of Schultz Cairn and 13.4 km south of the Tanami Road (Figs 2, 5). The sample is medium grained, consisting of quartz, plagioclase, K-feldspar and biotite, with accessory apatite, titanite and zircon. Biotite is locally replaced by chlorite and epidote and appears to have undergone low-temperature alteration at greenschist facies conditions. Zircons from the sample are pale brown to dark brown, and subhedral to euhedral. The crystals are up to 500 μm long and elongate, with aspect ratios up to 8:1. In CL images, concentric zoning is ubiquitous, and many crystals contain high-U, metamict domains.

Sixteen analyses were obtained from 16 zircons (Fig. 9g, Appendix 2). Three analyses are >5% discordant and do

not constrain the age of the monzogranite. Three analyses (Group X) yield $^{207}\text{Pb}^*/^{206}\text{Pb}^*$ dates of 2440–1875 Ma and are interpreted as the ages of inherited zircons. Ten analyses (Group I) yield a weighted mean $^{207}\text{Pb}^*/^{206}\text{Pb}^*$ date of 1788 ± 8 Ma (MSWD = 0.49), which is interpreted as a magmatic age. A discordia regression through 13 analyses in Groups I and D yields a lower intercept of 494 ± 50 Ma (MSWD = 0.87), which is interpreted as the age of low-temperature radiogenic-Pb loss.

GA 2001082003: monzogranite — Balwina Granite

The Balwina Granite forms a 9×5 km ovoid intrusion about 39 km west-northwest of Coyote (Fig. 2). In magnetic imagery, the intrusion forms a zone of moderate magnetization that is mantled by a narrow zone of strong magnetization that appears to reflect contact metamorphism of metasedimentary rocks of the Killi Killi Formation (Fig. 5). The sampled outcrops consist of seriate-textured, medium-grained quartz–plagioclase–K-feldspar–biotite monzogranite with rare biotite-rich xenoliths. Zircons separated from this sample are colourless to pale brown, subhedral to euhedral and exhibit concentric zoning. The crystals are up to 400 μm long and mainly elongate, with aspect ratios up to 9:1.

Forty-seven analyses of 29 zircons are concordant to strongly discordant (Fig. 10a, Appendix 2), and many of the discordant analyses indicate high U concentrations (up to 2800 ppm, Appendix 2). Thirty-five analyses are >5% discordant and/or indicate high common Pb (Group D). A discordia regression through 40 data points <1900 Ma and normally discordant, yields concordia intercepts of 1867 ± 9 and 604 ± 49 Ma (MSWD = 1.3). Nine analyses with discordance <5% and low common Pb yield a concordia age of 1866 ± 5 Ma (MSWD = 0.64). Although this date could be interpreted as the age of igneous crystallization, significantly younger dates obtained from other samples of the Balwina Granite (see below) suggest this date more likely reflects inheritance. Two analyses yield $^{207}\text{Pb}^*/^{206}\text{Pb}^*$ dates of 2485 and 2440 Ma, interpreted as the ages of older xenocrystic zircons. One analysis (Group P) indicates a $^{207}\text{Pb}^*/^{206}\text{Pb}^*$ date of 1826 ± 16 Ma, interpreted to reflect minor ancient loss of radiogenic Pb.

GA 72490306: biotite granodiorite — Balwina Granite

A sample of the Balwina Granite taken about 500 m west of sample GA 2001082003 (Figs 2, 5) was analysed to provide a more robust constraint on the timing of igneous crystallization. The sampled rock is a medium-grained, seriate-textured quartz–plagioclase–K-feldspar–biotite granodiorite that is intruded by aplite dykes. Zircons from this sample are colourless to dark brown or opaque, and anhedral to euhedral. The crystals are up to 400 μm long and mainly elongate, with aspect ratios up to 8:1. All zircons exhibit concentric zoning and some crystals contain high-U, metamict zones.

Thirty-eight analyses of 37 zircons are concordant to strongly discordant (Appendix 2), and the data are consistent with Pb loss at 600–500 Ma (Fig. 10b). Twenty-eight analyses are >5% discordant and/or indicate high common Pb (Group D).

Five analyses with discordance <5% and low common Pb (Group I) yield a weighted mean $^{207}\text{Pb}^*/^{206}\text{Pb}^*$ date of 1804 ± 8 Ma (MSWD = 0.49), interpreted as the age of igneous crystallization. Five analyses (Group X) yield $^{207}\text{Pb}^*/^{206}\text{Pb}^*$ dates of 2494–1857 Ma, interpreted as the ages of inherited components. The four youngest analyses in Group X form a single group with a weighted mean $^{207}\text{Pb}^*/^{206}\text{Pb}^*$ date of 1864 ± 8 Ma (MSWD = 0.95), which is similar to the youngest age component of sample GA 2001082003 of the Balwina Granite, supporting the interpretation that this age component reflects zircon inheritance.

GA 2003082001: biotite monzogranite — Balwina Granite

The Balwina Granite was also sampled from an area in the northwestern margin of the intrusion, about 4 km northwest of the other dated samples (Figs 2, 5), where it consists of grey, medium-grained, equigranular to seriate-textured quartz–plagioclase–K-feldspar–biotite monzogranite. Zircons from this sample are colourless to dark brown and anhedral to euhedral. The crystals are up to 200 μm long, and equant to elongate, with aspect ratios up to 5:1. All zircons exhibit concentric zoning, and some crystals contain high-U, metamict zones.

Forty-four analyses of 41 zircons are concordant to strongly discordant (Fig. 10c, Appendix 2). Thirty-six analyses are >5% discordant and/or indicate high common Pb (Group D). A discordia regression through normally discordant data <1850 Ma yields concordia

intercepts of 1807 ± 8 and 369 ± 88 Ma (MSWD = 0.87). Six analyses with discordance <5% and low common Pb (Group I) yield a weighted mean $^{207}\text{Pb}^*/^{206}\text{Pb}^*$ date of 1800 ± 6 Ma (MSWD = 0.35), interpreted as the age of igneous crystallization, and indistinguishable from the 1804 ± 8 Ma date obtained from the southeastern part of the intrusion. Two analyses (Group X) yield $^{207}\text{Pb}^*/^{206}\text{Pb}^*$ dates of 2487 and 2268 Ma, interpreted as the ages of xenocrystic zircons.

GA 2001082004: aplitic muscovite syenogranite dyke in Balwina Granite

A 30 cm-wide felsic dyke that intrudes the Balwina Granite was sampled from the area of sample GA 2001082003 to provide constraints on the age of magmatism (Figs 2, 5). This rock is fine-grained, aplitic quartz–K-feldspar (mostly microcline)–plagioclase–muscovite syenogranite. The rock is relatively fresh with only weak sericite dusting of the feldspars. Zircons from this sample are colourless to dark brown or opaque, and subhedral to euhedral. The crystals are up to 250 μm long and equant to elongate, with aspect ratios up to 5:1. Most zircons exhibit concentric zoning and some crystals contain high-U, metamict zones. Nearly all grains have fractures and limonite staining.

Forty-seven analyses of 37 zircons are concordant to strongly discordant (Fig. 10d), and many of the discordant analyses indicate high U concentrations (up to 1800 ppm, Appendix 2). Thirty-three analyses are >5% discordant

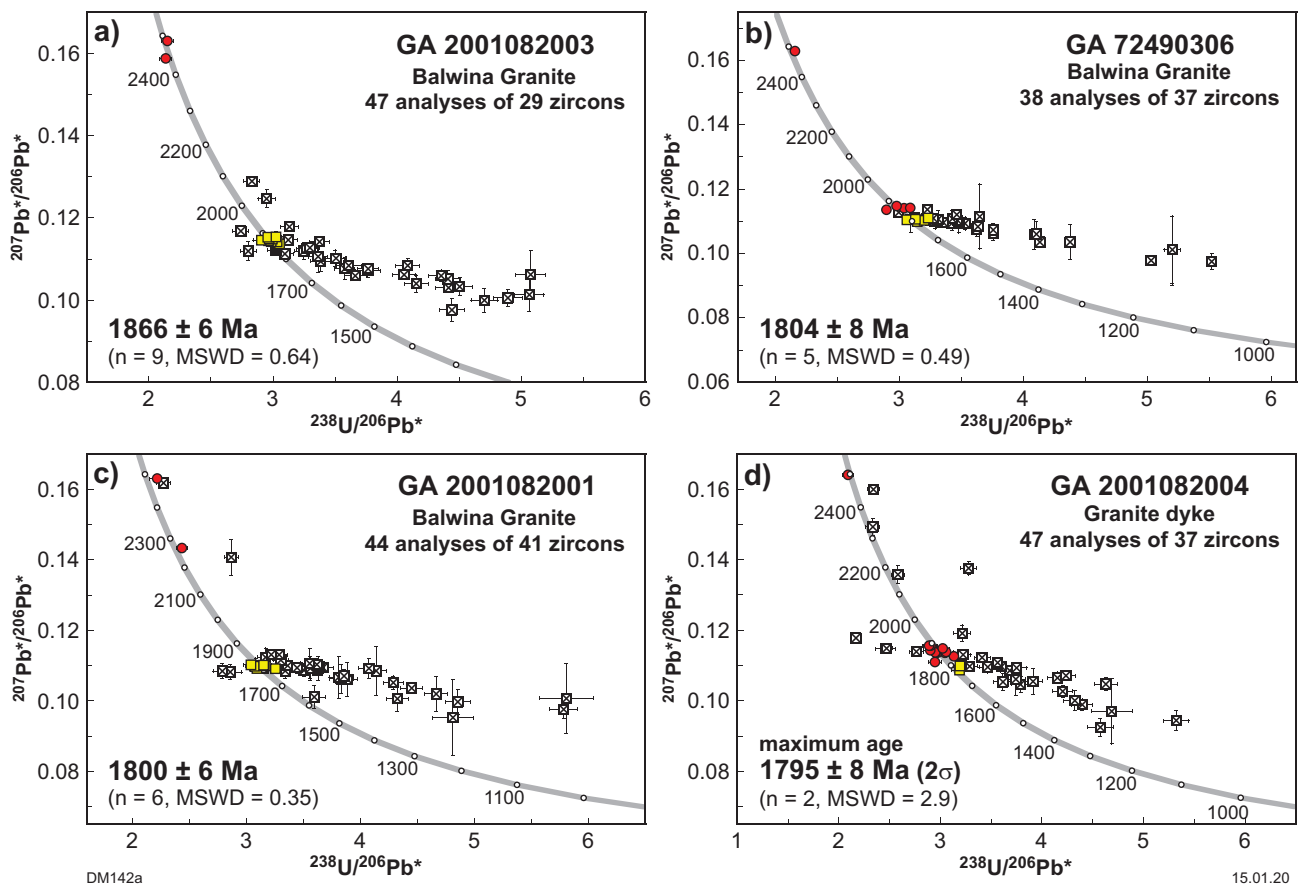


Figure 10. Concordia plots for samples of the Balwina Granite (a–c) and a felsic dyke in the Balwina Granite (d). Diagram features as described in Figure 9

and/or indicate high common Pb (Group D), and the pattern of discordance suggests that Pb loss occurred at about 700–600 Ma. Twelve analyses with discordance <5% and low common Pb (Group X) yield $^{207}\text{Pb}^*/^{206}\text{Pb}^*$ dates of 2497–1815 Ma, interpreted as the ages of inherited zircons. Two analyses (Group I) yield $^{207}\text{Pb}^*/^{206}\text{Pb}^*$ dates (1σ) of 1797 ± 4 and 1778 ± 11 Ma, with a mean of 1795 ± 8 Ma (2σ , MSWD = 2.9). This result is indistinguishable from the age of the host granite, indicating that either the dyke and granite are similar in age, or the zircons were inherited from the granite. The dyke is therefore assigned a maximum crystallization age of 1795 ± 8 Ma.

Discussion

Depositional age and provenance of the Tanami Group

Dead Bullock Formation

The depositional age of the Dead Bullock Formation remains imprecisely constrained. An 1844 ± 4 Ma date for the Inspiration Peak Monzogranite that intrudes the Dead Bullock Formation (Smith, 2001) has been taken as a minimum age for this unit. However, a second sample of the monzogranite from the 9.3 m interval of drillcore sampled by Smith (2001) yields a significantly younger date of 1802 ± 14 Ma (Iaccheri, 2019). The sampled interval of monzogranite is relatively homogeneous (Vandenberg et al., 2014), suggesting that both samples were from the same intrusive phase, but it remains uncertain which of these dates represents the magmatic crystallization age. A more robust minimum age constraint is provided by an 1839 ± 9 Ma date for metamorphic monazite in the Dead Bullock Formation (Petrella et al., 2019). Similar, but less precise minimum ages for the Dead Bullock Formation are provided by $^{40}\text{Ar}/^{39}\text{Ar}$ hornblende dates of 1840 ± 14 and 1840 ± 19 Ma obtained from metamorphosed mafic intrusive rocks within the unit (Li et al., 2014).

A stratigraphic age of 1838 ± 6 Ma was inferred by Cross and Crispe (2007) on the basis of a date from a feldspathic unit ~20 km northeast of the Tanami Goldfield, interpreted as a tuff within the Callie Member. Bagas et al. (2014) suggested that this date could instead represent the age of a felsic igneous intrusion, and thus should be considered as a minimum age for the host sedimentary rocks. The c. 1838 Ma date is also indistinguishable from the c. 1839 Ma date for metamorphic monazite formed during the Tanami Event, which would allow little time for deposition of the ~4 km-thick Killi Killi Formation that overlies the Dead Bullock Formation. The geological meaning of this date thus remains open to question, with uncertainties about the nature of the dated rock compounded by uncertainty regarding the stratigraphic position of the sedimentary host rocks. Metasedimentary rocks in this area have been assigned to the lower Killi Killi Formation by some workers (Ahmad and Scrimgeour, 2006; Ahmad et al., 2013b), and directly overlie magnetic units that appear to be an along-strike continuation of the Mount Charles Formation to the southwest.

Maximum age constraints for the Dead Bullock Formation are also equivocal because, with the possible exception of the Ferdies Member sample reported here, detrital zircons have yielded exclusively Archean ages. Two samples assigned to the Ferdies Member by Cross and Crispe (2007) include a feldspathic arenite in the southern part of the province with a range of Archean to early Paleoproterozoic detrital ages at 3235–3130, 2820–2740, 2710–2660 and 2560–2435 Ma; and a sample of arkosic conglomerate from the Groundrush deposit in the northern part of the province is dominated by an essentially unimodal age component at 2533 ± 3 Ma. However, it should be noted that Bagas et al. (2014) suggested that the unit sampled at Groundrush could be assigned to the uppermost part of the Callie Member on the basis of lithofacies associations. The sample of the Ferdies Member reported here (GA 2004085006) is also dominated by Neoproterozoic ages at c. 2519 Ma, but a single near-concordant zircon age at 1884 ± 8 Ma (1σ) is also present (Fig. 6a). This single zircon analysis provides the only direct age constraint placing deposition of the Ferdies Member as part of the Tanami Group rather than Archean basement, albeit a single analysis may not be a robust constraint. The conformable and transitional relationship between the Dead Bullock and Killi Killi Formations (Bagas et al., 2014) is also consistent with this interpretation.

The detrital zircon ages obtained for the Ferdies Member indicate that the ultimate sources of sediment for at least the lower part of the Dead Bullock Formation were dominantly Archean in age, considerably older than the inferred depositional age of this unit. This is consistent with published whole-rock Sm–Nd isotope data, which indicate that the Ferdies Member has a highly evolved isotope signature (Lambeck et al., 2010). Detrital zircon age components obtained from the Ferdies Member are similar to 2550–2510 Ma magmatic and inherited zircon ages obtained from Neoproterozoic basement rocks in the Billabong Complex (Kositcin et al., 2013a), suggesting that local basement rocks might have been a source of detritus. More distant sources are also possible, given that a significant age component at 2545–2510 Ma has also been identified in basement rocks of the Pine Creek Orogen (Cross et al., 2005b; Worden et al., 2006b; Hollis et al., 2009a). The ultimate sources of older Neoproterozoic to Mesoproterozoic zircons in the Ferdies Member sample from the southern part of the orogen dated by Cross and Crispe (2007) are unclear, with no rocks of this age recognized from the limited basement exposures within the North Australian Craton.

Stubbins Formation

Zircon data for a felsic igneous unit within the Stubbins Formation at the Osprey prospect (Fig. 5; GSWA 178801) include a dominant age component at 1874.0 ± 2.4 Ma and two younger individual zircon dates of 1852 ± 8 and 1835 ± 9 Ma (1σ). The 1874 ± 2 Ma date supersedes an earlier citation of a preliminary 1864 ± 3 Ma date by Bagas et al. (2008) and subsequent papers. The dominant age component is indistinguishable from the youngest detrital age component of 1874 ± 5 Ma in a Stubbins Formation sandstone from the Kookaburra prospect (GSWA 172279), and older than the 1865 ± 3 Ma detrital age component in a Stubbins Formation sandstone from the Sandpiper prospect

(GSWA 178809). The age spectra in the two Stubbins Formation sandstones are distinct from those of the Ferdies Member of the Dead Bullock Formation in containing this dominant Paleoproterozoic detrital age component, together with subordinate Archean detritus.

Bagas et al. (2008) interpreted the felsic meta-igneous unit as a volcanic horizon and the dominant c. 1874 Ma zircon age component (formerly cited as c. 1864 Ma) as its magmatic age, and thus the age of stratigraphic emplacement. However, noting the ages of detrital zircons in the host rock, it is possible that the c. 1874 Ma age represents zircon inheritance in an extrusive or hypabyssal intrusive rock that contains little or no magmatic zircon. There are other examples of felsic igneous units in the orogen lacking magmatic zircon that may support this interpretation. Another felsic unit within the Stubbins Formation sampled about 2.5 km to the northeast (GSWA 178834; drillhole LHD079: 151.8 – 152.5 m; MGA 485827 7835223, Zone 52) yielded only three anhedral zircon grains that were not dated because their form indicates xenocrysts in a rock with no magmatic zircon. Two other samples of felsic dykes intruding the Tanami Group have yielded only xenocrystic zircon (Smith, 2001). In this Report, the four dated samples of Balwina Granite indicate significant Paleoproterozoic zircon inheritance, and sample GA 2001082003 was found to contain no magmatic age component among 29 dated zircons. Although relatively euhedral zircons are present in the Stubbins Formation felsic unit (Fig. 8a), these are comparable in form to euhedral detrital zircons in Stubbins Formation sandstones (Fig. 8b,c). Given this context, the c. 1874 Ma age component in the felsic unit at the Osprey prospect is here more conservatively interpreted as a maximum age for the unit, rather than a magmatic or stratigraphic age. With these reservations, the most direct constraint on the age of the Stubbins Formation is the c. 1865 Ma maximum depositional age provided by sandstone sample GSWA 178809 in the upper part of the succession. Regional correlations of the Stubbins Formation, discussed below, imply that this is close to the deposition age.

Killi Killi Formation

Detrital zircon age spectra for the Killi Killi Formation obtained in this study are similar to those obtained for other samples of the unit, and comparable to those of the Stubbins Formation (Fig. 7b,d). The sample from the Dead Cat Rock area in the Northern Territory (GA 2004085001) has a dominant age component at 1876 ± 4 Ma, which forms a maximum depositional age, as well as a small number of older Paleoproterozoic to Archean grains. The sample from the Coyote prospect (GA 2001082009) has a dominant age component at 1872 ± 6 Ma and subsidiary age components at 2500–2400 Ma and 2200–2150 Ma. The youngest age component in this sample is within analytical uncertainty of that from another sample of the Killi Killi Formation from the Coyote prospect with a maximum depositional age of 1864 ± 6 Ma reported by Bagas et al. (2009). Detrital zircon dating of samples of the Killi Killi Formation from several locations in the Northern Territory by Cross and Crispe (2007) yielded similar dominant youngest detrital age components at c. 1868, 1867, 1866 and 1864 Ma, and subsidiary age components at c. 2500 Ma.

Taken together, the detrital zircon ages for the Killi Killi Formation indicate deposition took place at or after 1876–1864 Ma. Minimum age constraints for the unit are provided by the c. 1840 Ma Tanami Event and the overlying 1824–1815 Ma Ware Group.

Changes in provenance within the Tanami Group

The detrital zircon age spectra for metasedimentary rocks of the Tanami Group indicate a dominance of Archean detritus in the lower Dead Bullock Formation, and a dominant Paleoproterozoic 1870–1865 Ma age component with a subordinate c. 2500 Ma age component in the overlying Killi Killi Formation. The onset and nature of the transition between these two provenance signatures is uncertain due to a paucity of analysed samples from the upper Dead Bullock Formation, but appears to have taken place during deposition of this unit, if the correlation of the Stubbins Formation with the Dead Bullock Formation of Bagas et al. (2014) is valid (see discussion below). Inference depends in part on this, and other, correlations of geographically separated areas of Tanami Province sedimentary rocks, including those units at the Groundrush deposit dominated by 2500 Ma zircons that were assigned to the Ferdies Member by Cross and Crispe (2007), which Bagas et al. (2014) correlate instead with the top of the Dead Bullock Formation.

Two possible scenarios can be considered:

1. A single major shift in provenance from a dominance of Archean basement sources to sources that provided abundant detritus from 1870–1865 Ma granitic rocks.
2. A more complex transition, involving switches between such sources, and/or spatial variations in provenance.

The nature of this distinctive provenance shift has implications for correlating units that are separated from areas of well-defined stratigraphy by faulting or sedimentary cover, such as the Mount Charles and Stubbins Formations.

Whole-rock geochemistry in conjunction with detrital zircon studies provides a way to assess provenance changes in the Tanami Group (Lambeck et al., 2008, 2010). In a composite stratigraphic section of Dead Bullock Soak goldfield, Th/Sc and Cr/Th ratios (Fig. 11) show relatively consistent character and trends that reflect the relative proportions of felsic and mafic detritus (Lambeck et al., 2008). These data show that the Ferdies Member and the lower part of the Callie Member have consistently lower Th/Sc and higher Cr/Th ratios than the upper parts of the succession, reflecting a change from a mafic–felsic provenance to more felsic-dominated sources. This compositional distinction is also reflected in REE patterns, which show that the lower part of the succession has depleted LREE relative to Post-Archean Average Australian Shales (PAAS; Taylor and McLennan, 1985), whereas the upper part shows either no depletion of LREE, or slight enrichment (Lambeck et al., 2008, 2010).

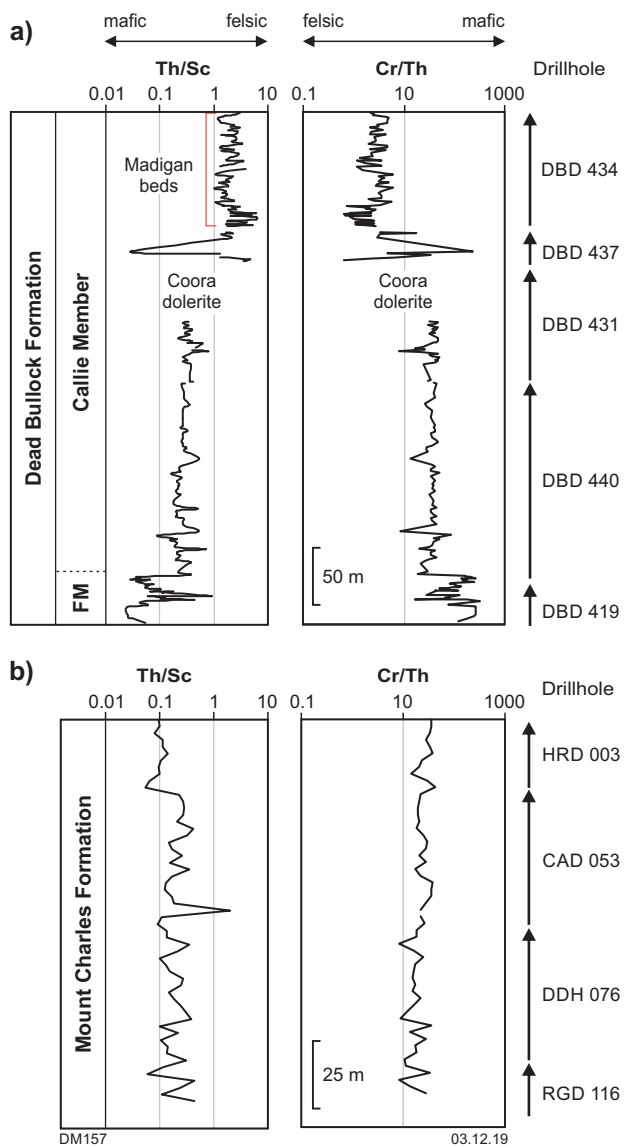


Figure 11. Whole-rock Th/Sc and Cr/Th ratios of metasedimentary rocks of the lower Tanami Group (after Lambeck et al., 2010), forming a composite log constructed from drillcore at: a) the Dead Bullock Soak goldfield; b) the Tanami Goldfield. Abbreviation: FM, Ferdies Member

The uppermost part of the succession analysed by Lambeck et al. (2008) in the Dead Bullock Soak goldfield comprises the informally named Madigan beds, a package of interlayered siltstone and greywacke that includes Fe-rich and graphitic units as well as chert bands and nodules (Smith et al., 1998). This unit represents a transition from a generally fine-grained metasedimentary succession containing Fe-rich, graphitic and chert-bearing layers in the informal Schist Hills Iron member (SHIM) of the Callie Member to fine- to medium-grained sandstones and siltstones of the overlying Killi Killi Formation. The Madigan beds were assigned by Crispe et al. (2007) and Lambeck et al. (2008) to the lowermost Killi Killi Formation, but Bagas et al. (2014) and Pendergast et al. (2017) favoured their inclusion within the uppermost Dead Bullock Formation on the basis of the presence of Fe-rich lithologies and chert. The whole-rock

geochemical data suggest that the main change in provenance took place before deposition of the Madigan beds, which has a relatively uniform geochemical signature consistent with the Killi Killi Formation elsewhere in the orogen (Fig. 12; Lambeck et al., 2010). Units in the uppermost Callie Member beneath the Madigan beds have a less regular geochemical signature, with significant deviations from what appears to be a baseline that is consistent with the Madigan beds. These units might, therefore, represent a brief transitional phase between the two provenance signatures. A mafic sill, the Coora dolerite, intrudes the succession beneath these units, and the succession beneath the sill is characterized by the more mafic-rich provenance signature.

The main change in sediment provenance defined by geochemistry thus occurs between the middle and upper parts of the Dead Bullock Formation. This stratigraphic position is towards the top of an aggradational sedimentary package, which transitions into a progradational package represented by the Killi Killi Formation (Lambeck et al., 2008). The change in geochemistry appears to be directly related to the change in the detrital zircon provenance signature, and the relatively narrow transitional zone between the two provenance signatures makes this a useful marker horizon for regional stratigraphic correlations.

On the basis of the above summary, units with dominantly Archean zircon age components and a significant mafic source component are likely to be part of the Dead Bullock Formation, rather than the Killi Killi Formation or a younger succession. It is possible that detritus was derived from Archean basement rocks at the margins of the basin rather than local sources within the basin, given the apparent lack of systematic facies variations in the Granites–Tanami Orogen that might indicate there were local emergent basement highs. This would be consistent with the generally well-rounded nature of Archean detrital zircons in the samples dated (Cross and Crispe, 2007). Units with a more felsic sediment source and a dominant Paleoproterozoic detrital zircon age component are consistent with the uppermost Callie Member or the overlying Killi Killi Formation, with the abundance of associated Fe-rich, graphitic or cherty metasedimentary rocks distinguishing between the two possibilities.

Possible correlations with the Halls Creek Group, Kimberley region

The timing of the change in provenance within the Tanami Group may be constrained by comparison with the similar-age Halls Creek Group in the Eastern Zone of the Lamboo Province, northwest of the Granites–Tanami Orogen (Figs 13, 14). In this area, dated felsic volcanic rocks provide time markers within a succession that is similar to the Tanami Group in terms of age, lithofacies, detrital zircon provenance and estimated thickness (Phillips et al., 2016). The lowermost units in these successions (Kairos member and Saunders Creek Formation) are relatively coarse grained, and transition into fining-upwards packages of thin-bedded to laminated, sediment-starved metasedimentary units that include chemical sediments (Ferdies Member to the lower to

middle Callie Member, and Brim Rockhole Formation). The fine-grained package is considerably thicker in the Tanami Group, which may indicate the presence of a depocentre in the Granites–Tanami Orogen (Lambeck et al., 2012). A progradational package of greywacke in the upper Callie Member (Madigan beds) is comparable to similar metasedimentary rocks in the Biscay Formation, and both successions transition into a thick (3–4 km), relatively homogeneous package of compositionally immature turbiditic sandstones and shales (Killi Killi and Olympio Formations).

The Saunders Creek and Brim Rockhole Formations contain a range of detrital zircon age components between c. 3600 and 2500 Ma, with one sample containing a c. 1909 Ma age component, similar to the age components obtained from units in the lower Dead Bullock and Mount Charles Formations. A felsic volcanic unit within the Brim Rockhole Formation is dated at 1881 ± 4 Ma (Phillips et al., 2016). The overlying metasedimentary units of the Biscay and Olympio Formations contain relatively uniform detrital zircon age signatures, comprising a dominant age component at 1860–1835 Ma and a minor component at c. 2500 Ma, similar to that of the Killi Killi and upper Stubbins Formations. The oldest felsic volcanic rock within the Olympio Formation has an age of 1856 ± 6 Ma, thereby constraining the main change in provenance signatures to between c. 1881 and 1856 Ma.

More detailed comparison of the Tanami and Halls Creek Groups may also provide information about the depositional age range of the Killi Killi Formation, which is not tightly constrained by geochronological data. The most likely correlative of the Killi Killi Formation in the Halls Creek Group, the Olympio Formation, contains felsic volcanic units dated at 1856 ± 6 and 1846 ± 4 Ma, and youngest detrital zircon age components of 1874–1857 Ma (Phillips et al., 2016). These detrital zircon age components are similar to those obtained from the Killi Killi Formation, which range from c. 1876 to 1864 Ma (Cross and Crispe, 2007; this study), though the youngest age components from the Olympio Formation range slightly younger. The uppermost parts of the Olympio Formation contain similar age components to the underlying units, but also incorporate a component of slightly younger ages at 1848 ± 5 and 1834 ± 8 Ma, which may reflect input from felsic igneous rocks in the area (Phillips et al., 2016).

Comparison between the Halls Creek and Tanami Groups thus suggests that deposition of the Killi Killi Formation could have commenced shortly before 1856 ± 6 Ma, the age of the felsic volcanic unit near the base of the Olympio Formation. Deposition of this relatively thick package may have continued to c. 1846 Ma, or younger, the age of the youngest volcanic unit in the Olympio Formation. The absence of c. 1846 and 1834 Ma age components in the dated samples of Killi Killi Formation might indicate that deposition did not continue as late as the uppermost Olympio Formation; however, this could instead reflect the localized occurrence of felsic igneous rocks of suitable age in the Halls Creek Orogen, and remains an open question. The depositional age of the Killi Killi Formation is thus inferred to overlap with deposition of the lower to middle Olympio Formation (i.e. approximately 1860–1845 Ma), with a possibility

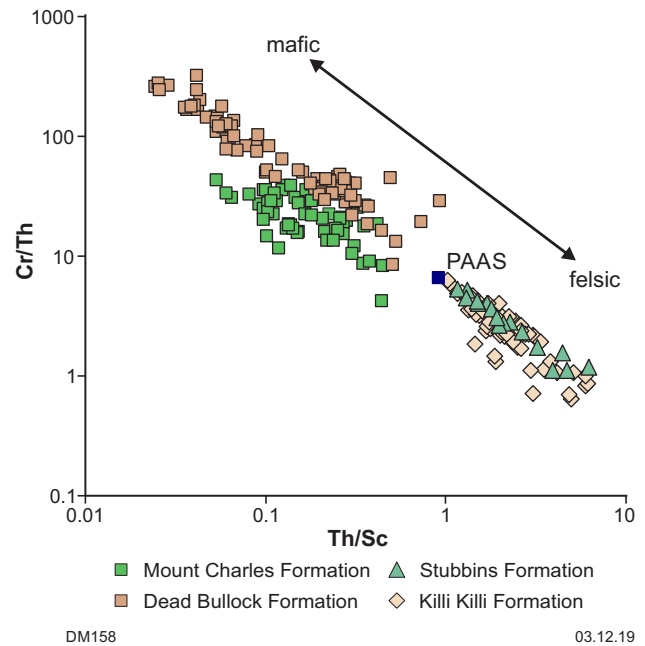


Figure 12. Whole-rock Th/Sc vs Cr/Th for metasedimentary rocks of the Tanami Group and inferred correlatives from samples across the Granites–Tanami Orogen (after Lambeck et al., 2010). Abbreviation: PAAS, Post-Archean Average Australian Shales

that it extends as young as the start of the Tanami Event, dated at c. 1840 Ma (Li et al., 2014; Petrella et al., 2019).

In this context, we note the various interpretations of the 1838 ± 6 Ma date obtained for a felsic rock assigned to the Callie Member of the Dead Bullock Formation (Cross and Crispe, 2007). Bagas et al. (2008) suggested the unit might be intrusive, but its identification as a tuff remains possible, consistent with the fine-grained, acicular shape of the dated zircons, which contain irregular axial cavities, and the friable character of the rock. However, its c. 1838 Ma age appears to be too young to date deposition of the upper Callie Member or lower Killi Killi Formation, which appear to have been deposited at about 1860–1855 Ma. The interpretation of this date and its stratigraphic affinity clearly form an important focus for future work.

Correlations with the Halls Creek Group may also provide constraints on the timing of deposition of units stratigraphically underlying the Killi Killi Formation. If the upper parts of the Dead Bullock and Stubbins Formations are broadly correlatives of the mafic-rich Biscay Formation, a minimum age for their deposition may be provided by correlation to the 1856 ± 6 Ma date for a volcanic unit in the lower part of the overlying Olympio Formation, which lacks mafic volcanic rocks. If this correlation is valid, then the depositional ages of the upper parts of the Dead Bullock and Stubbins Formations would be constrained to the period between the 1876–1864 Ma ages of their youngest detrital zircon age components and c. 1856 Ma. The lower parts of the Dead Bullock Formation could have been deposited closer to 1881 ± 4 Ma, by correlation to the age of a felsic volcanic rock in the Brim Rockhole Formation. This is consistent with the 1884 ± 8 Ma (1σ) age for the youngest single detrital zircon so far dated in the Ferdies Member.

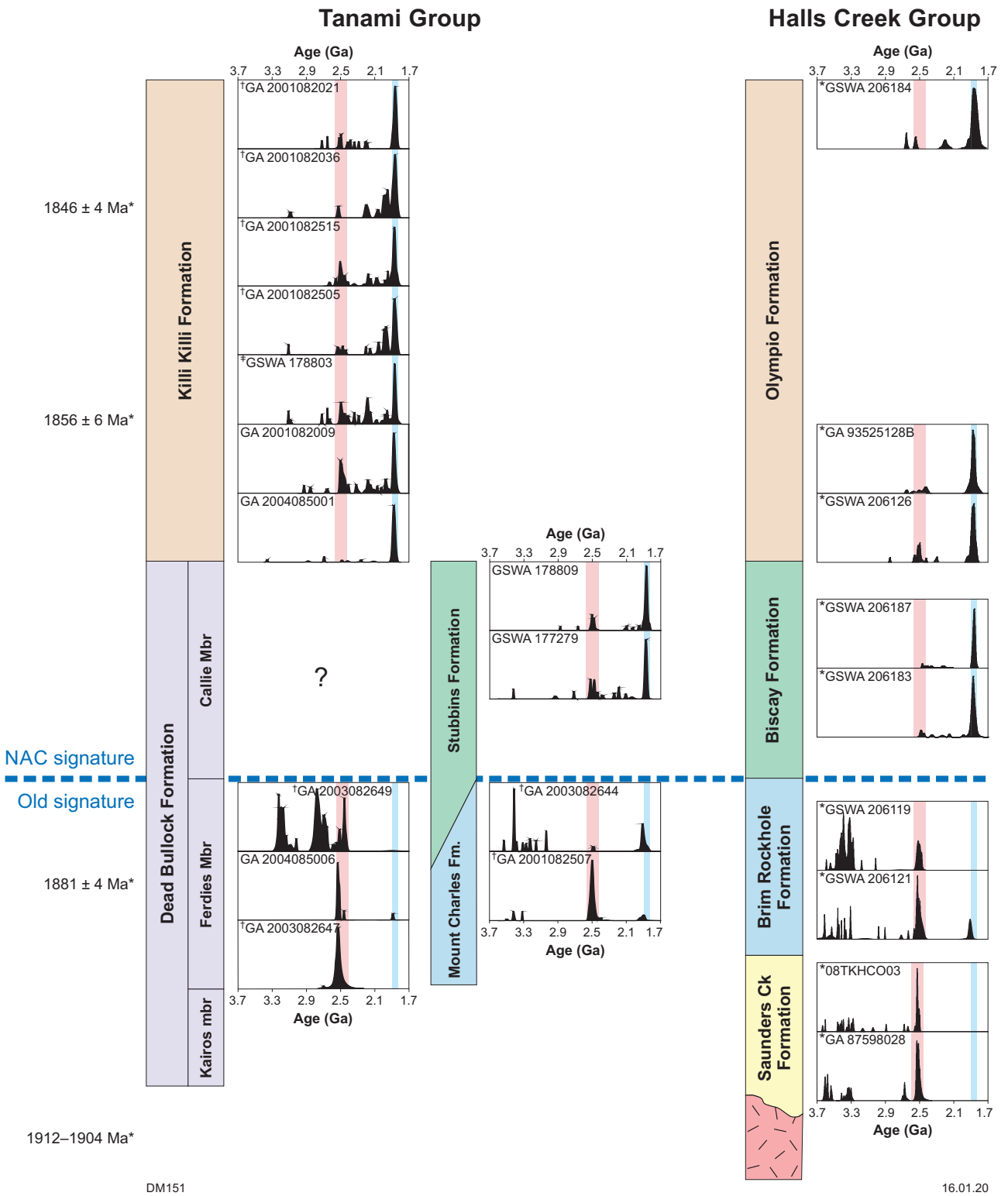


Figure 14. Combined detrital zircon age data $\leq 5\%$ discordant for the Halls Creek Group, Tanami Group and inferred correlatives. Dates adjacent to Halls Creek Group indicate approximate stratigraphic positions of dated volcanic units. * Phillips et al. (2016), † Cross and Crispe (2007), ‡ Bagas et al. (2009)

Stratigraphic correlations within the Granites–Tanami Orogen

Stubbins Formation

The detrital zircon and geochemical constraints described aid the assessment of regional correlations within the Tanami Group. Bagas et al. (2014) suggested that the Stubbins Formation is a correlative of the Dead Bullock Formation, rather than an older unit, on the basis of lithological associations and structural position. The samples of Stubbins Formation studied in this Report are from the uppermost part of this unit and yield dominant age components at c. 1874 and 1865 Ma, with a minor component at c. 2500 Ma. The age spectra, and the association with extensive mafic sills, are consistent with a stratigraphic position in the uppermost Dead Bullock Formation where it transitions into the lowermost Killi Killi Formation. Whole-rock geochemistry from this part of the Stubbins Formation near the Kookaburra prospect has high-Th/Sc ratios, low Cr contents and flat REE patterns normalized to PAAS (Lambeck et al., 2010), which is also consistent with this stratigraphic position. The Stubbins Formation has an inferred thickness of >2 km, similar to that of the Dead Bullock Formation (Bagas et al., 2014). Hence, it is possible that the lower parts of the Stubbins Formation are correlatives of the lower parts of the Dead Bullock Formation. The metasedimentary rocks in the lower part of the Stubbins Formation have not been dated or systematically sampled for whole-rock geochemistry to test this inference, but the suggestion implies that the Western Australian part of the Granites–Tanami Orogen might contain age-equivalents of the Au-localizing units in the lower Callie Member and Ferdies Member in the Northern Territory.

The Lyrebird prospect about 3 km northwest of the Kookaburra prospect in the Bald Hill area (Figs 2, 5) consists of Au-anomalous quartz veins in an exposed to shallowly covered area that could represent the lower part of the Stubbins Formation. The prospect occurs near the base of a series of laterally extensive dolerite sills and is largely hosted by turbiditic siliciclastic rocks, with no Fe-rich units noted in this area (Rohde and English, 2006). Although dolerite sills in the Stubbins Formation have an elevated magnetization in aeromagnetic images, the overall magnetization of the Stubbins Formation is significantly lower than that of the Dead Bullock Formation in the Dead Bullock Soak area (Fig. 5). If the correlation of the Stubbins Formation with the Dead Bullock Formation is correct, this suggests that lithologies in the lower parts of the Stubbins Formation may differ from correlative units in the Dead Bullock Soak area, which are inferred to have been deposited in a sediment-starved, relatively deep water depocentre (Lambeck et al., 2008). If turbiditic rocks in the Lyrebird area are representative of the lower Stubbins Formation, their deposition represents a more active sedimentary regime, and/or a shallower water setting, but currently there are few data available to evaluate the nature of the succession in this part of the orogen.

Mount Charles Formation

The stratigraphic position of the Mount Charles Formation in the Tanami Goldfield has been a subject of debate (Cross

and Crispe, 2007; Crispe et al., 2007; Ahmad et al., 2013b; Bagas et al., 2014). This is due in part to a lack of useful maximum depositional age constraints, with dated samples lacking detrital age components younger than c. 1900 Ma (Cross and Crispe, 2007). The Mount Charles Formation has been considered by some workers to be a c. 1800 Ma rift succession on the basis of field interpretations that it lacks the oldest generations of structures and unconformably overlies the Dead Bullock Formation (Crispe et al., 2007; Lambeck et al., 2010; Ahmad et al., 2013b). In contrast, Hawkins (2011) considered the Mount Charles Formation to be part of the Dead Bullock Formation on the basis of similarities in detrital zircon signatures and geochemistry. Bagas et al. (2014) also interpreted the Mount Charles Formation to be part of the Dead Bullock Formation, citing an unpublished c. 1825 Ma date for a dacitic dyke intruding the unit at the Hurricane–Repulse mine (Fig. 5). This interpretation places the Mount Charles Formation in a transitional zone between the Dead Bullock Formation and the Killi Killi Formation.

The detrital zircon age spectra obtained from the Mount Charles Formation are, however, significantly different from those of the upper Stubbins Formation, which is also correlated with the transitional zone between the Dead Bullock and Killi Killi Formations by Bagas et al. (2014). The detrital zircon ages are similar in some respects to those obtained from the Ferdies Member lower in the succession, though there are significant differences (Fig. 14). Sample GA 2003082644 of the Mount Charles Formation dated by Cross and Crispe (2007) is dominated by a c. 2500 Ma age component with a minor component of early Paleoproterozoic zircons, similar to zircon ages obtained for the Ferdies Formation in this study and at Groundrush (Cross and Crispe, 2007). Another sample of the Mount Charles Formation dated by Cross and Crispe (2007) contained only a minor c. 2500 Ma age component, and a larger proportion of scattered Archean dates between c. 3540 and 3040 Ma. This has no obvious correlative in the Tanami Group, but the closest age spectrum is a sample of the Ferdies Member dated by Cross and Crispe (2007), sample GA 2003082649, which contained only a minor c. 2500 Ma component and major Archean components at c. 3220, 3170, 2800 and 2700 Ma. This dominance of Archean detrital ages suggests that the Mount Charles Formation might be a correlative of units stratigraphically below the uppermost Dead Bullock Formation.

The youngest detrital zircon age components in the Mount Charles Formation at c. 1913 and 1905 Ma are derived from relatively euhedral grains, suggesting a proximal source. As noted by Cross and Crispe (2007), these zircons have similar ages to felsic rocks of the 1912–1904 Ma Sophie Downs Suite, which forms felsic-dominated basement to the Halls Creek Group about 275 km to the northwest (Phillips et al., 2016). Rocks of this age have not been identified elsewhere in the North Australian Craton and the Sophie Downs Suite may represent a distinctive source of sediment for the Mount Charles Formation. The lowermost part of the Halls Creek Group also contains units with detrital zircon ages consistent with derivation from the Sophie Downs Suite and, as noted above, is overlain by a thick metasedimentary succession dominated by c. 1865 Ma detrital zircons (Phillips et al., 2016). If the Sophie Downs Suite did indeed form a sediment source for the Mount Charles Formation, the absence of younger (1870–1865 Ma) detrital zircons suggests this was during

the earliest stages of sedimentation in the Granites–Tanami Orogen, rather than during a younger rifting event post-dating deposition of the Tanami Group.

Detrital zircon data for confirmed post-Tanami Group units also suggest that deposition of the Mount Charles Formation took place well before c. 1800 Ma. The 1824–1816 Ma Ware Group contains well-rounded detrital zircons with age components at 1880–1860 Ma and c. 2500 Ma, and also includes a component of euhedral zircons at 1831–1823 Ma (Cross and Crispe, 2007). The youngest age component is similar to the age of intrusive and extrusive felsic volcanism within the Ware Group itself, so may reflect a juvenile magmatic component in an environment otherwise dominated by sediment reworked from the underlying Tanami Group or correlatives (Cross and Crispe, 2007). The Pargee Sandstone and Gardiner Sandstone represent distinct sedimentary successions that post-date the Ware Group and contain detrital age components that are broadly similar to the Ware Group, with the Pargee Sandstone also containing a younger c. 1768 Ma age component. It is thus difficult to envisage the Mount Charles Formation as a c. 1800 Ma succession deposited between the Ware Group and Pargee Sandstone, since its youngest detrital age components are c. 1913 and 1905 Ma. A younger rift basin developed in this setting would likely have accumulated a significant component of reworked 1870–1815 Ma zircons from the underlying succession, as seen in the other post-Tanami Group sedimentary successions.

The limited geochronological data for the Mount Charles Formation thus suggest it was deposited as part of the Tanami Group, but further work is required to confirm its stratigraphic position. In particular, an inferred correlation with the Dead Bullock Formation conflicts with a field observation that places the Mount Charles Formation unconformably above the Killi Killi Formation near the Jim’s Find mine, and an interpretation that it contains fewer deformation events than the Tanami Group (Vandenberg et al., 2001; Crispe et al., 2007; Ahmad et al., 2013b). These workers suggested that the two generations of large-scale folding affecting the Mount Charles Formation are related to late-stage deformation (i.e. D₄ or later), contrasting with the interpretation of Bagas et al. (2009) that these fold generations formed during the Tanami Orogeny and Stafford Event. These conflicting structural interpretations require resolution to aid more robust correlations.

The potential stratigraphic correlations for the Mount Charles Formation can also be evaluated using lithology and geochemistry, but the effectiveness of this approach may be limited if sub-basins and volcanic centres were present during deposition, resulting in local variations in sedimentary facies, thickness and composition. Fault-bound depocentres infilled by the Stubbins Formation have been inferred in the western part of the orogen, where seismic data suggest the presence of west-northwesterly trending half-grabens that were partially inverted during younger deformation (Joly et al., 2010). Syndepositional extensional faults with displacements of up to several metres have been recognized within the Mount Charles Formation (Tunks and Cooke, 2007), which may be related to sub-basin development. Basaltic clasts in metasedimentary rocks of the Mount Charles Formation (Tunks and Cooke, 2007) are also likely to limit the applicability of geochemical

fingerprinting, as these are likely to be derived from proximal volcanic centres rather than reflect the regional sediment provenance.

In this context, the mafic–felsic geochemical signature of the Dead Bullock Formation (Lambeck et al., 2008, 2010) may also have been influenced by proximal mafic volcanism, though no mafic volcanic rocks have been identified within the formation itself. The sediment-starved nature of this package, which contains a significant component of chemical sedimentary rocks, would make its geochemistry particularly susceptible to small contributions from local mafic volcanic centres. If this is the case, the mafic geochemical signature of the Dead Bullock Formation might not necessarily be indicative of a large mafic component in the more distal source regions that supplied more quartz-rich sediment.

The potential difficulties associated with regional correlations of the Dead Bullock Formation and equivalents are less pronounced for the Killi Killi Formation, which is lithologically more homogeneous. This may be a consequence of more rapid depositional rates and infill of any depocentres that may have been present during deposition of the Dead Bullock Formation.

Browns Range Metamorphics

The Browns Range Metamorphics form a poorly exposed domain along the western and southern margins of the granite-cored Browns Range Dome (Fig. 2) and are unconformably overlain by the Gardiner Sandstone of the Birrindudu Basin. Exposures consist of feldspathic metasandstone, metaconglomerate and muscovite schist, with less common calc-silicate rock and metamorphosed banded iron-formation (Blake et al., 2000). The depositional age of this unit has been the subject of debate, with interpretations ranging from Mesoproterozoic–Neoproterozoic to middle Paleoproterozoic (Page et al., 1995b; Cross and Crispe, 2007; Ahmad et al., 2013b; Nazari-Dehkordi et al., 2017).

Arkosic metasedimentary rocks in the western part of the dome are dominated by Archean detrital zircons, with five samples each yielding a similar unimodal age component between c. 3146 and 3026 Ma, and Lu–Hf T_{DM} model ages of 3.38 – 3.27 Ga (Nazari-Dehkordi et al., 2017). The same study dated three granitic rocks from the area, each of which yielded a dominant zircon age component at 3103–3036 Ma and a minor component at 2522–2501 Ma. Nazari-Dehkordi et al. (2017) interpreted the c. 2500 Ma age component to be the magmatic age of the granitic rocks and that the Browns Range Metamorphics were thus deposited between c. 3000 and 2500 Ma. Zircon dating of two samples of quartz–muscovite schist from the same general area yielded comparable dominant detrital age components, but also found a few younger ages of 2540–2520 Ma, and a single near-concordant analysis at 2128 ± 30 Ma (1σ) (Lu et al., 2017i,j). A single zircon grain is not a robust constraint, but this date, coupled with similarities of the age components in the quartz–muscovite schists and the granitic rocks, raises the possibility that the c. 2500 Ma age component in the granitic rocks reflects inheritance. If this is the case, it is possible that the Browns Range Metamorphics were deposited after c. 2500 Ma.

Dating from the southern part of the dome provides clearer evidence that the protoliths to at least parts of the Browns Range Metamorphics were deposited in the Paleoproterozoic. Page et al. (1995b) reported a range of detrital zircon ages between c. 3460 and 2470 Ma for an arkose, and calculated a maximum depositional age of 2507 ± 22 Ma. Granitic rocks intruding the succession contain zircon age components between c. 3400 and 1870 Ma, with a significant component at c. 2500 Ma interpreted by Page et al. (1995b) as the igneous age. Cross and Crispe (2007) reassessed this interpretation using CL imagery and considered all the dated zircon in these samples to be inherited, with the c. 1870 Ma age component only representing a maximum age for magmatism. This view is in accord with igneous ages of 1805 ± 7 , 1796 ± 7 and 1780 ± 33 Ma for other samples of granitic rocks in the Browns Range Dome (Smith, 2001).

It is therefore possible that all the dated zircon age components in the granitic rocks of the western part of the dome reflect inheritance. If this is the case, then the Browns Range Metamorphics could be a correlative of the Dead Bullock Formation, which is also dominated by Archean detritus. This would remove the need to account for an apparent absence of the Tanami Group in the Browns Range Dome area, since the Gardiner Sandstone directly overlies the Browns Range Metamorphics. However, the dominantly felsic geochemical composition of the arkosic metasedimentary rocks of the Browns Range Metamorphics (Nazari-Dehkordi et al., 2017) differs from the dominantly mafic compositions of units in the Dead Bullock Formation (Lambeck et al., 2008, 2010). Although it is possible that this indicates the Browns Range Metamorphics are not a correlative of the Dead Bullock Formation, it is also possible that this difference reflects a lateral change in lithofacies (Nazari-Dehkordi et al., 2017), particularly if this area was distant from coeval mafic volcanic centres.

The interpretation of the geochronological data for the Browns Range Metamorphics remains inferential, but if these metasedimentary rocks do correlate with the Dead Bullock Formation, it raises the possibility that the unit has the potential to host orogenic Au mineralization. In this context, a linear positive magnetic anomaly along the southern margin of the dome, and irregular magnetic highs in the western part, could indicate the presence of Fe-rich or mafic units which form components of sedimentary packages that host mineralization in other parts of the orogen.

It should be noted that granitic gneiss of the Billabong Complex, which is generally regarded as Archean basement, contains 2550–2510 Ma zircon age components that are similar to those in granitic and metasedimentary rocks of the Browns Range Metamorphics (Page et al., 1995b; Kositcin et al., 2013a; Whelan et al., 2014). The youngest age component in these rocks at c. 2510 Ma forms euhedral zircon overgrowths and is interpreted as the magmatic crystallization age of the granitic precursor (Page et al., 1995b; Kositcin et al., 2013a). These granitic rocks differ from those in the Browns Range Metamorphics, however, in that they were metamorphosed at relatively high grade and contain a gneissic foliation. The Browns Range Metamorphics, in contrast, are weakly foliated and metamorphosed at greenschist facies (locally amphibolite facies), comparable to the tectonism that affected the Tanami Group and 1820–1790 Ma granitic rocks elsewhere in the orogen.

Age and provenance of the Gardiner Sandstone

The provenance age data collected for two samples of Gardiner Sandstone as part of this study complement other dated samples taken from the Coomarie Range by Cross and Crispe (2007) and the Browns Range Dome by Nazari-Dehkordi et al. (2017). All these samples have similar detrital zircon age spectra, ranging between c. 2600 and 1800 Ma, with significant age components at c. 1860 and 2500 Ma. Maximum depositional ages of 1829 ± 19 and 1841 ± 16 Ma (this study) and 1812 ± 8 Ma (Cross and Crispe, 2007) are significantly older than the 1768 ± 14 Ma maximum depositional age for the unconformably underlying Pargee Sandstone (Cross and Crispe, 2007), and so do not improve constraints on the depositional age. From the detrital zircon ages obtained by Nazari-Dehkordi et al. (2017), a maximum depositional age of 1768 ± 21 Ma ($n = 9$, MSWD = 1.7) can be calculated, which is indistinguishable from that of the Pargee Sandstone. This is the youngest maximum age available for the Gardiner Sandstone itself. A minimum age for deposition of the Gardiner Sandstone is provided by a U–Pb date of 1632 ± 3 Ma for xenotime overgrowths on detrital zircons (Vallini et al., 2007).

As noted by Cross and Crispe (2007), the abundance of c. 1860 and 2500 Ma zircons in the Gardiner Sandstone and their generally well-rounded shapes suggests derivation from reworked older parts of the succession, in particular the Tanami Group. This is consistent with the presence of clasts of vein quartz, greywacke, phyllitic metasedimentary rocks, quartzite and rare mafic volcanic rocks in conglomerate near the base of the unit, which suggests derivation from the Granites–Tanami Orogen (Blake et al., 1979).

Timing of the Tanami Event

Recent interpreted structural frameworks for the Granites–Tanami Orogen offer considerable differences in the number, character and timing of events (Table 2). This study does not attempt to resolve these differences, but the inferred depositional ages of the Tanami Group provide additional constraints on the timing of the Tanami Event (D_1).

The Tanami Event deformed the entire Tanami Group, marking the end of its deposition, and pre-dates deposition of the 1826–1814 Ma Ware Group. The Killi Killi Formation is the youngest unit affected by the Tanami Event, deposition of which appears to have continued to at least c. 1846 Ma. A date of 1839 ± 9 Ma for peak metamorphic xenotime in the Dead Bullock Soak Goldfield (Petrella et al., 2019) provides a direct constraint on the timing of tectonism. These age constraints indicate that the Tanami Event was similar in age to the Halls Creek Orogeny in the east Kimberley region, which commenced between 1837 ± 6 and 1832 ± 3 Ma (Bodorkos et al., 2000a), and ceased before 1808 ± 3 Ma (Page et al., 2001; Tyler et al., 2012). A correlation between the Tanami Event and the Halls Creek Orogeny has been suggested previously, consistent with the similar north-northeasterly trend of F_1 fold axes in the west and north of the Granites–Tanami Orogen and folding and faulting in the Halls Creek

Orogen (Huston et al., 2007; Crispe et al., 2007; Bagas et al., 2009). An inferred 1840–1826 Ma age for the Tanami Event is similar to age estimates of Crispe et al. (2007) and Ahmad et al. (2013b), but somewhat younger than an c. 1850 Ma age inferred in other studies, which are in part based on an inferred older onset of deformation in the Halls Creek Orogen (Bagas et al., 2009, 2014; Joly et al., 2010; Li et al., 2014).

No deformation age-equivalent to the Tanami Event has yet been identified in the Aileron Province to the southeast, where the earliest recognized tectonism is the 1810–1790 Ma Stafford Event (Scrimgeour, 2013). This apparent absence might indicate that the regional effects of the D₁ event are limited to the northwestern margin of the North Australian Craton.

Regional correlations and sedimentary provenance: 1880–1835 Ma

As noted above, the Tanami Group can be correlated with metasedimentary rocks of the Halls Creek Group in the Lamboo Province. Correlations may also be possible at a wider geographic scale, with 1880–1835 Ma metasedimentary packages elsewhere in the North Australian Craton having comparable lithologies and provenance to those in the Granites–Tanami Orogen (Figs 15, 16). Metasedimentary rocks in these areas also display correlated changes in lithofacies with time that imply common development of these depositional systems. This section reviews some of these potential correlations to provide context for the Granites–Tanami Orogen and geodynamic models of craton evolution.

Basal units dominated by Archean detritus (Detrital A provenance)

In areas of the North Australian Craton where Neoproterozoic basement is exposed or at shallow depths, the oldest known Paleoproterozoic metasedimentary units typically have detrital zircon age signatures dominated by Archean age components, which are distinct from those of overlying successions (Fig. 17). For convenient discussion, we denote this provenance signature as ‘Detrital A’. The depositional ages of these units may differ between regions, as can the relative proportions of age components, but the dominance of Archean detrital zircon ages in the lowermost parts of Paleoproterozoic successions appears to be consistent. For example, the basal units of the Halls Creek Group are dominated by c. 2500 Ma detrital zircon ages, similar to units in the basal Tanami Group, but have a larger component of 3600–3300 Ma ages (Phillips et al., 2016).

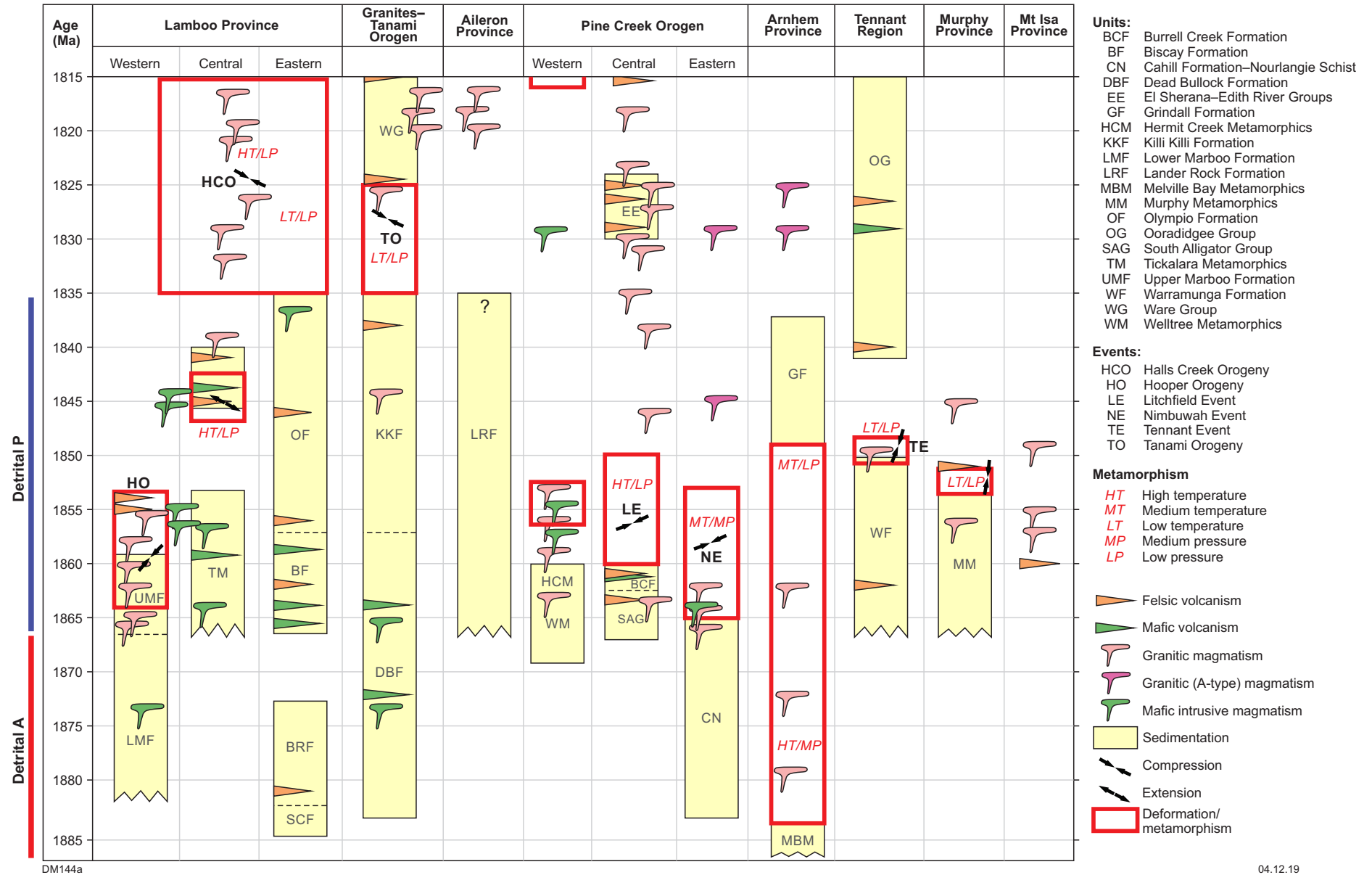
The oldest Paleoproterozoic units of the Pine Creek Orogen to the north of the Granites–Tanami Orogen (Fig. 1) are also dominated by Archean detritus. These include the c. 2020 Ma Woodcutters Supergroup in the Central Domain, which has detrital zircon ages consistent with those of the basement rocks it unconformably overlies (Cross et al., 2005a; Ahmad and Hollis, 2013), though some samples include age components at c. 3670 and 3125 Ma that do not have any known equivalents in exposed basement rocks (Hollis et al., 2010). Similar

Neoproterozoic-dominated signatures are also present in the Cahill Formation and Nourlangie Schist of the Nimbuhah Domain in the eastern part of the orogen, which were deposited after 1866 ± 11 Ma and intruded by granitic rocks at 1867–1857 Ma (Hollis et al., 2014). Hollis et al. (2014) noted that the c. 2500 Ma detrital zircons in these metasedimentary rocks have relatively juvenile Hf and mantle-like O isotope values. This differs from the more evolved and crustal-like Hf and O isotope characteristics of Archean basement rocks exposed in the Pine Creek Orogen, leading Hollis et al. (2014) to suggest that this material might have been derived from a more distal source, such as the Gawler Craton or the Dharwar Craton in India. However, Hf and O isotope compositions of zircons from the Billabong Complex in the Granites–Tanami Orogen show evidence of mixing between a juvenile, mantle-like source and a more evolved crustal source (Whelan et al., 2014), indicating that basement rocks are isotopically heterogeneous and external sediment sources are not necessarily required. A similar conclusion was made by Iaccheri et al. (2018), who suggested that differences in Hf and O isotope values for zircons in granitic rocks of the Granites–Tanami Orogen reflect compositionally distinct basement terranes.

In the Arnhem Province in the northeast of the craton, Neoproterozoic basement is not exposed and the oldest known units are metasedimentary rocks of the 1900–1880 Ma Melville Bay Metamorphics (Whelan et al., 2017). These rocks contain dominant age components at 2300–1900 Ma and minor components to c. 2609 Ma (Whelan et al., 2017; Kositcin et al., 2018; Reno et al., 2018). Similarly, no Neoproterozoic basement rocks have been identified in the Aileron Province, and the oldest exposed units are correlatives of the Killi Killi Formation, with detrital zircon signatures dominated by 1870–1865 Ma age components (see below). In the southeast of the Aileron Province, some metasedimentary units in the Entia Gneiss are dominated by c. 2500 Ma detritus, whereas others contain much younger detritus indicating deposition after c. 1780–1770 Ma (Wade et al., 2008; Beyer et al., 2013). These data could indicate local sediment derivation from an Archean basement source.

Turbidites dominated by 1870–1865 Ma detritus (Detrital P provenance)

Siliciclastic-dominated metasedimentary rocks deposited between c. 1870 and 1835 Ma are widespread across the North Australian Craton and overlie units with by Detrital A provenance (Figs 15, 16). These younger packages are characterized by a dominant 1870–1865 Ma detrital zircon age component and a subsidiary c. 2500 Ma age component (Fig. 18; Neumann et al., 2006; Cross and Crispe, 2007; Cloué-Long et al., 2008a,b; Worden et al., 2008b; Carson et al., 2009; Bodorkos et al., 2013; Carson, 2013; Hollis et al., 2013, 2014; Maidment et al., 2013; Phillips et al., 2016). For convenient discussion, this distinctive and uniform provenance signature is here denoted ‘Detrital P’ for the dominantly Paleoproterozoic age of detritus. The ubiquitous nature of the Detrital P signature is matched by the similar lithofacies of these packages, typically described as ‘turbiditic’, and the Detrital P provenance is carried forward into younger sedimentary successions by erosion and redeposition (e.g. the Ware Group and Pargee



04.12.19

Figure 15. Time–space plot for the North Australian Craton between 1885 and 1815 Ma. ‘Detrital A’ provenance refers to metasedimentary rocks dominated by Archean to early Paleoproterozoic detrital zircon ages; ‘Detrital P’ provenance refers to units dominated by 1875–1865 Ma detrital zircon, with a minor c. 2500 Ma age component. The Tennant Region column includes units in the Tomkinson, Warramunga and Davenport provinces

and Gardiner Sandstones in the Granites–Tanami Orogen). The widespread occurrence of 1870–1835 Ma sedimentary rocks with the Detrital P provenance, and their similar lithofacies, suggests a geographically extensive and linked sediment transport and deposition system.

In addition to the Biscay and Olympio Formations in the Eastern Zone of the Lamboo Province, metasedimentary rocks with the Detrital P signature were deposited in other parts of the province between c. 1875 and 1855 Ma. These include the upper Marboo Formation and Mount Joseph Migmatite in the Western Zone (Tyler et al., 1999; Kirkland et al., 2014; Lu et al., 2016c,e, 2017c,g, 2018a,c), and the Tickalara Metamorphics, Milba Formation and Winnama Formation in the Central Zone (Page et al., 1995a; Bodorkos et al., 1999, 2000b; Lu et al., 2016a,b,d, 2017h, 2018b,d,e, Mole et al., 2018). Both the Western and Central Zones have been interpreted as exotic terranes with respect to the Eastern Zone and North Australian Craton (e.g. Tyler et al., 1995; Griffin et al., 2000; Tyler et al., 2012; Lindsay et al., 2016; Kohanpour et al., 2017), but the presence of the Detrital P signature in all three terranes implies a connection at the time of deposition.

In the Aileron Province southeast of the Granites–Tanami Orogen, the Detrital P signature characterizes the

widespread Lander Rock Formation, which has a similar lithology and provenance signature to both the Killi Killi and Olympio Formations. Detrital zircon dating of this unit indicates youngest age components ranging between c. 1872 and 1835 Ma (Kinny, 2002; Cross et al., 2005c; Claoué-Long et al., 2008b; Bodorkos et al., 2013; Hollis et al., 2013), and minimum ages are provided by 1820–1770 Ma granitic rocks that intrude the unit (Scrimgeour, 2013).

The Detrital P signature is also present in 1865–1860 Ma metasedimentary rocks of the Pine Creek Orogen (Worden et al., 2008b). The Cosmo Supergroup in the Central Domain contains turbiditic metasedimentary rocks with the Detrital P signature that are dated by intercalated 1863–1861 Ma felsic volcanic rocks (Worden et al., 2008a). This felsic volcanism was coeval with the emplacement of voluminous granitic rocks of the 1867–1857 Ma Nimbuwah Complex in the Nimbuwah Domain farther to the east, where no sedimentation of this age is known. The amphibolite to granulite facies Welltree and Hermit Creek Metamorphics of the Litchfield Domain in the western Pine Creek Orogen appear to be higher metamorphic grade correlatives of the upper Cosmo Supergroup (Ahmad and Hollis, 2013). The Hermit Creek Metamorphics have the Detrital P signature, with protoliths deposited after 1868 ± 5 Ma (Worden et al.,

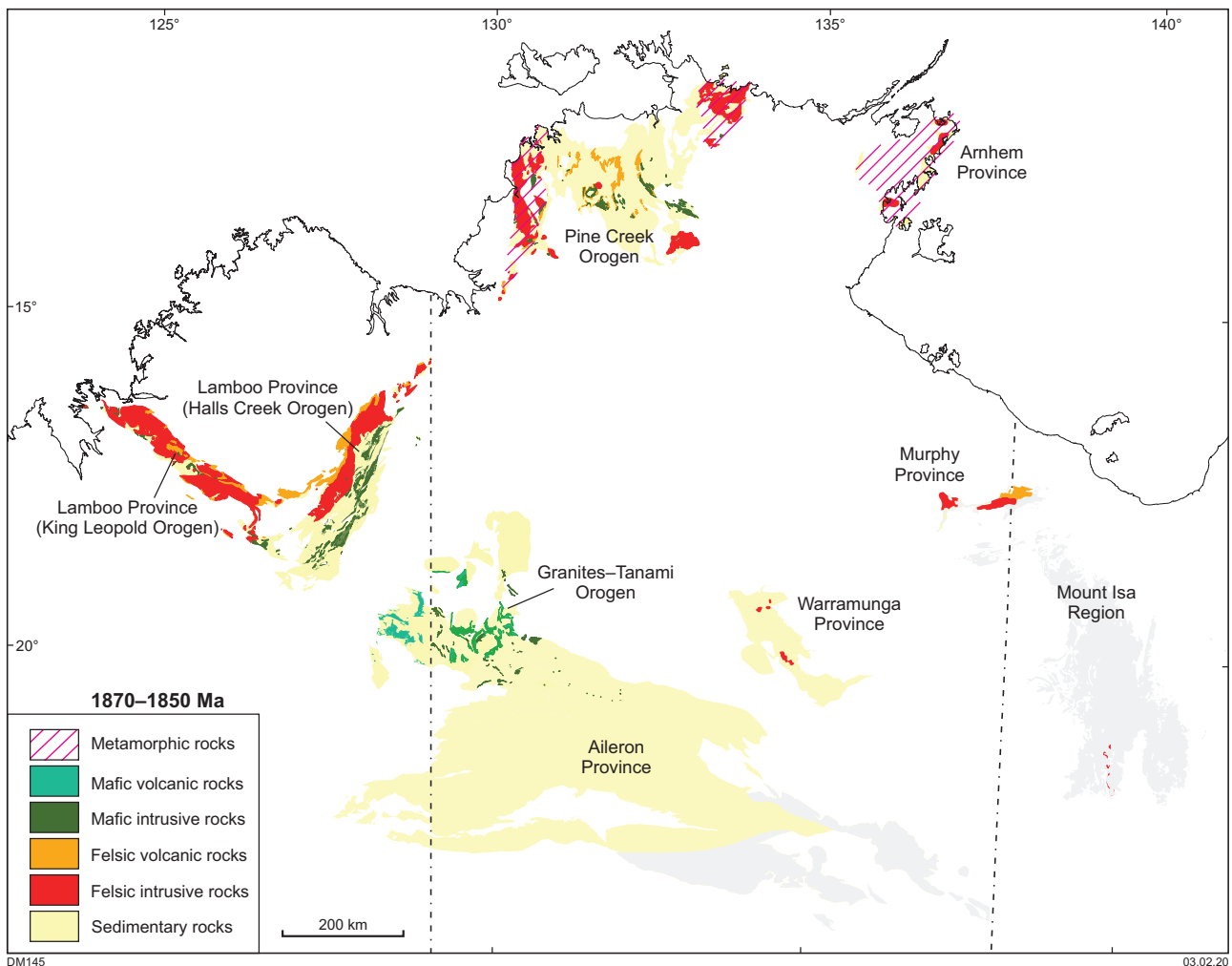


Figure 16. Distribution of areas in the North Australian Craton (exposed and interpreted beneath shallow cover) that preserve a record of 1870–1850 Ma sedimentation, magmatism and tectonism. Based on Ahmad and Scrimgeour (2006) and GSWA (2016a)

2008b). These rocks experienced high-temperature, low-pressure metamorphism at 1855–1853 Ma and were intruded by granitic rocks at a similar time (1863–1850 Ma) in an interpreted extensional setting (Carson et al., 2008; Ahmad and Hollis, 2013).

The oldest exposed rocks in the Tennant Region in the central part of the craton are turbiditic metasedimentary rocks of the Warramunga Formation within the Warramunga Province, which have dominant age components at c. 1861 Ma and minor components at c. 2500 Ma (Compston, 1995; Maidment et al., 2013). Minor felsic volcanic rocks in the Warramunga Formation and correlative units were emplaced at 1862 ± 9 and 1862 ± 5 Ma (Compston, 1995; Smith, 2001) and sedimentation possibly continued until deformation and felsic magmatism of the c. 1850 Ma Tennant Event (McPhie, 1993; Maidment et al., 2013).

The Detrital P signature is also present in the oldest rocks of the Murphy Province, the Murphy Metamorphics, in the eastern part of the craton (Fig. 1). This unit consists of turbiditic shale and greywacke with lesser ironstone, quartzite and chert (Ahmad et al., 2013a) and contains dominant detrital zircon age components of 1867 ± 7 and 1853 ± 4 Ma, with a smaller proportion of early Paleoproterozoic to Neoproterozoic grains (Hanley, 1996; Hollis et al., 2010). This sedimentation ceased with intrusion of granitic rocks dated at 1856 ± 3 and 1845 ± 3 Ma and the eruption of 1851 ± 3 Ma felsic volcanic rocks

that unconformably overlie the Murphy Metamorphics (Page et al., 2000).

The Arnhem Province in the northeast of the craton is dominated by the emplacement of S-type granitic rocks with associated high-grade metamorphism at 1872–1862 Ma (Kositcin et al., 2015a, Whelan et al., 2017; Reno et al., 2018). Turbiditic rocks of the post-orogenic Grindall Formation were deposited between 1862 and 1830 Ma, but differ from other units of similar age in the craton in that they do not contain zircon age components younger than c. 1930 Ma (Kositcin et al., 2015a, 2018; Whelan et al., 2017).

In the Mount Isa region in the far eastern part of the North Australian Craton (Fig. 1), the oldest exposed units comprise 1864–1852 Ma granitic rocks and coeval felsic volcanic rocks but no 1880–1835 Ma sedimentary rocks are known (Bierlein et al., 2008, 2011; Neumann et al., 2009).

Source of Detrital P detritus

Though not everywhere precisely constrained, the timing of initial deposition of sedimentary units with the Detrital P provenance signature appears to be close to the age of the dominant detrital age component within these rocks (Fig. 13). This means that the source region(s) for the Detrital P detritus should be characterized by exhumation, uplift and erosion synchronous with, or immediately

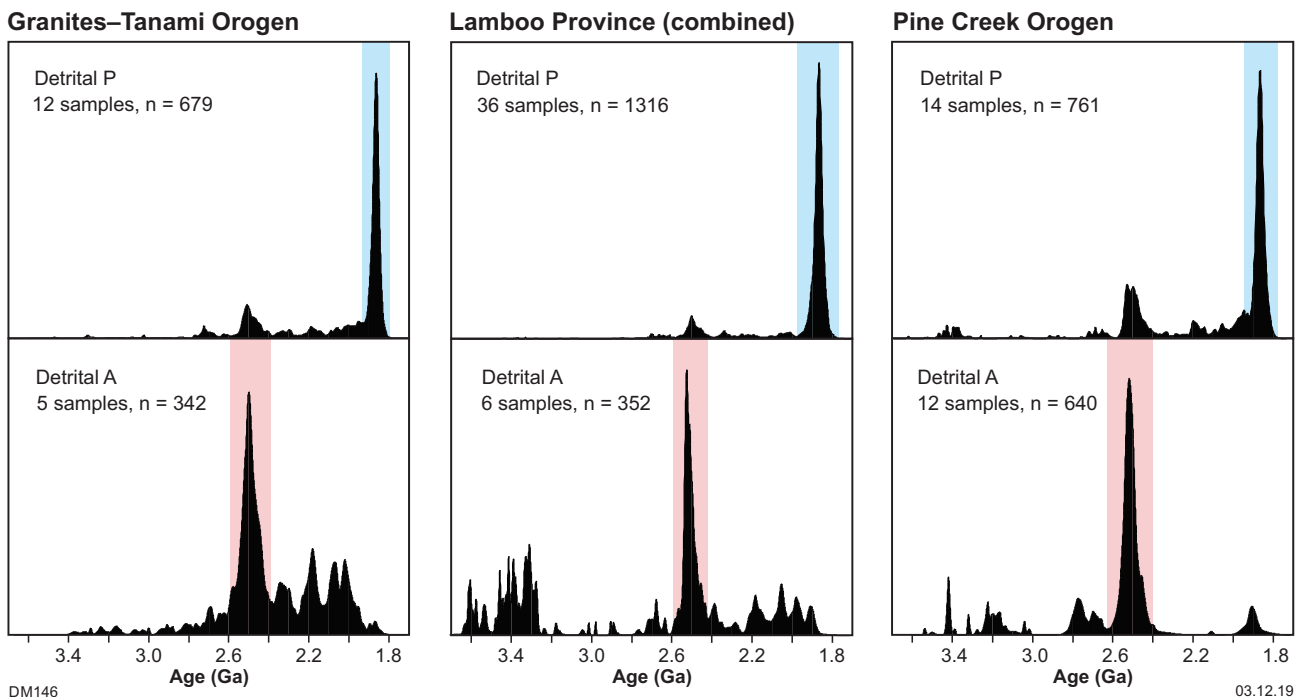


Figure 17. Composite probability density diagrams for detrital zircon dating of 1885–1835 Ma metasedimentary rocks in the Granites–Tanami Orogen, Lamboo Province (Western, Central and Eastern Zones) and the Pine Creek Orogen. Metasedimentary rocks with the Detrital A provenance signature (lower plots) are dominated by c. 2500 Ma ages and a range of early Paleoproterozoic to Archean ages. These units may reflect the input of basement sources during the early phases of sedimentation. Units with the Detrital P provenance signature (upper plots) are dominated by c. 1865 Ma ages, with a subsidiary c. 2500 Ma age component, and reflect a more homogeneous provenance that covered much of the North Australian Craton after 1870–1865 Ma. Granites–Tanami Orogen data from Smith (2001), Cross and Crispe (2007), Worden et al. (2008b), Bagas et al. (2009), Kirkland and Wingate (2010) and this study. Lamboo Province data from Bodorkos et al. (1999, 2000b), Tyler et al. (1999), Page and Hoatson (2000), Worden et al. (2008b), Lu et al. (2016a–e, 2017a–d, 2018a–e) and Phillips et al. (2016). Pine Creek Orogen data from Worden et al. (2006a,b, 2008b), Hollis et al. (2010), Carson et al. (2011a), Beyer et al. (2013), Carson (2013), and Kositcin et al. (2013b)

post-dating, emplacement of voluminous 1870–1860 Ma felsic igneous rocks. The near-euhedral shape of many 1870–1860 Ma detrital zircons (e.g. Fig. 8) reflects this first cycle of zircon reworking, but does not necessarily indicate a proximal source, since subaqueous transport of sediment does not typically cause rapid rounding of detrital grains (Garzanti, 2017).

Granitic and felsic volcanic rocks of suitable age are exposed in the present-day northern, northwestern and northeastern margins of the North Australian Craton, including the Western Zone of the Lamboo Province, the Pine Creek Orogen, and the Arnhem and Mount Isa Provinces (Figs 15, 16). Inboard of these areas, there are few granitic rocks of this age known, with slightly younger granitic rocks dated at c. 1856 and 1845 Ma in the Murphy Province (Page et al., 2000), c. 1850 Ma in the Warramunga Province (Compston, 1995; Maidment et al., 2013), and a single granite in the far southeast of the Aileron Province dated at c. 1852 Ma (Kositcin et al., 2015b). Felsic volcanic and volcanoclastic rocks (\pm mafic volcanic rocks) dated to the period 1870–1855 Ma are also volumetrically minor inboard of the northern margins of the craton, with limited felsic volcanic rocks present in the Eastern Zone of the Lamboo Province, the Granites–Tanami Orogen and the Warramunga Province (Smith, 2001; Bagas et al., 2008; Phillips et al., 2016).

Although 1870–1860 Ma felsic rocks are present in several regions, not all of these are likely to have been the dominant source of the large volume of sediment preserved in the widespread Detrital P metasedimentary packages. The Western Zone of the Lamboo Province — here considered to have been part of the North Australian Craton at this time — experienced folding and uplift during the c. 1860 Ma Hooper Orogeny, which overlapped with emplacement of felsic igneous rocks of the 1867–1849 Ma Paperbark Supersuite (Tyler and Griffin, 1990; Tyler et al., 2012). However, the degree of uplift and exhumation during the Hooper Orogeny may not have been large, since turbiditic sedimentation in the area continued locally until c. 1855 Ma, 1862–1854 Ma volcanic and hypabyssal intrusive rocks are preserved in the orogen, and relatively low peak metamorphic pressures are recorded (Tyler et al., 1999). The Central Domain of the Pine Creek Orogen, which contains 1863–1861 Ma felsic volcanic rocks, appears to have been an active basin until at least c. 1855 Ma (Ahmad and Hollis, 2013), similar to the Litchfield Province in the west, which experienced high-temperature, low-pressure metamorphism ascribed to extension at c. 1855 Ma (Carson et al., 2008). Granitic rocks in the Murphy and Warramunga Provinces are slightly younger than the main Detrital P age component, and were depositional sites at the onset of Detrital P sedimentation at c. 1865 Ma, only experiencing significant deformation at c. 1850 Ma (Maidment et al., 2013). In the Kalkadoon–Leichhardt Subprovince of the Mount Isa Province, 1864–1849 Ma granitic and felsic volcanic rocks form the oldest known units in the region (Bierlein et al., 2008, 2011; Neumann et al., 2009; Carson et al., 2011b), but no deformational event has been recognized that might have resulted in significant exhumation and uplift at c. 1865 Ma.

The northeastern parts of the craton, including the Nimbuwah Domain of the Pine Creek Orogen and the Arnhem Province, do preserve evidence suggesting that they formed part of a significant uplifted orogen with the potential to supply large volumes of sediment at 1865–1855 Ma. The Nimbuwah Domain experienced moderate-temperature, relatively high-

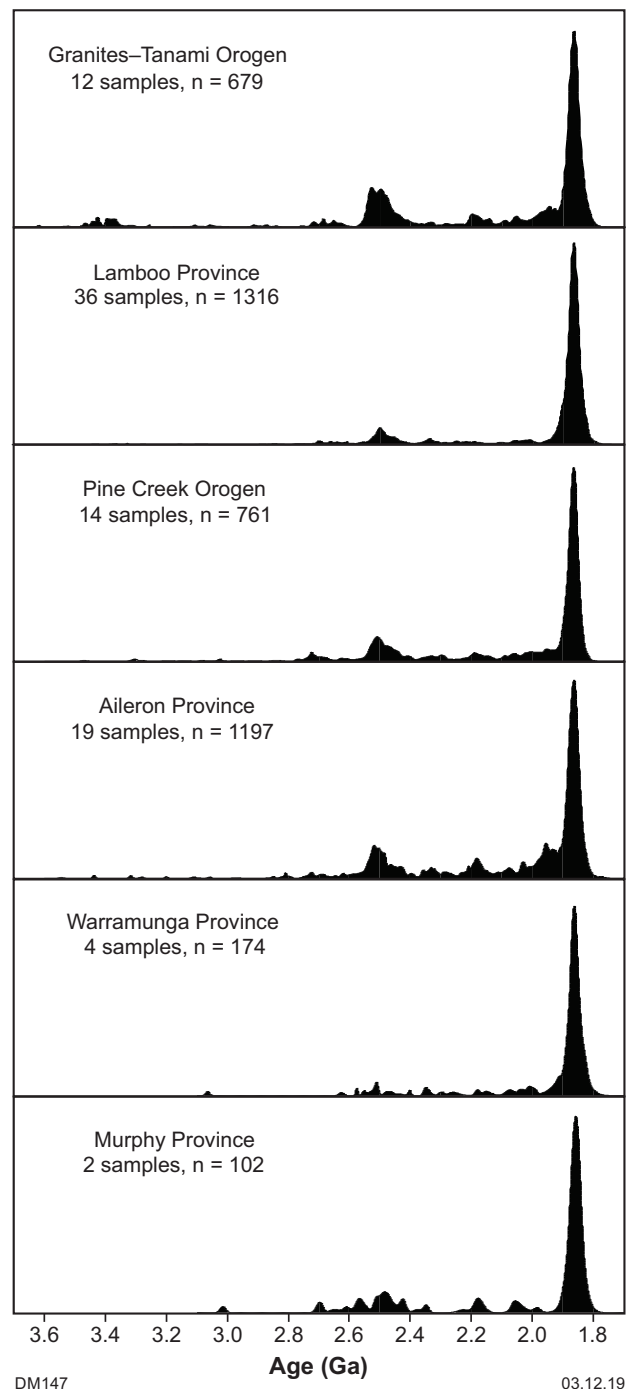


Figure 18. Composite probability density diagrams for detrital zircon dating of 1870–1835 Ma metasedimentary rocks with the ‘NAC signature’ in different domains of the North Australian Craton. The age spectra are remarkably consistent and suggest a common provenance, possibly from the northeastern margin of the craton. Data sources for the Granites–Tanami Orogen, Lamboo Province and Pine Creek Orogen are as noted in Figure 13. Aileron Province data from Smith (2001), Cross et al. (2005c), Worden et al. (2004, 2006a), Claué-Long et al. (2008b), Carson et al. (2009, 2011a), Beyer et al. (2013), Bodorkos et al. (2013) and Hollis et al. (2013). Warramunga Province data from Compston (1995) and Maidment et al. (2013). Murphy Province data from Hollis et al. (2010) and Kositcin et al. (2014)

pressure metamorphism of 450–600°C at 8–10 kbar during the c. 1865 Ma Nimbuwah Event (Hollis et al., 2009b), which likely involved compressional thickening of the crust. Sedimentation in this area appears to have ceased during deformation, and did not recommence until after c. 1820 Ma, following an additional greenschist facies folding event (Hollis et al., 2009b). Sedimentation farther to the east in the Arnhem Province ceased by c. 1880 Ma, earlier than in the Nimbuwah Domain, and was followed by granulite facies metamorphism and the development of isoclinal folding and associated steep to subvertical foliations. Metamorphism followed a clockwise pressure–temperature–time (P – T – t) path, with peak metamorphic conditions of >825°C and 6–8 kbar at 1879 ± 6 Ma, followed decompression and cooling through about 3 kbar and 670°C by 1849 ± 6 Ma, and was accompanied by the emplacement of S-type granitic rocks (Reno et al., 2017; Whelan et al., 2017). This tectonism was followed by deposition of turbiditic sedimentary rocks, before emplacement of A-type granitic rocks at 1829–1825 Ma (Haines et al., 1999; Kositcin et al., 2015a; Whelan et al., 2017).

Granitic rocks dated at 1875–1860 Ma were eroded during the uplift and exhumation of the Arnhem Province and Nimbuwah Domain are thus primary candidates within the North Australian Craton for the source of Detrital P sediment, which was dispersed, homogenized and deposited over a broad area to the south and southwest. Some sediment may also have been derived from 1865–1855 Ma felsic volcanic and granitic rocks of the Western Lamboo Province. The subsidiary Neoproterozoic age component in the provenance may be indicative of a smaller proportion of exhumed Neoproterozoic basement in the sediment source areas. Neoproterozoic granitic rocks dated at 2640–2510 Ma (Hollis et al., 2009a,b) in the Nimbuwah Domain may represent part of this basement domain. The very large volume of sedimentary rocks deposited during this period across a wide area implies a source region considerably more extensive than the limited areas now preserved in the Nimbuwah Domain and Arnhem Province.

The comparison of zircon age components and geological histories described above provides a first-order constraint on the potential sources of the Detrital P sediment. Further constraints are provided by comparing the isotope characteristics of detrital zircons from metasedimentary rocks with magmatic zircons from igneous rocks of similar age in the postulated source regions (e.g. Howard et al., 2009). Presently, there are data for only one sample of the Nimbuwah Complex, a c. 1866 Ma granitic rock with zircon ϵ_{Hf} values of –6.2 to –2.5 and $\delta^{18}\text{O}$ values of 6.5 to 8.9 ‰ (Beyer et al., 2013). Similar zircon Hf isotope values have also been obtained from four 1867–1865 Ma granitic rocks of the Paperbark Supersuite in the far western Lamboo Province, which have ϵ_{Hf} values between –6.4 and –0.8 (GSWA 95416, 95449 95459 and 95464, from GSWA, 2016). These isotope values are within the relatively limited range of values obtained for 1870–1860 Ma detrital zircons in samples of Detrital P metasedimentary units in the Granites–Tanami Orogen and Lamboo Province, which have ϵ_{Hf} values from –7 to +2, and $\delta^{18}\text{O}$ values from 6.5 to 9.5 ‰ (Phillips et al., 2016; Iaccheri et al., 2018). Although more data are required to better characterize potential sediment sources, the limited available data are consistent with the proposed source areas in the northern parts of the North Australian Craton.

There are few paleocurrent measurements to provide additional constraints on the source of Detrital P sediment.

Hancock (1991) reported a small number of measurements from the Marboo Formation of the Western Lamboo Province, which indicated south- and southwest-dipping paleoslopes. Broadly comparable paleoflow directions have been obtained from limited indicators in the Saunders Creek Formation (northwest–southeast axis) and Olympio Formation (north–northeast–south–southwest axis) in the Eastern Zone (Hancock and Rutland, 1984; Hancock, 1991). The 1861–1862 Ma Burrell Creek Formation in the Central Domain of the Pine Creek Orogen contains paleoflow indicators near Pine Creek indicating a locally northerly trending current direction (Stuart-Smith et al., 1993), which differs from an inferred westerly source of detritus based on grain size variations (Needham and Stuart-Smith, 1984; Ahmad and Hollis, 2013). The available paleocurrent data are thus broadly consistent with at least one area of uplift north of the Lamboo Province and west of the Pine Creek Orogen, that is, beyond the currently preserved craton margin, but there are too few data to allow robust interpretations of regional sediment transport paths.

Evolution of the North Australian Craton: 1885–1830 Ma

Proto-craton assembly before c. 1885 Ma

The widespread 1885–1830 Ma metasedimentary successions in the North Australian Craton show striking similarities in provenance patterns and lithofacies associations, particularly after c. 1865 Ma. This implies a geographically extensive basin system developed on, or marginal to, crystalline basement assembled prior to basin formation. In some areas, for example, the Lamboo Province and possibly the Granites–Tanami Orogen, essentially conformable relationships between metasedimentary successions with the Detrital P provenance and underlying units deposited at 1885–1865 Ma suggests that this basin may have initiated at c. 1885 Ma. It thus follows that tectonism within the North Australian Craton post-dating formation of this basin system was not a result of convergence between terranes, but may have instead been driven by plate margin interactions outside the currently preserved craton margins, or was wholly intraplate.

It is notable that previous geodynamic models for the evolution of the Lamboo Province conflict with an interpretation of craton assembly prior to c. 1885 Ma. Most current models consider the Lamboo Province to have been assembled after this time, as a result of convergence between an exotic Kimberley Craton and the proto-North Australian Craton, with final collision during the 1837–1808 Ma Halls Creek Orogeny (Tyler et al., 1995; Griffin et al., 2000; Sheppard et al., 2001; Lindsay et al., 2016; Kohanpour et al., 2017; Mole et al., 2018). This interpretation is based on differences between crustal domains within the province, considered to be exotic terranes, and on the compositions of igneous rocks, some of which have compositions comparable to modern arcs. Limited detrital zircon dating of 1885–1830 Ma metasedimentary rocks in initial studies showed some differences in detrital zircon age components between the Western and Eastern Zones of the province (Tyler et al., 1999). However, as noted above, more recent work in the Western and Central Zones shows that many

units have Detrital P provenance signatures, and detrital zircon oxygen isotope characteristics comparable to those of similar-age rocks of the Halls Creek Group in the Eastern Zone and the Granites–Tanami Orogen (e.g. Kirkland et al., 2014; Lu et al., 2016a–e, 2017a–d, 2018a–e; Iaccheri et al., 2018; Mole et al., 2018). Hence, one possibility is that there are no exotic elements in the Lamboo Province, and that the similar provenance of metasedimentary rocks reflects a connection with the rest of the North Australian Craton at c. 1865 Ma. If this interpretation is correct, the geochemistry of igneous rocks in the Halls Creek Orogen may require re-evaluation in terms of intraplate processes, such as reworking of previously subduction-modified lithosphere.

Back-arc development from c. 1885 Ma?

The spatial patterns of felsic ± mafic magmatism and locally developed, low-pressure, high-temperature metamorphism (Fig. 16; Tyler et al., 1999; Carson et al., 2008), indicate that the locus of 1870–1855 Ma tectonism was situated around the northern margins of the currently preserved craton. In this area, most 1870–1855 Ma granitic rocks are potassic I-type or S-type, with low Sr/Y, and relatively evolved Sm–Nd and Lu–Hf isotope signatures, consistent with melting of Archean crustal sources under relatively high geothermal gradients (Budd et al., 2001). These granitic rocks can be placed in a broadly extensional continental setting, which may also have been the driver for subsidence, sedimentation and mafic magmatism during this period. Hollis and Glass (2012) suggested a continental arc setting for granitic rocks of the Nimbuwah Complex, based on the magnesian, calc-alkaline geochemical affinities of these rocks. However, similar-age mafic rocks in this area lack a clear arc-like signature (Hollis and Glass, 2012), raising the possibility that the geochemical signature of the granitic rocks was inherited from older basement rocks, consistent with the relatively evolved Sm–Nd and Hf isotope signatures of the felsic intrusions.

Many 1870–1845 Ma mafic rocks in northern Australia show elevated concentrations of large ion lithophile elements (LILE) and low concentrations of high field strength elements (HFSE). These signatures are consistent with emplacement in a regionally extensive continental back-arc setting, although they are not uniquely diagnostic. Mafic rocks in the Litchfield Province of the Pine Creek Orogen have geochemical signatures consistent with either a back-arc or oceanic arc setting (Glass, 2011), but a lack of other evidence for an oceanic setting for these rocks suggests that a back-arc is more likely. Mafic volcanic rocks of the c. 1865 Ma Tickalara Metamorphics in the Lamboo Province are hosted by metasedimentary rocks with the Detrital P provenance signature, and have geochemical characteristics that can be interpreted in terms of a back-arc/ensialic rift setting, or an oceanic arc (Sheppard et al., 1999). Basalts of a similar age within the Biscay Formation have characteristics similar to those emplaced in continental passive margins (Sheppard et al., 1999), while slightly younger mafic–ultramafic rocks emplaced in the Lamboo Province at c. 1845 Ma have characteristics consistent with a continental back-arc (Mole et al., 2018). The presence of 1865–1840 Ma metasedimentary units with the Detrital P provenance across the Lamboo Province limits the possibility of exotic terranes within the province, and collectively, the geochemistry of these mafic rocks can be interpreted in

the context of an extensional continental setting, possibly a back-arc if the geochemistry of these rocks was related to contemporary subduction. In the Arnhem Province, the oldest metasedimentary rocks were deposited after c. 1900 Ma, and experienced high-grade metamorphism at c. 1880 Ma. Associated mafic rocks have geochemical characteristics interpreted to reflect emplacement in a back-arc setting, consistent with the high geothermal gradient established at c. 1880 Ma (Whelan et al., 2017).

A back-arc setting at c. 1864 Ma has also been proposed for the Granites–Tanami Orogen on the basis of geochemical characteristics of mafic extrusive and intrusive rocks within the Stubbins Formation (Bagas et al., 2008; Li et al., 2013). These authors considered back-arc development to be related to a subduction zone between the Granites–Tanami Orogen and the Aileron Province, but if both terranes were contiguous at this time, any subduction would be constrained to have been external to this area. Partially inverted, west-northwesterly trending half-grabens inferred from seismic data by Joly et al. (2010) might reflect preservation of extensional structures associated with deposition of the Tanami Group. The 1885–1865 Ma architecture of the northern margins of the craton is not as well understood, but the presence of voluminous granitic rocks, high-temperature, low-pressure metamorphism and sedimentation may indicate that extension and crustal attenuation was greater in this area compared with areas to the south. This apparent polarity of tectonism suggests that if a subduction zone was the driver for intraplate extension, it may have been located to the north of the currently preserved craton margin (Fig. 19), though it should be noted that the nature of the southern margin of the craton is largely unconstrained for this period.

Crustal shortening in the northeastern North Australian Craton at 1870–1860 Ma

Moderate- to high-pressure metamorphism and deformation in the Arnhem Province and Nimbuwah Domain is consistent with a compressional orogenic event between c. 1880 and 1850 Ma that overprinted a previously established extensional domain with a relatively high geothermal gradient, possibly in a back-arc setting (Fig. 19). In the Arnhem Province, deformation during this period consists of asymmetric isoclinal folds with a locally developed, northwest- to northeast-steeply dipping foliation that developed synchronously with S-type granite emplacement. A clockwise P – T – t path peaking at up to ~8 kbar was followed by ~4 kbar of decompression by c. 1850 Ma, consistent with significant uplift and exhumation during an extended period of orogenesis (Whelan et al., 2017). In the Nimbuwah Domain, peak metamorphic conditions of 8–10 kbar attained during the c. 1865 Ma Nimbuwah Event may have been associated with west-verging folding and thrusting (Hollis et al., 2009b; Ahmad and Hollis, 2013). It is possible that the granitic magmatism emplaced in both the Nimbuwah Domain and Arnhem Province during this period reflects the combined effects of a high geothermal gradient established during back-arc formation at c. 1885 Ma and structural thickening during 1870–1860 Ma deformation.

The earlier onset of deformation and a hiatus in sedimentation in the Arnhem Province compared with the

Nimbuwah Domain may reflect a diachronous westwards propagation of deformation during the crustal shortening event. Areas farther to the south also experienced deformation at a slightly younger time, with east–west-trending isoclinal folding in the Murphy Province constrained to about 1853–1851 Ma, whereas upright, east–west trending folding in the Warramunga Province is constrained to c. 1850 Ma (Maidment et al., 2013). Further work is needed to determine whether the drivers for these events are related, or if they represent discrete events.

The possible drivers for deformation in the northeastern part of the craton are not well constrained, but conceivably reflect interactions along a subduction zone to the north or northeast of the currently preserved craton margin. In such a setting, crustal shortening could be a result of processes such as terrane accretion, a change in subduction dip, or rapid convergence relative to subduction (Cawood et al., 2009).

Hollis and Glass (2012) discussed the driver for this deformation, and proposed two alternatives: 1) compression caused by collision of the Kimberley Craton from the west, driving east-directed subduction between the Central and Nimbuwah Domains of the Pine Creek Orogen, or closure of an intraplate basin; 2) deformation as a result of west-directed subduction between the Nimbuwah Domain and Arnhem Province, related to arrival of a terrane from the east. In both models, granitic rocks of the Nimbuwah Complex are interpreted to be part of a magmatic arc, although, as noted above, other interpretations are possible. A collision of an inferred Kimberley Craton from the west is not favoured here, because the Kimberley Craton was either not an exotic terrane, as suggested by detrital zircon data, or collided with the proto-North Australian Craton at least 20 million years after the Nimbuwah Event (Griffin et al., 2000; Tyler et al., 2012). There is also no evidence to suggest that the Arnhem Province is exotic with respect to the Pine Creek Orogen, so if deformation was related to a plate margin to the east, it would have been situated outboard of the Arnhem Province, which has been interpreted to extend a significant distance east and north beneath the Gulf of Carpentaria (Frogtech Geoscience, 2018).

Granitic rocks intruded in the northwestern part of the craton at 1865–1855 Ma, after the onset of deformation in the northeast, do not have a clear association with significant crustal thickening. Carson et al. (2008) suggested that 1860–1855 Ma tectonism in the western Pine Creek Orogen was related to extension, and sedimentation in the western and central parts of the orogen may have continued to c. 1855 Ma (Ahmad and Hollis, 2013). In the Lamboo Province, deposition of younger parts of the succession locally continued through the period 1865–1840 Ma (e.g. Bodorkos et al., 2000b; Phillips et al., 2016), synchronous with mafic and ultramafic magmatism and high-temperature, low-pressure metamorphism that might also reflect intraplate extension. One possibility is that back-arc extension continued in the northwestern part of the craton during localized compressional deformation in the northeast. Another possibility is that granitic magmatism may have been generated by a short-lived compressional event during this extensional period, of which the c. 1860 Ma Hooper Orogeny in the western Lamboo Province may be an example.

Basin disruption at c. 1835 Ma

There are limited data constraining the youngest depositional ages of Detrital P turbiditic successions. In some areas, sedimentation appears to have been disrupted at 1855–1850 Ma (Fig. 15), particularly near the current northern craton margins, and in some parts of the interior (e.g. the Warramunga Province). Sedimentation in the Granites–Tanami Orogen and the Lamboo Province appears to have been the most long-lived, extending as young as c. 1840 Ma, when the Tanami Event/Halls Creek Orogeny commenced.

After 1840–1835 Ma there is a marked change in the character of sedimentation across the North Australian Craton. Sedimentary rocks formed between c. 1840 and 1815 Ma were typically deposited in fluvial to shallow-marine settings, marking a pronounced shallowing of water depths following the deposition of 1885–1840 Ma metasedimentary rocks. These 1840–1815 Ma successions commonly contain significant felsic volcanic rocks and lesser mafic volcanic rocks. They include the Ware Group in the Granites–Tanami Orogen, the Edith River and El Sherana Groups in the Central Domain of the Pine Creek Orogen and the Ooradidgee Group in the Tennant Region (Fig. 15). Sedimentation at this time was more localized than the older succession, consistent with restricted extensional depocentres, and was coincident with the emplacement of A-type granitic rocks in the northeastern Pine Creek Orogen and Arnhem Province (Ahmad and Hollis, 2013; Whelan et al., 2017). This post-orogenic extensional phase appears to mark a shift in the regional geodynamic setting, possibly involving a change to tectonism driven by events on the southern margin of the craton (see discussion below). It is notable that extension in the northeastern part of the craton at 1830–1815 Ma was broadly coeval with crustal shortening associated with the Tanami Event/Halls Creek Orogeny to the west. It is unclear whether these extensional and compressional regimes were related to a single tectonic driver or reflect essentially unrelated processes associated with different craton margins.

Granitic rocks and the Stafford Event: 1825–1790 Ma

Ages and compositions of granitic rocks in the Granites–Tanami Orogen

The geochronological data collected for granitic rocks of the Granites–Tanami Orogen as part of this study are complicated by significant ancient Pb loss, but the interpreted 1807–1800 Ma magmatic crystallization ages (Table 3) are consistent with those of other granitic rocks in the Western Australian part of the orogen. Dating reported by Bagas et al. (2010) also found complications from ancient Pb loss, and thus calculated ages using regressions through both concordant and discordant analyses. Upper intercept dates of 1797 ± 9 Ma for the Balwina Granite and 1796 ± 24 Ma for the Lewis Granite (Bagas et al., 2010) are indistinguishable from dates obtained in this study from multiple samples. An upper intercept date of 1793 ± 8 Ma for the Slatey Creek Granite (Bagas et al., 2010), not

dated in this study, is consistent with emplacement during the same magmatic event. The combined granite age dataset indicates this magmatism is associated with the 1810–1790 Ma Stafford Event.

Granitic rocks of the Granites–Tanami Orogen in the Northern Territory have been extensively dated and most have ages between c. 1816 and 1791 Ma (Smith, 2001; Cross et al., 2005a; Iaccheri, 2019). An 1844 ± 8 Ma date for the Inspiration Peak Monzogranite (Smith, 2001) is an outlier in this dataset, but as discussed above, this date conflicts with an 1802 ± 14 Ma age for the same intrusive body (Iaccheri, 2019), and as such its geological meaning is uncertain. The 1825 ± 5 Ma Winnecke Granophyre and 1821 ± 4 Ma Water Tower Tonalite (Birthday Suite intrusions) represent magmatism coeval with the emplacement of felsic volcanic rocks of the 1825–1815 Ma Ware Group. Unpublished dates of c. 1827 and 1825 Ma for felsic dykes cited by Bagas et al. (2014) overlap with this older magmatism. A histogram of 49 dates for 1815–1790 Ma granitic rocks (Fig. 20) suggests that magmatism may comprise several discrete pulses, as noted by Dean (2001), with modes at c. 1814, 1807, 1802 and 1793 Ma. There is no discernible difference between the ages of magnetic and non-magnetic phases of this magmatism (i.e. the Frederick and Grimwade Suites, respectively). The apparent crosscutting relationship between the non-magnetic and magnetic phases of the Lewis Granite in magnetic images thus appears to reflect distinct magmas batches emplaced during the same magmatic event.

Most of the granitic rocks in the Granites–Tanami Orogen are Sr-depleted and Y-undepleted, consistent with melting of source rocks at moderate depths under an elevated geothermal gradient (Budd et al., 2001). In contrast, three samples assigned to the Lewis Granite by Bagas et al. (2010) from the Selby Hills area in the far west of the orogen have high Sr/Y (40.9, 44.1 and 145.3). These rocks are more sodic ($K_2O/Na_2O = 0.48 - 0.64$), are relatively depleted in HREE ($La/Yb = 9.7 - 26.3$, with $Yb = 0.38 - 1.24$ ppm) and lack a negative Eu anomaly. These characteristics are similar to those of high silica adakites (Martin et al., 2005), possibly indicative of melting of, or interaction with, a mafic-dominated lower crust, where garnet is stable and plagioclase is unstable. Sm–Nd isotope data for one of these granitic rocks indicates a relatively isotopically evolved composition, with a T_{DM}^2 model age of 2.52 Ga, comparable to other samples from the Lewis Granite, which have T_{DM}^2 model ages of 2.53 and 2.70 Ga (Bagas et al., 2010). This suggests that the source of these granitic rocks may be dominated by mafic Neoproterozoic basement. The granitic rocks in this area have not been dated, so their relationship with the other granitic units in the area is uncertain. Relatively sodic high Sr/Y granitic rocks with geochemical characteristics similar to those in the Selby Hills area have also been identified at several localities in the Northern Territory, and most were included in the Frederick Suite by Dean (2001). Two of these intrusions have been dated. One component of the composite granitic body coring the Coomarie Dome (tentatively assigned by Dean [2001] to the what is now termed the Grimwade Suite) yielded a U–Pb zircon date of 1815 ± 5 Ma, whereas the Inspiration Peak Monzogranite has yielded U–Pb zircon dates of 1844 ± 4 Ma (Smith, 2001) and 1802 ± 14 Ma (Iaccheri, 2019).

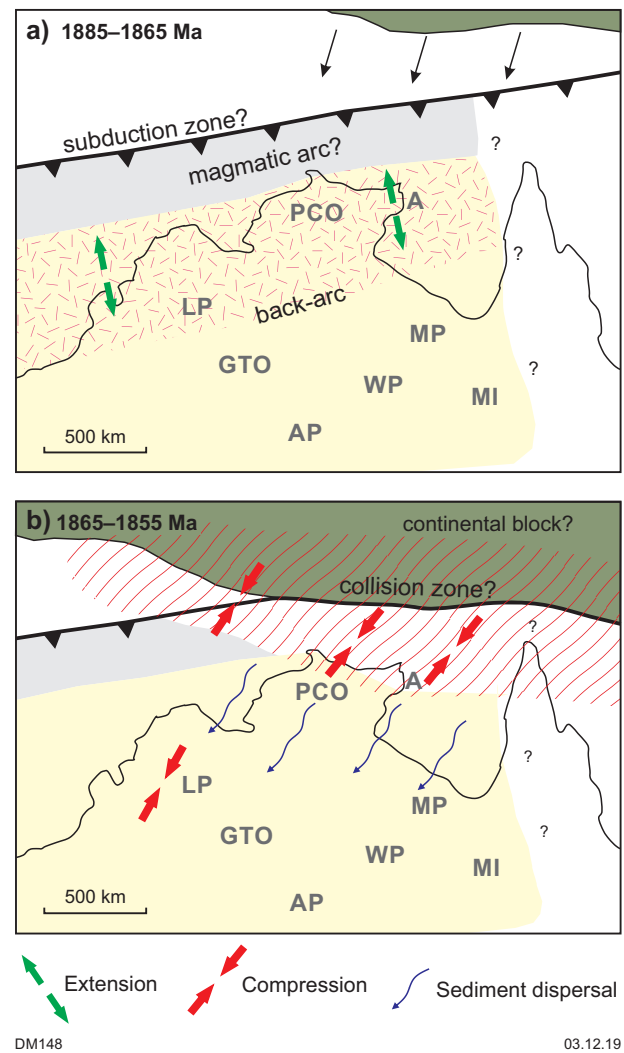


Figure 19. Possible geodynamic setting of regional sedimentation and magmatism in the North Australian Craton between 1885 and 1855 Ma: a) 1885–1865 Ma — extension-related tectonism and basin formation occurred in a broad back-arc setting related to subduction north of the preserved craton margin; b) plate margin interactions in the northeast at c.1865 Ma generated an orogen that shed sediment southwards across the craton (Detrital P provenance). Abbreviations: A, Arnhem Province; AP, Aileron Province; GTO, Granites–Tanami Orogen; MI, Mount Isa region; LP, Lamboos Province; PCO, Pine Creek Orogen; WP, Warramunga Province

The granitic rocks in the Granites–Tanami Orogen were thus generated over a period of more than 25 million years, likely within a domain having an elevated geothermal gradient. Most granitic rocks were derived from moderate crustal depths, with a smaller component derived from partial melting of mafic-rich lower crust. Relatively evolved zircon Hf and whole-rock Nd isotope values for the granitic rocks are consistent with involvement of both Archean basement and Tanami Group metasedimentary rocks, with the age spectrum of inherited zircons mirroring the Detrital P signature (Iaccheri, 2018). A complex mix of sources was envisaged by Iaccheri (2018), on the basis of wide ranges of isotope values for individual granitic rocks, and a spectrum of mantle-like and elevated zircon $\sigma^{18}O$ values.

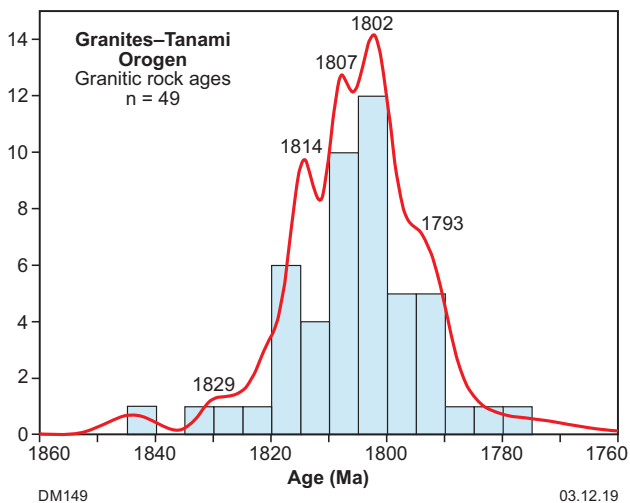


Figure 20. Histogram of ages for 1820–1780 Ma granitic rocks in the Granites–Tanami Orogen, incorporating data from this study, Page (1996c), Smith, (2001), Cross et al. (2005a), Bagas et al. (2010) and Iachheri et al. (2018)

1825–1790 Ma belt of magmatism and tectonism

Granitic rocks in the Granites–Tanami Orogen form part of a large belt of broadly coeval magmatism, approximately 100–150 km wide, which extends about 800 km from the southern Lamboo Province to the southeastern Aileron Province (Fig. 21; Green, 2002; Scrimgeour, 2013; Howlett et al., 2015). In the Granites–Tanami Orogen and northern Aileron Province, 1825–1790 Ma magmatism was voluminous and felsic-dominated, with comparable geochemical and isotope signatures (Green, 2002). In the southeastern Aileron Province, coeval magmatism contains a considerably higher proportion of mafic rocks, including mafic volcanic rocks, sills, dykes and larger intrusions emplaced between c. 1820 and 1780 Ma (Hoatson et al., 2005; Clauoué-Long and Hoatson, 2005; Scrimgeour, 2013; Beyer et al., 2016; Weisheit et al., 2016). In the western Aileron Province, low-K tholeiitic sills are considered to have been emplaced in an extensional setting as part of this magmatic event (Scrimgeour, 2013). Coeval sedimentation was sandstone-dominated in the central Aileron Province and siltstone- and carbonate-dominated in the southeast (Scrimgeour, 2013). No sedimentation of this age has been identified in the Granites–Tanami Orogen, possibly indicating a general northwards shallowing of depositional settings, or greater degrees of uplift and erosion in the Granites–Tanami Orogen during and after the Stafford Event.

The voluminous felsic and mafic magmatic rocks emplaced during the 1810–1790 Ma Stafford Event in the Aileron Province were associated with localized low-pressure, high-temperature metamorphism and rapid lateral changes in metamorphic grade (Scrimgeour, 2013). In the Mount Stafford area in the central Aileron Province, metamorphism was not associated with penetrative deformation, though melt migration into extensional shear zones and boudin necks has been observed (Greenfield et al., 1996). Elsewhere in the

central and northern Aileron Province, north- to northeast-trending upright folds have been assigned to this event (Scrimgeour, 2013). In the Granites–Tanami Orogen, F_2 and F_3 fold generations are assigned to the Stafford Event (Table 2), which was typically greenschist facies in this area, with higher grades only locally developed adjacent to intrusions (Bagas et al., 2010).

To the northwest of the Granites–Tanami Orogen, the Eastman Granite and San Sou Monzogranite in the southern Halls Creek Orogen are dated at 1804 ± 5 and 1788 ± 6 Ma, respectively (Fig. 21; Page et al., 2001). Two other granitic rocks from this area with dates of c. 1817 and 1808 Ma are currently considered to be part of the north-northeasterly trending Sally Downs Supersuite, which includes granitic rocks as old as c. 1850 Ma (Page et al., 2001). It is, however, possible that the 1817–1788 Ma granitic rocks in the southern Halls Creek Orogen are all part of the west-northwesterly trending magmatic belt. In the Kimberley Basin, farther to the northwest, similar-age mafic sills of the Hart Dolerite and coeval basaltic rocks of the Carson Volcanics comprise the voluminous (300 000 km³) Hart–Carson large igneous province (LIP) (Tyler et al., 2006; Sheppard et al., 2012, Orth, 2015; Ramsay et al., 2019). Granophyre within the Hart Dolerite has a U–Pb zircon age of 1799 ± 17 Ma (Sheppard et al., 2012) and a U–Pb baddeleyite age of 1795 ± 15 Ma (Sheppard et al., 2012). Recent geochronology of gabbroic rocks provided a more precise U–Pb crystallization age of 1793 ± 1 Ma (Ramsay et al., 2019). Emplacement of the Hart–Carson LIP within the subsiding Kimberley Basin therefore overlapped with the latter stages of the dominantly felsic Stafford Event magmatism in the Granites–Tanami Orogen and Aileron Province.

Geodynamic setting of the Stafford Event

The craton-scale patterns of magmatism and tectonism between c. 1825 and 1790 Ma provide regional context for interpreting the geodynamic setting of the Stafford Event. In the southeastern Aileron Province, bimodal magmatism, sedimentation, high thermal gradients and VMS-style mineralization have been interpreted in terms of extension, possibly within a back-arc basin developed inboard of a convergent continental margin to the south (Hoatson et al., 2005; Scrimgeour, 2006; Cawood and Korsch, 2008; Howlett et al., 2015; McGloin et al., 2016). High thermal gradients in this area were maintained for an extended period, until at least c. 1700 Ma (Clauoué-Long et al., 2008c; Reno et al., 2017). Elsewhere in the Aileron Province, widespread low-pressure, high-temperature metamorphism and near-isobaric cooling at this time is also consistent with an extensional setting (Cawood and Korsch, 2008). Felsic magmatism in this setting may be a consequence of an elevated geothermal gradient resulting from crustal thinning and emplacement of mafic rocks. Deformation assigned to this event may reflect short-lived contraction driven by plate margin processes within an otherwise extensional setting.

In contrast to the dominantly extensional setting proposed for the Aileron Province, Bagas et al. (2010) suggested that granitic magmatism, folding and orogenic Au mineralization in the Granites–Tanami Orogen was a result of crustal thickening during a collision with the Aileron

Province. These authors interpreted the geochemistry of 1865–1850 Ma mafic rocks in the Stubbins and Mount Charles Formations in terms of emplacement in a back-arc basin northwest of a subduction zone proposed to have separated the Granites–Tanami Orogen and the Aileron Province (Bagas et al., 2008; Li et al., 2013). A major deep crustal feature evident in seismic data near the boundary between the two domains is associated with thickening of the crust from about 42 km to 60 km (Goleby et al., 2009), and is coincident with the southern edge of the east-northeasterly trending Willowra gravity high (Fig. 3; Bagas et al., 2008). The Willowra feature marks a major change in the orientation of the lower crustal structural grain and has been proposed as a collisional suture between the Granites–Tanami Orogen and the Aileron Province (Goleby et al., 2009; Bagas et al., 2010; Betts et al., 2016). However, a minimum age for this feature is provided by the Killi Killi and Lander Rock Formations, which form a continuous sedimentary package that overlies the Willowra feature in the deeper crust (Claoué-Long, 2006; Goleby et al., 2009). The Dead Bullock Formation and its correlatives are conformable with the overlying Killi Killi Formation, so it follows that any collision of the Granites–Tanami Orogen and Aileron Province pre-dated deposition of the entire 1885–1835 Ma Tanami Group. On this basis, the

1825–1790 Ma felsic magmatism cannot be related to a collision between these two domains.

An alternative explanation of Stafford Event tectonism in the Granites–Tanami Orogen expands the dominantly extensional regime of the southeastern Aileron Province northwestwards, and invokes transient shortening events during a long-lived period of extension. This is consistent with locally developed high-temperature, low-pressure metamorphism, and relatively high geothermal gradients implied by the low Sr/Y values of most granitic rocks in the Granites–Tanami Orogen. While it is true that extensional collapse of a collisional orogen could produce similar granitic compositions (Li et al., 2013), the minimum timing constraints on any such collision imposed by 1885–1835 Ma sedimentary rocks that cover the lower crustal structure between the two domains precludes a continental collision immediately pre-dating the Stafford Event. In addition, the Tanami and Ware Group sedimentary rocks that pre-date the Stafford Event are of relatively low metamorphic grade, except near contacts with granitic rocks, and show no evidence that deep burial occurred during the Stafford Event. The interpretation of only partially inverted extensional structures in seismic data (Joly et al., 2010) is also difficult to reconcile with a major collision after deposition of the Tanami Group.

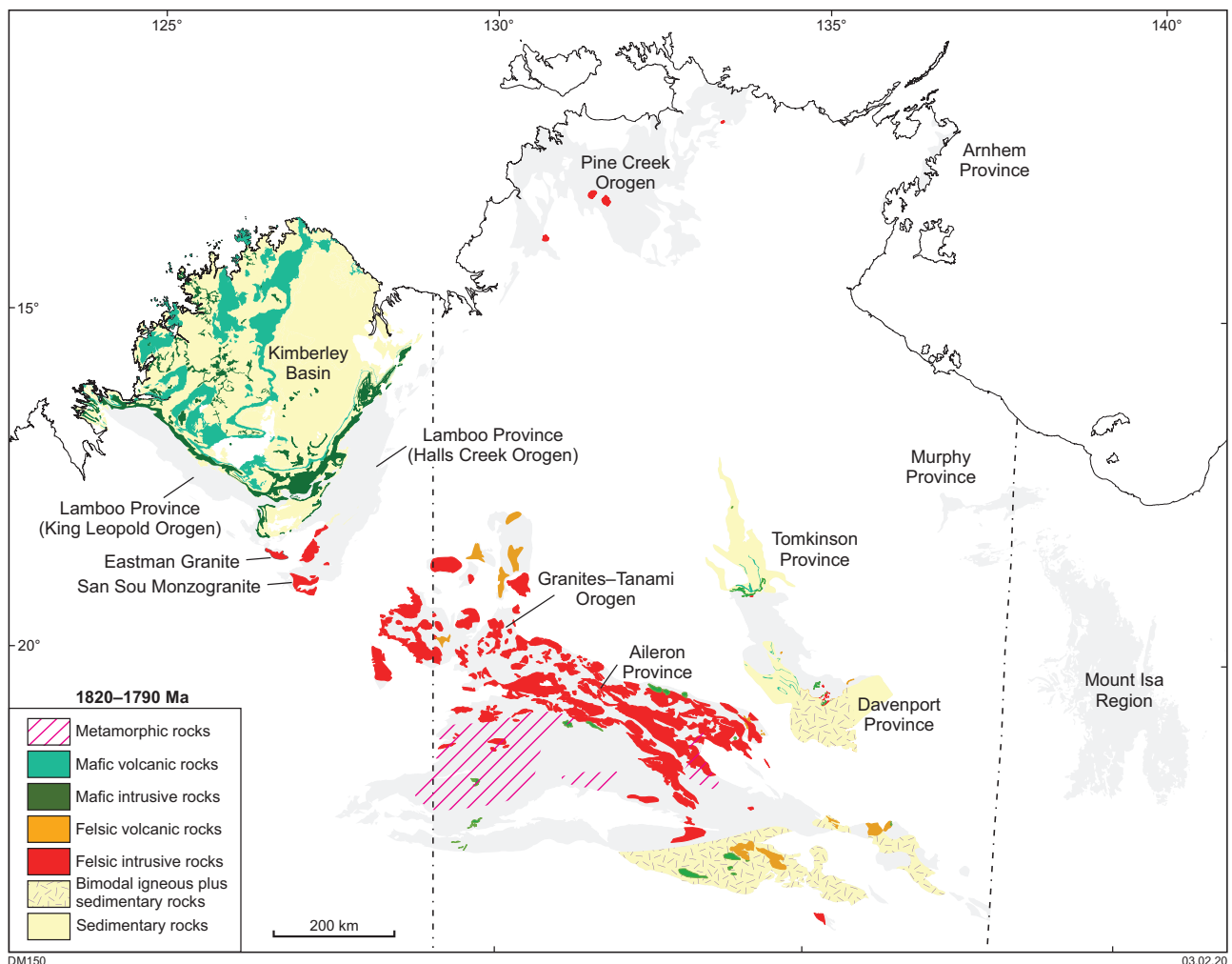


Figure 21. Distribution of areas in the North Australian Craton (exposed and interpreted beneath shallow cover) that preserve a record of 1820–1790 Ma sedimentation, magmatism and tectonism. Based on Ahmad and Scrimgeour (2006), Scrimgeour (2013) and GSWA (2016a)

Widespread upright folding (D_2 – D_3 events in Table 2), fault movement and orogenic Au mineralization in the Granites–Tanami Orogen at c. 1800 Ma indicate that some crustal shortening took place during the period of magmatism. It is possible that these compressional phases were relatively short-lived events within the >25 million year period of magmatism, focused on a domain that was rheologically weak as a result of this magmatism and an associated high geothermal gradient. In this scenario, the apparent temporal ‘pulses’ of granitic magmatism during the Stafford Event (Fig. 20) might reflect switching between compression and extension.

It is possible that the felsic and lesser mafic magmatic rocks of the 1825–1815 Ma Birthday Suite represent the earliest phase of magmatism associated with the Stafford Event in the Granites–Tanami Orogen. An extensional setting for the Birthday Suite was suggested by Dean (2001) on the basis of its bimodal character, similar to the extensional setting proposed for the 1829–1822 Ma felsic volcanic and lesser basaltic rocks in the El Sherana and Edith River Groups in the Pine Creek Orogen, with which the Ware Group has been correlated (Crispe et al., 2007; Ahmad and Hollis, 2013; Ahmad et al., 2013b). If this is the case, the Stafford Event may span the period 1825–1790 Ma rather than the 1810–1790 Ma range typically assigned to this event. Minor c. 1800 Ma dolerite dykes in the Granites–Tanami Orogen, interpreted to reflect post-collisional extension by Li et al. (2013), could instead be a consequence of intraplate extension unrelated to a collision.

Within the Granites–Tanami Orogen, the volumetrically smaller, relatively sodic granitic rocks with high Sr/Y and steep REE patterns are indicative of deep melting of mafic-rich sources (Dean, 2001). Zircons in these high Sr/Y granitic rocks have $\delta^{18}\text{O}$ values only slightly higher than mantle values, and evolved Hf isotope signatures, implying a lower crustal source dominated by mafic Archean rocks that have not interacted with surficial processes (Iaccheri, 2018). The relatively deep melting implies some crustal thickening took place prior to, or synchronous with, granite emplacement. Given the constraints outlined above, any major structural thickening is likely to have taken place before deposition of the Tanami Group, though some thickening during the D_1 event is possible. In the dominantly extensional setting proposed here for the Stafford Event, sodic, high Sr/Y granitic rocks were formed by partial melting of mafic-dominated Archean lower crust during extension, while potassic, low Sr/Y granitic rocks were sourced from more extensive melting of crust of intermediate composition at shallower crustal depths. A similar process has been invoked for Quaternary adakitic volcanic rocks in Papua New Guinea, where older subduction- and collision-modified lithosphere was tapped during younger rifting (Haschke and Ben-Avraham, 2005).

A dominantly extensional setting for 1820–1790 Ma magmatism in the Granites–Tanami Orogen is consistent not only with the adjacent Aileron Province, but also with coeval extensional settings apparent in other parts of the craton. In the Kimberley region, compressional deformation of the Halls Creek Orogeny commenced at c. 1837 Ma (Bodorkos et al., 2000a) and ceased before intrusion of an 1808 ± 3 Ma granitic rock that cross cuts structures formed during this event (Page et al., 2001; Tyler et al., 1998). The Kimberley Basin unconformably overlies rocks affected by the Halls Creek Orogeny, and

formed a broad, shallow depression infilled by fluvial to shallow-marine sedimentary rocks deposited after 1814 ± 10 Ma (Ramsay et al., 2017; Phillips et al., 2017). Progressive, gentle subsidence was accompanied by the emplacement of voluminous mafic rocks of the c. 1793 Ma Hart–Carson large igneous province in the middle part of the succession (Tyler et al., 2006; Sheppard et al., 2012). A mantle plume-related origin is not required to explain the geochemical characteristics of this magmatism (Tyler et al., 2006), and the setting is more consistent with passive extension, with magmatism post-dating initiation of the basin, and no evidence of plume-related regional uplift. The greatest thickness of mafic rocks is in the southwest of the Kimberley Basin, and they thin towards the northeast (Tyler et al., 2006). This suggests a locus of extension situated along the southwest margin of the basin, along strike from the west-northwesterly trending belt of 1820–1790 Ma magmatism across central Australia. The transition between dominantly mafic magmatism in the Kimberley region and dominantly felsic magmatism in central Australia is marked by the Halls Creek Orogen (Fig. 21). The reasons for the difference in magmatic character on either side of the orogen are currently unclear, but the orogen is likely to have remained a zone of relative weakness following the Halls Creek Orogeny, since it experienced slow average rates of cooling following deformation and magmatism (Bodorkos and Reddy, 2004). This orogen thus appears to have formed a discontinuity that separated crustal domains that responded to extension in a different manner.

Further regional context for Stafford Event magmatism in the Granites–Tanami Orogen is provided by magmatism and sedimentation of a similar age in the Davenport and Tomkinson Provinces, northeast of the Aileron Province (Fig. 21). In this area, tectonism during the 1820–1800 Ma period is described as extensional (the Murchison Event) and was associated with the emplacement of bimodal volcanic and intrusive rocks in a shallow-marine to fluvial depositional setting (Blake et al., 1987; Claoué-Long et al., 2008a; Donnellan, 2013). U–Pb zircon dating of felsic volcanic rocks and a mafic dyke have yielded ages of 1814–1805 Ma (Claoué-Long et al., 2008a; Kositsin et al., 2013b). The magmatic rocks are most voluminous and occur over a broader stratigraphic range in the south (Davenport Province), and are represented by only a single basaltic unit in the north (Tomkinson Province). This suggests that the area of greatest extension may have been in the south, immediately adjacent to the 1820–1790 Ma Aileron Province granitic rocks.

The tectonic driver for extension inferred across the North Australian Craton at this time is not clear, but if the back-arc basin setting interpreted for the southeastern Aileron Province is correct (Weisheit et al., 2016; Reno et al., 2017), it is possible that all magmatism along the belt was a result of processes related to convergence along the southern craton margin. This would imply that this margin had a similar orientation to the magmatic belt, that is, west-northwesterly in current coordinates.

The patterns of tectonism noted above have similarities with extensional, or retreating, accretionary orogens (Collins, 2002; Cawood et al., 2009). These orogens are characterized by the development of large back-arc basin systems during prolonged slab rollback and are associated with widespread felsic and minor mafic magmatism,

regional low-pressure, variable-temperature metamorphism and the development of rift basins. The extensional regime developed in this setting is commonly interrupted by short-lived compressional events caused by the arrival of blocks of more buoyant crust into the subduction zone, or periods where slab rollback was stationary or advancing relative to the overriding plate. Deformation and orogenic Au mineralization in the Granites–Tanami Orogen during the Stafford Event was broadly coeval with unconformity-related U mineralization in the Pine Creek Orogen (Mercadier et al., 2013) and could be a response to one or more of these transient compressional events. Relating the magmatism to convergence along the southern margin of the craton requires that this margin was open along its entire length, and that the West Australian Craton had not yet amalgamated with the North Australian Craton. This is consistent with recent studies that suggest this collision could have taken place as late as c. 1300 Ma (Anderson, 2015; Maidment, 2017).

After c. 1780 Ma, the locus of tectonism migrated southwards, and possibly rotated counter-clockwise, to form a broadly east–west trending belt across the southern half of the Aileron Province. Tectonism between c. 1780 and 1740 Ma comprised widespread felsic and mafic magmatism, high-temperature, medium-pressure metamorphism, and localized sedimentation (Scrimgeour, 2013). Some of the felsic magmatism in the southeast Aileron Province during this period has been interpreted to be arc-related (Foden et al., 1988; Zhao and McCulloch, 1995; Beyer et al., 2016), and the setting for the southern Aileron Province is consistent with a back-arc (Howlett et al., 2015). One possibility is that this southwards migration of tectonism reflects an evolving convergent margin driven by processes such as slab rollback.

Neoproterozoic–Paleozoic isotopic disturbance

Many of the zircon samples in this study contain evidence of isotopic disturbance, particularly in high-U zircons, or zircons with irregular dark-CL domains (e.g. Fig. 8c,d). Some of these discordia trends are consistent with Pb loss during recent weathering, but a significant number also show clear evidence of ancient Pb loss (Table 3). Lower concordia intercepts are difficult to define with precision, particularly where multiple age components are present and recent Pb loss also took place. However, the samples show consistent discordia towards ages in the latest Neoproterozoic to early Paleozoic (approximately 650–400 Ma). Similar discordia were noted in Granites–Tanami Orogen dating by Bagas et al. (2010), with lower intercept dates in the range 600–400 Ma. Other instances are noted in dating of granitic rocks in the Browns Range Dome in the northwest of the orogen (Nazari-Dehkordi et al., 2017) and a smaller number of samples of granitic rocks in the central and southeastern part of the orogen (Smith, 2001; Cross et al., 2005a). Slightly younger lower intercept ages were obtained in thermal ionization mass spectrometry zircon dating by Cooper and Ding (1997), but their dated samples were multigrain mixtures of zircons which necessarily blend age components.

Neoproterozoic to early Paleozoic isotopic disturbance is most commonly observed in the northwestern and western

parts of the orogen and only sporadically farther to the southeast. Candidate processes for isotopic disturbance include ancient near-surface weathering or hydrothermal fluid flow driven by thermal or tectonic processes. Tectonic drivers could include intraplate deformation that affected central Australia between c. 650 and 400 Ma: the Petermann Orogeny in the Musgrave Province; the King Leopold Orogeny in the Lamboo Province; the Miles and Paterson Orogenies of the Paterson Orogen; or multiple events that comprise the Alice Springs Orogeny in central Australia. However, the observation that the apparent 600–400 Ma Pb loss is best developed in the northwest of the Granites–Tanami Orogen may implicate, instead, the local emplacement of the Antrim Plateau Volcanics, which forms part of the 510–500 Ma Kalkarindji LIP (Glass and Phillips, 2006; Glass et al., 2013; Jourdan et al., 2014; Marshall et al., 2018). The thickest and most extensive area of this magmatism is located to the northwest of the Granites–Tanami Orogen, thinning from about 1100 m in the eastern Kimberley region to about 500 m in the area 80 km northeast of the Browns Range Dome (Gole and Ashley, 2003; Gole and Lee, 2005, 2006). Erosional remnants are >30 m thick in the Granites–Tanami Orogen, where they extend southwards as a discontinuous belt <30 km wide (Blake et al., 1979). One possibility is that the U–Pb isotopic disturbance observed in zircons in the northwestern part of the orogen is a result of thermally driven fluid flow in crust in the vicinity of this major magmatic and thermal event.

Conclusions

Dating of detrital zircons from the Tanami Group, combined with data from previous studies, shows that the lower part of the succession (lower Dead Bullock Formation) is dominated by Archean detritus (Detrital A provenance), whereas the upper part (Killi Killi Formation) is dominated by 1870–1865 Ma ages with a minor 2500 Ma age component (Detrital P provenance). The Mount Charles Formation in the Tanami Goldfield is also dominated by Detrital A provenance and may be a correlative of the lower Dead Bullock Formation. The upper Stubbins Formation in Western Australia has a Detrital P provenance, with maximum depositional ages of 1874–1865 Ma. The detrital zircon age spectrum and felsic geochemical signature of this part of the unit is comparable with the Killi Killi Formation, while the presence of mafic units and laminated chemical sedimentary rocks is similar to that of the Dead Bullock Formation, and may indicate a stratigraphic position as a correlative of a transitional zone between the two units. The undated lower part of the Stubbins Formation is potentially a correlative of stratigraphically lower parts of the Dead Bullock Formation. A felsic igneous unit in the Stubbins Formation, previously interpreted as a volcanic horizon dating deposition at c. 1864 Ma, is here reinterpreted to contain only xenocrystic zircon and thus not constrain the timing of sedimentation more tightly than the maximum depositional ages of the host metasedimentary rocks. The 1885–1835 Ma Halls Creek Group in the Lamboo Province is comparable to the Tanami Group in terms of lithostratigraphy, changes in provenance and thickness, and the Tanami Group is likely to have been deposited over a similar age range.

The abundance of Archean detrital zircon ages in the lower Tanami Group (1885–1870 Ma) is also typical of the oldest Paleoproterozoic units overlying Neoproterozoic basements elsewhere in the North Australian Craton, and may reflect derivation from basement sources within the craton. Basins developed at this time may have formed in a back-arc setting associated with south-directed subduction north of the currently preserved craton margin. Granitic rocks emplaced at 1870–1865 Ma in the northern margins of the craton were associated with high-temperature, low-pressure metamorphism and may reflect zones of greater extension.

Younger (1865–1835 Ma) turbiditic metasedimentary rocks with the Detrital P signature are widespread across the North Australian Craton and are interpreted to represent parts of a linked sedimentary system that provides a minimum age constraint for craton assembly. Deformation at c. 1865 Ma in the northeastern part of the craton may represent part of a larger orogen that impinged on the postulated back-arc. Uplift and exhumation as part of this event may have exposed 1870–1865 Ma granitic rocks to provide a source for the dominant age component in the Detrital P provenance signature.

Dating of the Lewis and Balwina Granites in the Western Australian part of the Granites–Tanami Orogen yielded magmatic ages of 1807–1800 Ma, indicating that they form part of the widespread 1825–1790 Ma felsic magmatism emplaced during the Stafford Event. Magmatism of this age forms a belt extending >800 km from the southeast Aileron Province to the southern Lamboo Province. Regional geological constraints suggest this magmatism was emplaced in a dominantly extensional setting, though folding and orogenic Au mineralization in the Granites–Tanami Orogen c. 1800 Ma indicates at least some crustal shortening took place during this period. Magmatism, low-pressure, high-temperature metamorphism and sedimentation between c. 1825 and 1790 Ma may reflect prolonged back-arc extension related to subduction along the southern margin of the craton. Transient shortening events interrupting this extension may reflect changes in plate margin conditions, forming a driver for orogenic Au mineralization in the Granites–Tanami Orogen.

The post-orogenic Gardiner Sandstone of the Birrindudu Basin contains detrital zircon age components that appear to reflect reworking of the underlying Tanami Group and the depositional age of this unit remains imprecisely constrained to 1768–1632 Ma. Isotopic disturbance in many zircon samples from the Granites–Tanami Orogen occurred between the latest Neoproterozoic and early Paleozoic, and is most strongly developed in the northwestern and western parts of the orogen. Although this could reflect uplift and weathering related to 650–300 Ma intraplate deformation, the spatial patterns of disturbance suggests it may have been related to emplacement of the c. 510 Ma Kalkarindji LIP.

References

- Adams, GJ 1991, Structural evolution and ore genesis of The Granites gold deposits, Northern Territory: The University of Adelaide, BSc (Hons) thesis, 243p. (unpublished).
- Adams, GJ, Both, RA and James, P 2007, The Granites gold deposits, Northern Territory, Australia: evidence for an early syn-tectonic ore genesis: *Mineralium Deposita*, v. 42, p. 89–105.
- Ahmad, M and Hollis, JA 2013, Chapter 5: Pine Creek Orogen, in *Geology and mineral resources of the Northern Territory compiled by M Ahmad and TJ Munson*: Northern Territory Geological Survey, Special Publication 5, p. 5:1–5:133.
- Ahmad, M, Munson, TJ and Wygralak, AS 2013a, Chapter 8: Murphy Province, in *Geology and mineral resources of the Northern Territory compiled by M Ahmad and TJ Munson*: Northern Territory Geological Survey, Special Publication 5, p. 8:1–8:8.
- Ahmad, M and Scrimgeour, IR 2006, Geological map of the Northern Territory (1:2 500 000 scale): Northern Territory Geological Survey.
- Ahmad, M, Vandenberg, LC and Wygralak, AS 2013b, Chapter 11: Tanami Region, in *Geology and mineral resources of the Northern Territory compiled by M Ahmad and TJ Munson*: Northern Territory Geological Survey, Special Publication 5, p. 11:1–11:41.
- Anderson, J 2015, Metamorphic and isotopic characterisation of Proterozoic belts at the margins of the North and West Australian Cratons: University of Adelaide, PhD thesis, 149p. (unpublished).
- Bagas, L, Anderson, JAC and Bierlein, FP 2009, Palaeoproterozoic evolution of the Killi Killi Formation and orogenic mineralization in the Granites–Tanami Orogen, Western Australia: *Ore Geology Reviews*, v. 35, p. 47–67.
- Bagas, L, Bierlein, FP, Anderson, JAC and Maas, R 2010, Collision-related granitic magmatism in the Granites–Tanami Orogen: *Precambrian Research*, v. 177, p. 212–226.
- Bagas, L, Bierlein, FP, English, L, Anderson, J, Maidment, D and Huston, DL 2008, An example of a Paleoproterozoic back-arc basin: petrology and geochemistry of the ca. 1864 Ma Stubbins Formation as an aid towards an improved understanding of the Tanami Orogen, Western Australia: *Precambrian Research*, v. 166, no. 1–4, p. 168–184.
- Bagas, L, Boucher, R, Li, B, Miller, J, Hill, P, Depauw, G, Pascoe, J and Eggers, B 2014, Paleoproterozoic stratigraphy and gold mineralisation in the Granites–Tanami Orogen, North Australian Craton: *Australian Journal of Earth Sciences*, v. 61, p. 89–111, doi:10.1080/08120099.2013.784220.
- Bagas, L, Huston, DL, Anderson, J and Mernagh, TP 2007a, Paleoproterozoic gold deposits in the Bald Hill and Coyote areas, Western Tanami, Western Australia: *Mineralium Deposita*, v. 42, p. 127–144.
- Bagas, L, Huston, DL, Anderson, JAC and Bierlein, FP 2007b, Coyote gold deposit, Granites–Tanami Orogen, Western Australia, in *Geological Survey of Western Australia Annual Review 2005–06*: Geological Survey of Western Australia, p. 81–85.
- Betts, PG, Armit, RJ, Stewart, J, Aitken, ARA, Ailleres, L, Donchak, P, Hutton, L, Withnall, I and Giles, D 2016, Australia and Nuna, in *Supercontinent Cycles Through Earth History edited by ZX Li, DAD Evans and JB Murphy*: Geological Society, London: Special Publication 424, p. 47–81, doi:10.1144/SP424.2.
- Betts, PG and Giles, D 2006, The 1800–1100 Ma tectonic evolution of Australia: *Precambrian Research*, v. 144, p. 92–125.
- Beyer, EE, Hollis, JA, Whelan, JA, Glass, LM, Donnellan, N, Yaxley, G, Armstrong, R, Allen, C and Scherstén, A 2013, Summary of results NTGS laser ablation ICPMS and SHRIMP U–Pb, Hf and O, geochronology project: Pine Creek Orogen, Arunta Region, Georgina Basin and McArthur Basin, July 2008 – May 2011: Northern Territory Geological Survey, Record 2012-007, 205p.
- Beyer, EE, Reno, BL, Whelan, JA and Weisheit, A 2016, Geochemical evidence for an evolving tectonic setting in the northeastern Aileron Province, central Australia, in *Abstracts: Uncover Earth's Past to Discover Our Future, AESC 2016 — Australian Earth Sciences Convention, Adelaide, 26–30 June*: Geological Society of Australia, p. 40.

- Bierlein, FP, Black, LP, Hergt, J and Mark, G 2008, Evolution of pre-1.8 Ga basement rocks in the western Mt Isa Inlier, northeastern Australia — insights from SHRIMP U–Pb dating and in-situ Lu–Hf analysis of zircons: *Precambrian Research*, v. 163, p. 159–173.
- Bierlein, FP, Maas, R and Woodhead, J 2011, Pre-1.8 Ga tectono-magmatic evolution of the Kalkadoon–Leichhardt Belt: implications for the crustal architecture and metallogeny of the Mount Isa Inlier, northwest Queensland, Australia: *Australian Journal of Earth Sciences*, v. 58, p. 887–915.
- Black, LP, Kamo, SL, Allen, CM, Davis, DW, Aleinikoff, JN, Valley, JW, Mundil, R, Campbell, IH, Korsch, RJ, Williams, IS and Foudoulis, CF 2004, Improved $^{206}\text{Pb}/^{238}\text{U}$ microprobe geochronology by the monitoring of trace-element-related matrix effect: SHRIMP, ID–TIMS, ELA–ICP–MS and oxygen isotope documentation for a series of zircon standards: *Chemical Geology*, v. 205, p. 115–140.
- Black, LP, Kamo, SL, Williams, IS, Mundil, R, Davis, DW, Korsch, RJ and Foudoulis, CF 2003, The application of SHRIMP to Phanerozoic geochronology: a critical appraisal of four zircon standards: *Chemical Geology*, v. 200, p. 171–188.
- Blake, DH, Hodgson, IM and Muhling, PC 1979, Geology of The Granites–Tanami region, Northern Territory and Western Australia: Bureau of Mineral Resources, Geology and Geophysics, Bulletin 197, 91p.
- Blake, DH, Hodgson, IM and Smith, PA 1975, Geology of the Birrindudu and Tanami 1:250 000 sheet areas, Northern Territory: Bureau of Mineral Resources, Report 174, 70p.
- Blake, DH, Stewart, AJ, Sweet, IP and Hone, IG 1987, Geology of the Proterozoic Davenport province, central Australia: Bureau of Mineral Resources, Bulletin 226, 108p.
- Blake, DH, Tyler, IM and Warren, RG 2000, Gordon Downs, Western Australia – 1:250,000 Geological Series (2nd Edition): Australian Geological Survey Organisation, Explanatory Notes SE/52–10, 58p.
- Bodorkos, S, Beyer, EE, Edgoose, CJ, Whelan, JA, Webb, G, Vandenberg, LC and Hallett, L 2013, Summary of results. Joint NTGS–GA geochronology project: central and eastern Arunta Region, January 2008 – June 2011: Northern Territory Geological Survey, Record–2013-003, 74p.
- Bodorkos, S, Cawood, PA and Oliver, HS 2000a, Timing and duration of syn-magmatic deformation in the Mabel Downs Tonalite, northern Australia: *Journal of Structural Geology*, v. 22, p. 1181–1198.
- Bodorkos, S, Cawood, PA, Oliver, NHS and Nemchin, AA 2000b, Rapidity of orogenesis in the Paleoproterozoic Halls Creek Orogen, northern Australia: evidence from SHRIMP zircon data, CL zircon images, and mixture modeling studies: *American Journal of Science*, v. 300, no. 1, p. 60–82.
- Bodorkos, S, Oliver, NHS and Cawood, PA 1999, Thermal evolution of the central Halls Creek Orogen, northern Australia: *Australian Journal of Earth Sciences*, v. 46, p. 453–465.
- Bodorkos, S and Reddy, SM 2004, Proterozoic cooling and exhumation of the northern Central Halls Creek Orogen, Western Australia: constraints from a reconnaissance $^{40}\text{Ar}/^{39}\text{Ar}$ study: *Australian Journal of Earth Sciences*, v. 51, p. 591–609.
- Budd, AR, Wyborn, LAI and Bastrakova, IV 2001, The metallogenic potential of Australian Proterozoic granites: *Geoscience Australia, Record 2001/12*, 152p.
- Carson, CJ 2013, The Victoria and Birrindudu Basins, Victoria River region, Northern Territory, Australia: a SHRIMP U–Pb detrital zircon and Sm–Nd study: *Australian Journal of Earth Sciences*, v. 60, p. 175–196, doi:10.1080/08120099.2013.772920.
- Carson, CJ, Clauoué-Long, J, Stern, R, Close, DF, Scrimgeour, IR and Glass, LM 2009, Summary of results, Joint NTGS–GA geochronology project: Central and eastern Arunta Region and Pine Creek Orogen, July 2006 – May 2007 (CD): Northern Territory Geological Survey, Record 2009-001.
- Carson, CJ, Hollis, JA, Glass, LM, Close, DF, Whelan, JA and Wygralak, A 2011a, Summary of results, Joint NTGS–GA geochronology project: Pine Creek Orogen, eastern Arunta Region, Murphy Inlier and Amadeus Basin, July 2007 – June 2009: Northern Territory Geological Survey, Record 2010-004, 84p.
- Carson, CJ, Hutton, LJ, Withnall, IW, Perkins, WG, Donchak, PJT, Parsons, A, Blake, PR, Sweet, IP, Neumann, NL and Lambeck, A 2011b, Summary of results: Joint GSQ–GA NGA geochronology project, Mount Isa region, 2009–2010: Queensland Geological Survey, Record 2011/03, 212p.
- Carson, CJ, Worden, KE, Scrimgeour, IR and Stern, RA 2008, The Palaeoproterozoic evolution of the Litchfield Province, western Pine Creek Orogen, northern Australia: Insight from SHRIMP U–Pb zircon and in situ monazite geochronology: *Precambrian Research*, v. 166, p. 145–167.
- Cawood, PA and Korsch, RJ 2008, Assembling Australia: Proterozoic building of a continent: *Precambrian Research*, v. 166, no. 1–4, p. 1–38.
- Cawood, PA, Kröner, A, Collins, WJ, Kusky, TM, Mooney, WD and Windley, BF 2009, Accretionary orogens through Earth history, in *Earth Accretionary Systems in Space and Time edited by PA Cawood and A Kröner*: Geological Society, London, Special Publication 318, p. 1–36.
- Clauoué-Long, J 2006, Arunta–Tennant–Tanami: the early evolution to ca. 1700 Ma, in *Evolution and metallogenesis of the North Australian Craton, Conference Abstracts edited by P Lyons and DL Huston: Evolution and metallogenesis of the North Australian Craton, Alice Springs, 20 June 2006*: Geoscience Australia, Record 2006/16, p. 3–7.
- Clauoué-Long, J, Maidment, D and Donnellan, N 2008a, Stratigraphic timing constraints in the Davenport Province, central Australia: A basis for Palaeoproterozoic correlations: *Precambrian Research*, v. 166, p. 204–218.
- Clauoué-Long, J, Maidment, D, Hussey, K and Huston, D 2008c, The duration of the Strangways Event in central Australia: Evidence for prolonged deep crust processes: *Precambrian Research*, v. 166, p. 246–262.
- Clauoué-Long, JC, Compston, W, Roberts, J and Fanning, CM 1995, Two Carboniferous ages: a comparison of SHRIMP zircon dating with conventional zircon ages and $^{40}\text{Ar}/^{39}\text{Ar}$ analysis, in *Geochronology, time scales and global stratigraphic correlation edited by WA Berggren, DV Kent, M-P Aubry and J Hardenbol*: Society for Sedimentary Geology, Special Publication 54, p. 3–21.
- Clauoué-Long, JC, Edgoose, C and Worden, K 2008b, A correlation of Aileron Province stratigraphy in central Australia: *Precambrian Research*, v. 166, no. 1–4, p. 230–245.
- Clauoué-Long, JC and Hoatson, D 2005, Proterozoic mafic–ultramafic intrusions in the Arunta Region, central Australia. Part 2: Event chronology and regional correlations: *Precambrian Research*, v. 142, no. 3–4, p. 134–158, doi:10.1016/j.precamres.2005.08.006.
- Collins, WJ 2002, Nature of extensional accretionary orogens: *Tectonics*, v. 21, no. 4, p. 6–1–6–12, doi:10.1029/2000TC001272.
- Compston, DM 1995, Time constraints on the evolution of the Tennant Creek Block, northern Australia: *Precambrian Research*, v. 71, p. 107–129.
- Compston, W, Williams, IS and Meyer, C 1984, U–Pb geochronology of zircons from lunar breccia 73217 using a sensitive high mass-resolution ion microprobe: *Journal of Geophysical Research*, v. 89, no. S02, p. B525–B534.
- Cooper, JA and Ding, PQ 1997, Zircon ages constrain the timing of deformation events in the The Granites–Tanami region, northwest Australia: *Australian Journal of Earth Sciences*, v. 44, p. 777–787.
- Crispe, AJ, Vandenberg, LC and Scrimgeour, IR 2007, Geological framework of the Archean and Paleoproterozoic Tanami Region, Northern Territory: *Mineralium Deposita*, v. 42, p. 3–26.
- Cross, A, Clauoué-Long, J, Scrimgeour, IR, Crispe, A and Donnellan, N 2005a, Summary of results. Joint NTGS–GA geochronology project: northern Arunta and Tanami regions, 2000–2003: Northern Territory Geological Survey, Record 2005-003, 69p.
- Cross, A, Clauoué-Long, JC, Scrimgeour, IR, Ahmad, M and Kruse, PD 2005b, Summary of results. Joint NTGS–GA geochronology project: Rum Jungle, basement to the southern Georgina Basin and eastern Arunta Region, 2001–2003: Northern Territory Geological Survey, Record 2005-006, 42p.

- Cross, A, Claoué-Long, JC, Scrimgeour, IR, Close, DF and Edgoose, CJ 2005c, Summary of results, Joint NTGS–GA geochronology project: southern Arunta Region: Northern Territory Geological Survey, Record 2004-003, 61p.
- Cross, AJ and Crispe, AJ 2007, SHRIMP U–Pb analyses of detrital zircon: a window to understanding the Paleoproterozoic development of the Tanami Region, northern Australia: *Mineralia Deposita*, v. 42, p. 27–50.
- Cross, AJ, Fletcher, IR, Crispe, AJ, Huston, DL and Williams, N 2005d, New constraints on the timing of deposition and mineralisation in the Tanami Group, in *Annual Geoscience Exploration Seminar (AGES) 2005*, Record of abstracts: Northern Territory Geological Survey, Record 2005-001, p. 44–45.
- Cutovinos, A, Beier, PR, Kruse, PD, Abbott, ST, Dunster, JN and Brescianini, RF 2002, Limbunya, Northern Territory (2nd edition): Northern Territory Geological Survey, 1:250 000 geological map series explanatory notes SE 52-15, 36p.
- Dean, AA 2001, Igneous rocks of the Tanami Region (electronic pre-release edition): Northern Territory Geological Survey, Record 2001-003, 78p.
- Donnellan, N 2013, Chapter 16: Tomkinson Province, in *Geology and mineral resources of the Northern Territory compiled by M Ahmad and TJ Munson*: Northern Territory Geological Survey, Special Publication 5, p. 16:1–16:27.
- Fanning, CM 1991, Ion microprobe U–Pb zircon dating of a tuffaceous horizon within the Kunja Siltstone, Victoria River Basin, Northern Territory: Australian National University, Research School of Earth Sciences, Report for Pacific Oil and Gas Pty Ltd (unpublished).
- Foden, JD, Buick, IS and Mortimer, GE 1988, The petrology and geochemistry of granitic gneisses from the east Arunta Inlier, central Australia — implications for Proterozoic crustal development: *Precambrian Research*, v. 40/41, p. 233–259.
- Fraser, G 2002, Timing of regional tectonism and Au-mineralisation in the Tanami Region: $^{40}\text{Ar}/^{39}\text{Ar}$ geochronological constraints, in *Annual Geoscience Exploration Seminar (AGES) 2002*, Record of abstracts: Northern Territory Geological Survey, Record 2002-0003.
- Fraser, GL, Bagas, L and Huston, DL 2012, $^{40}\text{Ar}/^{39}\text{Ar}$ evidence for the timing of Paleoproterozoic gold mineralisation at the Sandpiper deposit, Tanami Region, northern Australia: *Australian Journal of Earth Sciences*, no. 59, p. 399–409.
- Frogtech Geoscience 2018, SEEBASE study and GIS for greater McArthur Basin: Northern Territory Geological Survey, Digital Information Package DIP 017.
- Frost, BR, Barnes, CG, Collins, WJ, Arculus, RJ, Ellis, DJ and Frost, CD 2001, A geochemical classification for granitic rocks: *Journal of Petrology*, v. 42, no. 11, p. 2033–2048.
- Garzanti, E 2017, The maturity myth in sedimentology and provenance analysis: *Journal of Sedimentary Research*, v. 87, p. 353–365.
- Gehrels, GE 2009, Age pick program, University of Arizona Laserchron Center, US, <<https://sites.google.com/a/laserchron.org/laserchron/home>>.
- Geological Survey of Western Australia 2016a, 1:500 000 State interpreted bedrock geology of Western Australia, 2016, digital data layer: Geological Survey of Western Australia, viewed 2 December 2019, <www.dmp.wa.gov.au/geoview>.
- Geological Survey of Western Australia 2016b, Compilation of geochronology information, 2016, digital data layer: Geological Survey of Western Australia, viewed 2 December 2019, <www.dmp.wa.gov.au/geoview>.
- Glass, LM 2011, Palaeoproterozoic island-arc-related mafic rocks of the Litchfield Province, western Pine Creek Orogen, Northern Territory: Northern Territory Geological Survey, Record 2010-005, 39p.
- Glass, LM, Ahmad, M and Munson, TJ 2013, Chapter 30: Kalkarindji Province, in *Geology and mineral resources of the Northern Territory compiled by M Ahmad and TJ Munson*: Northern Territory Geological Survey, Special Publication 5, p. 30:1–30:17.
- Glass, LM and Phillips, D 2006, The Kalkarindji continental flood basalt province: a new Cambrian large igneous province in Australia with possible links to faunal extinctions: *Geology*, v. 34, no. 6, p. 461–464, doi:10.1130/G22122.1.
- Gole, M and Ashley, J 2003, Antrim project: combined annual report for ELs 22642–22644 and 22749–22751 for the period up to 31/12/2002: Northern Territory Geological Survey, Open File Company Report CR2003-0019, 305p. (unpublished).
- Gole, M and Lee, S 2005, Antrim Project, NT: third partial relinquishment report for exploration licences 22643 and 22644, period ending 17/10/2005: Northern Territory Geological Survey, Open File Company Report CR2005-0678, 73p. (unpublished).
- Gole, M and Lee, S 2006, Antrim Project, NT: third partial relinquishment report for exploration licences 22643 and 22644, period ending 17/10/2005: Northern Territory Geological Survey, Open File Company Report CR2005-0678 (AusQuest Ltd Report 2006/7), 73p. (unpublished).
- Goleby, BR, Huston, DL, Lyons, P, Vandenberg, L, Bagas, L, Davies, BM, Jones, LEA, Gebre-Mariam, M, Johnson, W, Smith, T and English, L 2009, The Tanami deep seismic reflection experiment: an insight into gold mineralization and Paleoproterozoic collision in the North Australian Craton: *Tectonophysics*, v. 472, no. 1–4, p. 169–182.
- Green, M 2002, Granite petrogenesis in the northern Arunta Province, in *Annual Geoscience Exploration Seminar (AGES) 2002*, Record of abstracts: Northern Territory Geological Survey, Record 2002-0003.
- Greenfield, JE, Clarke, GL, Bland, M and White, RW 1996, In-situ migmatite and hybrid diatexite at Mount Stafford, central Australia: *Journal of Metamorphic Geology*, v. 14, p. 413–426.
- Griffin, TJ, Page, RW, Sheppard, S and Tyler, IM 2000, Tectonic implications of Palaeoproterozoic post-collisional, high-K felsic igneous rocks from the Kimberley region of northwestern Australia: *Precambrian Research*, v. 101, p. 1–23.
- Haines, PW, Rawlings, DJ, Sweet, IP, Pietsch, BA, Plumb, KA, Madigan, TL and Krassay, AA 1999, Blue Mud Bay SD 53-7 (second edition): explanatory notes: Northern Territory Geological Survey and Australian Geological Survey Organisation, 1:250 000 Geological Map Series explanatory notes, 107p.
- Hancock, SL 1991, Tectonic development of the Lower Proterozoic basement in the Kimberley district of northwestern Western Australia: University of Adelaide, PhD thesis (unpublished).
- Hancock, SL and Rutland, RWR 1984, Tectonics of an early Proterozoic geosuture: the Halls Creek Orogenic Sub-province, northern Australia: *Journal of Geodynamics*, v. 1, p. 387–432.
- Hanley, LM 1996, Geochronology, mineral chemistry, geochemistry and petrography of diamond-associated rocks in the Coanjula Region, Northern Territory: The University of Western Australia, Perth, BSc (Hons) thesis (unpublished).
- Hanley, LM and Wingate, MTD 2000, SHRIMP zircon age for an Early Cambrian dolerite dyke: an intrusive phase of the Antrim Plateau Volcanics of northern Australia: *Australian Journal of Earth Sciences*, v. 47, p. 1029–1040.
- Hawkins, AJ 2011, The Tanami gold mine, Northern Territory: a critical evaluation of the remaining resource and exploration model: The University of Western Australia, MSc thesis, 240p. (unpublished).
- Haschke, M and Ben-Avraham, Z 2005, Adakites from collision-modified lithosphere: *Geophysical Research Letters*, v. 32, no. 15, doi:10.1029/2005GL023468.
- Hendrickx, MA, Slater, KR, Crispe, AJ, Dean, AA, Vandenberg, LC and Smith, JB 2000, Palaeoproterozoic stratigraphy of the Tanami Region: regional correlations and relation to mineralisation – preliminary results: Northern Territory Geological Survey, Record 2000-0013, 66p.
- Hoatson, DM, Sun, S-S and Claoué-Long, JC 2005, Proterozoic mafic–ultramafic intrusion in the Arunta Region, central Australia, Part 1: Geological setting and mineral potential: *Precambrian Research*, v. 142, no. 3–4, p. 93–133.

- Hollis, JA, Beyer, E, Whelan, JA, Kemp, AIS, Scherstén, A and Greig, A 2010, Summary of results, NTGS laser U–Pb and Hf geochronology project: Pine Creek Orogen, Murphy Inlier, McArthur Basin and Arunta Region, July 2007 – June 2008: Northern Territory Geological Survey, Record 2010-001.
- Hollis, JA, Carson, CJ and Glass, LM 2009a, SHRIMP U–Pb zircon geochronological evidence for Neoproterozoic basement in western Arnhem Land, northern Australia: *Precambrian Research*, v. 174, no. 3–4, p. 364–380.
- Hollis, JA, Carson, CJ, Glass, LM, Kositsin, N, Scherstén, A, Worden, KE, Armstrong, RA, Yaxley, GM, Kemp, AIS and EIMF 2014, Detrital zircon U–Pb–Hf and O isotope character of the Cahill Formation and Nourlangie Schist, Pine Creek Orogen: implications for the tectonic correlation and evolution of the North Australian Craton: *Precambrian Research*, v. 246, p. 35–53.
- Hollis, JA and Glass, LM 2012, Howship and Oenpelli, Northern Territory, 5572, 5573: Northern Territory Geological Survey, 1:100 000 Geological Map Series Explanatory Notes.
- Hollis, JA, Kirkland, CL, Spaggiari, CV, Tyler, IM, Haines, PW, Wingate, MTD, Belousova, EA and Murphy, RC 2013, Zircon U–Pb–Hf isotope evidence for links between the Warumpi and Aileron Provinces, west Arunta region: Geological Survey of Western Australia, Record 2013/9, 30p.
- Hollis, JA, Scherstén, A, Glass, LM and Carson, CJ 2009b, Stratigraphic and tectonic evolution of the Nimbawah Domain: a separate terrane to the rest of the Pine Creek Orogen?, *in* Annual Exploration Geoscience Seminar (AGES) 2009, Record of Abstracts: Northern Territory Geological Survey, Record 2009-002, p. 21–26.
- Howard, KE, Hand, M, Barovich, KM, Reid, A, Wade, BP and Belousova, EA 2009, Detrital zircon ages: Improving interpretation via Nd and Hf isotopic data: *Chemical Geology*, v. 262, p. 277–292.
- Howlett, D, Raimondo, T and Hand, M 2015, Evidence for 1808–1770 Ma bimodal magmatism, sedimentation, high-temperature deformation and metamorphism in the Aileron Province, central Australia: *Australian Journal of Earth Sciences*, v. 62, p. 831–852.
- Huston, DL, Blewett, RS and Champion, DC 2012, Australia through time: a summary of its tectonic and metallogenic evolution: *Episodes*, v. 35, no. 1, p. 23–43.
- Huston, DL, Vandenberg, L, Wygralak, AS, Memagh, TP, Bagas, L, Crispe, A, Lambeck, A, Cross, A, Fraser, G, Williams, N, Worden, K, Meixner, T, Goleby, B, Jones, L, Lyons, P and Maudment, D 2007, Lode-gold mineralization in the Tanami region, northern Australia: *Mineralium Deposita*, v. 42, p. 175–204.
- Iaccheri, LM 2019, Composite basement along the southern margin of the North Australian Craton: Evidence from in-situ zircon U–Pb–O–Hf and whole-rock Nd isotopic compositions: *Lithos*, v. 324–325, p. 733–746., doi:10.1016/j.lithos.2018.11.006
- Iaccheri, LM, Kemp, AIS and EIMF 2018, Detrital zircon age, oxygen and hafnium isotope systematics record rigid continents after 2.5 Ga: *Gondwana Research*, v. 57, p. 90–118.
- Ireland, TJ and Mayer, TE 1984, The geology and mineralization of The Granites gold deposits, Northern Territory, *in* Proceedings: The Australasian Institute of Mining and Metallurgy Annual Conference, Darwin, Northern Territory, 5–9 August 1984: Australian Institute of Mining and Metallurgy, p. 397–406.
- Joly, A, McCuaig, TC and Bagas, L 2010, The importance of early crustal architecture for subsequent basin-forming, magmatic and fluid flow events. The Granites–Tanami Orogen example: *Precambrian Research*, v. 182, no. 1–2, p. 15–29.
- Jourdan, F, Hodges, K, Sell, B, Schaltegger, U, Wingate, MTD, Evins, LZ, Söderlund, U, Haines, PW, Phillips, D and Blenkinsop, T 2014, High-precision dating of the Kalkarindji large igneous province, Australia, and synchrony with the Early–Middle Cambrian (Stage 4–5) extinction: *Geology*, v. 42, no. 6, p. 543–546, doi:10.1130/G35434.1.
- Kinny, PD 2002, SHRIMP U–Pb geochronology of Arunta Province samples from the Mount Liebig and Lake Mackay 1:250 000 mapsheets: Northern Territory Geological Survey, Technical Note 2002-015.
- Kirkland, CL and Wingate, MTD 2010, 177278: schistose metagreywacke, Bald Hill; Geochronology Record 922: Geological Survey of Western Australia, 4p.
- Kirkland, CL, Wingate, MTD, Hollis, J and Phillips, C 2014, 206154: pelitic migmatite, Paperbark Bore; Geochronology Record 1204: Geological Survey of Western Australia, 6p.
- Kohanpour, F, Gorczyk, W, Lindsay, MD and Occhipinti, S 2017, Examining tectonic scenarios using geodynamic numerical modelling: Halls Creek Orogen, Australia: *Gondwana Research*, v. 46, p. 95–113.
- Kositsin, N, Beyer, EE, Whelan, JA, Close, DF, Hallett, L and Dunkley, DJ 2013a, Summary of results, Joint NTGS–GA geochronology project: Arunta Region, Ngalia Basin, Tanami Region and Murphy Province, July 2011–June 2012: Northern Territory Geological Survey, Record 2013-004, 31p.
- Kositsin, N, Carson, CJ, Hollis, JA, Glass, LM, Close, DF, Whelan, JA, Webb, G and Donnellan, N 2013b, Summary of Results. Joint NTGS–GA geochronology project: Arunta region, Davenport Province and Pine Creek Orogen July 2009 – June 2011: Northern Territory Geological Survey, Record 2012-008, 49p.
- Kositsin, N, Kraus, S and Whelan, JA 2015a, Summary of results, Joint NTGS–GA SHRIMP geochronology project: Arnhem Province, July 2014 – June 2015: Northern Territory Geological Survey, Record 2015-010, 28p.
- Kositsin, N, Reno, BL and Whelan, JA 2015b, Summary of results, Joint NTGS–GA geochronology project: Arunta Region, July 2014–June 2015: Northern Territory Geological Survey, Record 2015-007, 18p.
- Kositsin, N, Whelan, JA, Hallett, L and Beyer, EE 2014, Summary of results, Joint NTGS–GA geochronology project: Amadeus Basin, Arunta Region and Murphy Province, July 2012 – June 2013: Northern Territory Geological Survey, Record 2014-005, 24p.
- Kositsin, N, Whelan, JA, Reno, BL, Kraus, S and Beyer, EE 2018, Summary of results, Joint NTGS–GA geochronology project: Arnhem Province, July 2014 – June 2016: Northern Territory Geological Survey, Record 2018-008, 37p.
- Lambeck, A, Barovich, K, George, AD, Cross, A, Huston, D and Meixner, T 2012, Proterozoic turbiditic depositional system (Tanami Group) in the Tanami region, northern Australia, and implications for gold mineralization: *Australian Journal of Earth Sciences*, v. 59, p. 383–397.
- Lambeck, A, Huston, D and Barovich, K 2010, Typecasting prospective Au-bearing sedimentary lithologies using sedimentary geochemistry and Nd isotopes in poorly exposed Proterozoic basins of the Tanami region, Northern Australia: *Mineralium Deposita*, v. 45, p. 497–515, doi:10.1007/s00126-010-0281-z.
- Lambeck, A, Huston, D, Maudment, D and Southgate, PN 2008, Sedimentary geochemistry, geochronology and sequence stratigraphy as tools to typecast stratigraphic units and constrain basin evolution in the gold mineralised Palaeoproterozoic Tanami Region, Northern Australia: *Precambrian Research*, v. 166, p. 185–203.
- Li, B, Bagas, L, Gallardo LA, Said, N, Diwu, C and McCuaig, TC 2013, Back-arc and post-collisional volcanism in the Palaeoproterozoic Granites–Tanami Orogen, Australia: *Precambrian Research*, v. 224, p. 570–587.
- Li, B, Bagas, L and Jourdan, F 2014, Tectono-thermal evolution of the Palaeoproterozoic Granites–Tanami Orogen, North Australian Craton: Implications from hornblende and biotite $^{40}\text{Ar}/^{39}\text{Ar}$ geochronology: *Lithos*, v. 206–207, p. 262–276.
- Lindsay, MD, Occhipinti, S, Aitken, ARA, Metelka, V, Hollis, J and Tyler, I 2016, Proterozoic accretionary tectonics in the east Kimberley region, Australia: *Precambrian Research*, v. 278, p. 265–282.
- Lovett, DR, Giles, CW, Edmonds, W, Gum, JC and Webb, RJ 1993, The geology and exploration of the Dead Bullock Soak gold deposits, The Granites–Tanami Goldfield, NT, *in* Proceedings of AusIMM centenary conference, Adelaide, South Australia, 30 March – 4 April 1993: Australasian Institute of Mining and Metallurgy, p. 73–80.
- Lu, Y, Wingate, MTD and Hollis, JA 2017a, 212317: pelitic migmatite, Mount Joseph; Geochronology Record 1389: Geological Survey of Western Australia, 4p.

- Lu, Y, Wingate, MTD, Hollis, JA, Maidment, DW and Phillips, C 2017b, 215562: metasandstone, Neville Gorge; Geochronology Record 1467: Geological Survey of Western Australia, 7p.
- Lu, Y, Wingate, MTD, Kirkland, CL, Maidment, DW, Phillips, C and Hollis, JA 2016a, 206106: pelitic migmatite, Sydney Harbour Yard; Geochronology Record 1340: Geological Survey of Western Australia, 6p.
- Lu, Y, Wingate, MTD, Kirkland, CL, Maidment, DW, Phillips, C and Hollis, JA 2016b, 206128: pelitic schist, Panton mine; Geochronology Record 1341: Geological Survey of Western Australia, 6p.
- Lu, Y, Wingate, MTD, Kirkland, CL, Maidment, DW, Phillips, C and Hollis, JA 2016c, 212344: pelitic schist, Napier Creek; Geochronology Record 1348: Geological Survey of Western Australia, 6p.
- Lu, Y, Wingate, MTD, Kirkland, CL, Maidment, DW, Phillips, C and Hollis, JA 2016d, 206131: migmatitic pelitic gneiss, Six Mile Bore; Geochronology Record 1342: Geological Survey of Western Australia, 5p.
- Lu, Y, Wingate, MTD, Kirkland, CL, Maidment, DW, Phillips, C and Hollis, JA 2016e, 206173: psammitic schist, Lissadell Road; Geochronology Record 1346: Geological Survey of Western Australia, 5p.
- Lu, Y, Wingate, MTD, Maidment, DW and Phillips, C 2017c, 218305: metasilstone, O'Donnell Brook; Geochronology Record 1468: Geological Survey of Western Australia, 7p.
- Lu, Y, Wingate, MTD, Maidment, DW and Phillips, C 2017d, 218315: psammitic gneiss, Stock Route Bore; Geochronology Record 1469: Geological Survey of Western Australia, 7p.
- Lu, Y, Wingate, MTD, Maidment, DW and Phillips, C 2018a, 218310: metasandstone, Bow River; Geochronology Record 1543: Geological Survey of Western Australia, 6p.
- Lu, Y, Wingate, MTD, Maidment, DW and Phillips, C 2018b, 218318: muscovite–chlorite schist, Palms Yard; Geochronology Record 1544: Geological Survey of Western Australia, 7p.
- Lu, Y, Wingate, MTD, Maidment, DW and Phillips, C 2018c, 218330: lithic metasandstone, Ragged Range; Geochronology Record 1545: Geological Survey of Western Australia, 6p.
- Lu, Y, Wingate, MTD, Maidment, DW and Phillips, C 2018d, 218333: psammitic gneiss, Two Mile Yard; Geochronology Record 1546: Geological Survey of Western Australia, 6p.
- Lu, Y, Wingate, MTD, Morin-Ka, S and Beardsmore, TJ 2017e, 213028: quartz–muscovite schist, GD5 Bore; Geochronology Record 1399: Geological Survey of Western Australia, 5p.
- Lu, Y, Wingate, MTD, Morin-Ka, S and Beardsmore, TJ 2017f, 213029: muscovite schist, GD5 Bore; Geochronology Record 1400: Geological Survey of Western Australia, 4p.
- Lu, Y, Wingate, MTD, Phillips, C and Maidment, DW 2018e, 216661: lithic sandstone, Sophie Downs homestead; Geochronology Record 1510: Geological Survey of Western Australia, 7p.
- Ludwig, KR 1998, On the treatment of concordant uranium–lead ages: *Geochimica et Cosmochimica Acta*, v. 62, p. 665–676.
- Ludwig, KR 2003, User's Manual for Isoplot 3.00: a geochronological toolkit for Microsoft Excel: Berkeley Geochronology Center, Special Publication 4, 70p.
- Ludwig, KR 2009, Squid 2.50, a user's manual: Berkeley Geochronology Centre, Berkeley, California, USA, 95p. (unpublished).
- Maidment, DW 2017, Geochronology from the Rudall Province, Western Australia: implications for the amalgamation of the West and North Australian Cratons: Geological Survey of Western Australia, Report 161, 95p.
- Maidment, DW, Huston, DL, Donnellan, N and Lambeck, A 2013, Constraints on the timing of the Tennant Event and associated Au–Cu–Bi mineralization in the Tennant Region, Northern Territory: *Precambrian Research*, v. 237, p. 51–63.
- Marshall, PE, Halton, AM, Kelley, SP, Widdowson, M and Sherlock, SC, 2018, New $^{40}\text{Ar}/^{39}\text{Ar}$ dating of the Antrim Plateau Volcanics, Australia: clarifying an age for the eruptive phase of the Kalkarindji continental flood basalt province: *Journal of the Geological Society*, v. 175, p. 974–985.
- Martin, H, Smithies, RH, Rapp, R, Moyen, J-F and Champion, DC 2005, An overview of adakite, tonalite–ironhjemetite–granodiorite (TTG), and sanukitoid: relationships and some implications for crustal evolution: *Lithos*, v. 79, p. 1–24.
- Mayer, TE 1990, The Granites gold field, in *Geology of the mineral deposits of Australia and Papua New Guinea edited by FE Hughes*: The Australasian Institute of Mining and Metallurgy, Monograph 14, p. 719–724.
- McGloin, MV, Maas, R, Weisheit, A, Meffre, S, Thompson, J, Zhukova, I, Stewart, J, Hutchinson, G, Trumbull, R and Creaser, R 2016, Palaeoproterozoic copper mineralisation in the Aileron Province: new findings on temporal, spatial and genetic features, in *Annual Geoscience Exploration Seminar (AGES) Proceedings*, Alice Springs, Northern Territory, 28–29 March 2017: Northern Territory Geological Survey, Darwin, Northern Territory, p. 63–74.
- McPhie, J 1993, The Tennant Creek porphyry revisited: A synsedimentary rhyolitic sill with peperite margins, Early Proterozoic, Northern Territory: *Australian Journal of Earth Sciences*, v. 40, p. 545–558.
- Mercadier, J, Skirrow, RG and Cross, AJ 2013, Uranium and gold deposits in the Pine Creek Orogen (North Australian Craton): a link at 1.8 Ga?: *Precambrian Research*, v. 238, p. 111–119.
- Mole, DR, Barnes, SJ, Le Vaillant, M, Martin, LAJ and Hicks, J 2018, Timing, geochemistry and tectonic setting of Ni–Cu sulfide-associated intrusions of the Halls Creek Orogen, Western Australia: *Lithos*, v. 314–315, p. 425–446.
- Myers, JS, Shaw, RD and Tyler, IM 1996, Tectonic evolution of Proterozoic Australia: *Tectonics*, v. 15, p. 1431–1446.
- Nakamura, A and Milligan, PR 2015, Total Magnetic Intensity (TMI) Grid of Australia 2015 — sixth edition: Geoscience Australia, dataset, <<http://researchdata.ands.org.au/total-magnetic-intensity-sixth-edition>>.
- Nazari-Dehkordi, T, Spandler, C, Oliver, NHS, Chapman, J and Wilson, R 2017, Provenance, tectonic setting and source of Archean metasedimentary rocks of the Browns Range Metamorphics, Tanami Region, Western Australia: *Australian Journal of Earth Sciences*, v. 64, no. 6, p. 723–741.
- Needham, RS and Stuart-Smith, PG 1984, The relationship between mineralisation and depositional environment in the Early Proterozoic metasediments of the Pine Creek Geosyncline, in *Proceedings: The Australasian Institute of Mining and Metallurgy Annual Conference*, Darwin, Northern Territory, 5–9 August 1984, p. 201–213.
- Neumann, NL, Gibson, GM and Southgate, PN 2009, New SHRIMP age constraints on the timing and duration of magmatism and sedimentation in the Mary Kathleen Fold Belt, Mt Isa Inlier, Australia: *Australian Journal of Earth Sciences*, v. 56, p. 965–983.
- Neumann, NL, Southgate, PN, Gibson, GM and McIntyre, A 2006, New SHRIMP geochronology for the Western Fold Belt of the Mount Isa Inlier: developing a 1800–1650 Ma event framework: *Australian Journal of Earth Sciences*, v. 53, p. 1023–1039.
- Nicholson, PM 1990, Tanami gold deposit, in *Geology of the mineral deposits of Australia and Papua New Guinea edited by FE Hughes*: The Australasian Institute of Mining and Metallurgy, Monograph 14, p. 715–718.
- Orth, K 2007, Geology and volcanology of the Ware Group and Winnecke Granophyre, northern Tanami Region, Northern Territory: Northern Territory Geological Survey, Record 2007/002, 38p.
- Orth, K 2015, The Carson–Hart Large Igneous Province intrusive complex: implications for Speewah-style vanadium–titanium–iron mineralization in the Kimberley region, in *GSWA 2015 extended abstracts: promoting the prospectivity of Western Australia*: Record 2015/2, p. 19–22.
- Page, R 1996a, Sample ID 87495026, Winnecke Granophyre: Geoscience Australia, Geochron Delivery database, viewed 7 September 2017, <www.ga.gov.au/geochron-sapub-web/geochronology/shrimp/search.htm>.
- Page, R 1996b, Sample ID 87495029, Mount Winnecke Formation: Geoscience Australia, Geochron Delivery database, viewed 7 September 2017, <www.ga.gov.au/geochron-sapub-web/geochronology/shrimp/search.htm>.

- Page, R 1996c, Sample ID 87495026, Winnecke Granophyre: Geoscience Australia, Geochron Delivery database, viewed 7 September 2017, <www.ga.gov.au/geochron-sapub-web/geochronology/shrimp/search.htm>.
- Page, R 1996d, Sample ID 87495029, Mount Winnecke Formation: Geoscience Australia, Geochron Delivery database, viewed 7 September 2017, <www.ga.gov.au/geochron-sapub-web/geochronology/shrimp/search.htm>.
- Page, RW, Griffin, TJ, Tyler, IM and Sheppard, S 2001, Geochronological constraints on tectonic models for Australian Palaeoproterozoic high-K granites: *Journal of the Geological Society*, v. 158, p. 535–545.
- Page, RW and Hoatson, DM 2000, Geochronology of the mafic–ultramafic intrusions, in *Geology and economic potential of the Palaeoproterozoic layered mafic–ultramafic intrusions in the East Kimberley, Western Australia* edited by DM Hoatson and DH Blake: Australian Geological Survey Organisation, Bulletin 246, p. 163–172.
- Page, RW, Hoatson, DM, Sun, S and Foudoulis, C 1995a, High-precision geochronology of Palaeoproterozoic layered mafic–ultramafic intrusions in the East Kimberley: Australian Geological Survey Organisation Research Newsletter, v. 22, p. 7–8.
- Page, RW, Jackson, MJ and Krassay, AA 2000, Constraining sequence stratigraphy in north Australian basins: SHRIMP U–Pb zircon geochronology between Mt Isa and McArthur River: *Australian Journal of Earth Sciences*, v. 47, p. 431–459.
- Page, RW, Sun, S-S and Blake, DH 1995b, Geochronology of an exposed late Archean basement terrane in The Granites–Tanami Region: Australian Geological Survey Organisation (AGSO) Research Newsletter 22, p. 19–20.
- Pendergast, WJ, Baggott, MS and Schmeider, S 2017, Dead Bullock Soak including Callie, in *Australian ore deposits* edited by GN Phillips: The Australasian Institute of Mining and Metallurgy: Monograph 32, p. 551–556.
- Petrella, L, Thébaud, N, LaFlamme, C, Miller, J, McFarlane, C, Occhipinti, S, Turner, S and Perazzo, S 2019, Contemporaneous formation of vein-hosted and stratabound gold mineralization at the world-class Dead Bullock Soak mining camp, Australia: *Mineralium Deposita*, doi:10.1007/s00126-019-00902-7.
- Phillips, C, Maidment, DW and Lu, Y 2017, Revised tectono-stratigraphy of the Kimberley Basin, northern Western Australia, in *GSWA 2017 extended abstracts: promoting the prospectivity of Western Australia*: Geological Survey of Western Australia, Record 2017/2, p. 33–37.
- Phillips, C, Orth, K, Hollis, JA, Kirkland, CL, Bodorkos, S, Kemp, AIS, Wingate, MTD, Lu, Y, Iaccheri, L and Page, RW 2016, Geology of the Eastern Zone of the Lamboo Province, Halls Creek Orogen, Western Australia: Geological Survey of Western Australia, Report 164, 57p.
- Ramsay, RR, Eves AE, Denyszyn, SW, Wingate, MTD, Fiorentini, M, Gwalani, LG and Rogers KA 2019, Geology and geochronology of the Palaeoproterozoic Hart Dolerite, Western Australia: *Precambrian Research*, v. 335, 105482, doi.org/10.1016/j.precamres.2019.105482.
- Ramsay, RR, Eves, AE, Wingate, MTD, Fiorentini, ML, Batt, G, Rogers, K, Gwalani, LG and Martin, S 2017, Detrital zircon geochronology of the Speewah G1 of Earth Sciences, v. 64, p. 419–434.
- Reno, BL, Whelan, JA, Kraus, S, Thompson, JM and Meffre, S 2017, Summary of results, NTGS laser ablation ICP-MS in situ monazite geochronology project: Arnhem Province, Gove and Blue Mud Bay 1:250 000 map sheets: Northern Territory Geological Survey, Record 2017-007, 35p.
- Reno, BL, Whelan, JA, Kraus, S, Thompson, JM and Meffre, S 2018, NTGS laser ablation ICP-MS in situ zircon petrochronology project: Arnhem Province, Gove 1:250 000 mapsheet, July 2014 – June 2016: Northern Territory Geological Survey, Record 2017-009, 38p.
- Reno, BL, Weisheit, A, Beyer, EE, McGloin, MV and Kositsin, N 2017, Proterozoic tectonothermal evolution of the northeastern sector of the Aileron Province, in *Annual Geoscience Exploration Seminar (AGES) Proceedings*, Alice Springs, Northern Territory, 28–29 March 2017: Northern Territory Geological Survey, Darwin, Northern Territory, p. 56–62.
- Rohde, C and English, L 2006, Combined annual report E80/1526, 1735, 1905, 1976, 1986, 2036, 2091, 2452, 2453, 3275 and M80/562-564 Gardner project C97/2004 from 1 January 2005 to 31 December 2005; Tanami Exploration NL: Geological Survey of Western Australia, Statutory mineral exploration report, A72058 (unpublished).
- Scott, J 1993, The structural setting of the Proterozoic gold mineralization at Bunkers Hill open cut mine, The Granites, Northern Territory: The University of Adelaide, BSc (Hons) thesis (unpublished).
- Scrimgeour, I and Sandiford, M 1993, Early Proterozoic metamorphism at The Granites gold mine, Northern Territory: implications for the timing of fluid production in high-temperature, low-pressure terranes: *Economic Geology*, v. 88, p. 1099–1113.
- Scrimgeour, IR 2003, Developing a revised framework for the Arunta region, in *Annual Geoscience Exploration Seminar (AGES) 2003*, Record of abstracts: Northern Territory Geological Survey, Record 2003–001, p. 1–3.
- Scrimgeour, IR 2006, The Arunta Region: links between tectonics and mineralisation, in *Annual Geoscience Exploration Seminar (AGES) 2006*, Record of abstracts: Northern Territory Geological Survey, Record 2006-002, p. 7–10.
- Scrimgeour, IR 2013, Chapter 12: Aileron Province, in *Geology and mineral resources of the Northern Territory compiled by M Ahmad and TJ Munson*: Northern Territory Geological Survey, Special Publication 5, p. 12:1–12:74.
- Sheppard, S, Griffin, TJ, Tyler, IM and Page, RW 2001, High- and low-K granites and adakites at a Palaeoproterozoic plate boundary in northwestern Australia: *Journal of the Geological Society*, v. 158, p. 547–560.
- Sheppard, S, Page, RW, Griffin, TJ, Rasmussen, B, Fletcher, IR, Tyler, IM, Kirkland, CL, Wingate, MTD, Hollis, J and Thorne, AM 2012, Geochronological and isotopic constraints on the tectonic setting of the c. 1800 Ma Hart Dolerite and the Kimberley and Speewah Basins, northern Western Australia: Geological Survey of Western Australia, Record 2012/7, 28p.
- Sheppard, S, Tyler, IM, Griffin, TJ and Taylor, RW 1999, Palaeoproterozoic subduction-related and passive margin basalts in the Halls Creek Orogen, northwest Australia: *Australian Journal of Earth Sciences*, v. 46, p. 679–690.
- Smith, JB 2001, Summary of results, Joint NTGS–AGSO age determination program 1999–2001: Northern Territory Geological Survey, Record 2001–007, 53p.
- Smith, MEH, Lovett, DR, Pring, PI and Sando, BG 1998, Dead Bullock Soak gold deposits, in *Geology of Australian and Papua New Guinean Mineral Deposits* edited by DA Berkman and DH Mackenzie: The Australasian Institute of Mining and Metallurgy, Monograph 22, p. 449–460.
- Stacey, JS and Kramers, JD 1975, Approximation of terrestrial lead isotope evolution by a two-stage model: *Earth and Planetary Science Letters*, v. 26, p. 207–221.
- Steiger, RH and Jäger, E 1977, Subcommittee on geochronology: convention on the use of decay constants in geo- and cosmochronology: *Earth and Planetary Science Letters*, v. 36, p. 359–362.
- Stevenson, DB, Bagas, L, Aitken, ARA and McCuaig, TC 2013, A geophysically constrained multi-scale litho-structural analysis of the Trans-Tanami Fault, Granites–Tanami Orogen, Western Australia: *Australian Journal of Earth Sciences*, v. 60, p. 745–768.
- Stuart-Smith, PG, Needham, RS, Page, RW and Wyborn, LAI 1993, *Geology and Mineral Deposits of the Cullen Mineral Field, Northern Territory*: Australian Geological Survey Organisation, Bulletin 229, 145p.
- Taylor, SR and McLennan, SM 1985, *The continental crust: its composition and evolution*: Blackwell Scientific Publications, Oxford, UK, 312p.
- Tunks, AJ 1996, *Structure and origin of gold mineralization, Tanami Mine, Northern Territory*: University of Tasmania, PhD thesis (unpublished).

- Tunks, AJ and Cooke, DR 2007, Geological and structural controls on gold mineralization in the Tanami District, Northern Territory: *Mineralium Deposita*, v. 42, no. 1, p. 107–126, doi:10.1007/s00126-006-0097-z.
- Tyler, IM and Griffin, TJ 1990, Structural development of the King Leopold Orogen, Kimberley region, Western Australia: *Journal of Structural Geology*, v. 12, p. 703–714.
- Tyler, IM, Griffin, TJ, Page, RW and Shaw, RD 1995, Are there terranes within the Lamboo Complex of the Halls Creek Orogen?, *in* Geological Survey of Western Australia Annual Review 1993–94: Geological Survey of Western Australia, p. 37–46.
- Tyler, IM, Griffin, TJ and Sheppard, S 1998, Geology of the Dockrell 1:100 000 sheet: Geological Survey of Western Australia 1:100 000 Geological Series Explanatory Notes, 24p.
- Tyler, IM, Hocking, RM and Haines, PW 2012, Geological evolution of the Kimberley region of Western Australia: *Episodes*, v. 35, p. 298–306.
- Tyler, IM, Page, RW and Griffin, TJ 1999, Depositional age and provenance of the Marboo Formation from SHRIMP U–Pb zircon geochronology: Implications for the early Palaeoproterozoic tectonic evolution of the Kimberley region, Western Australia: *Precambrian Research*, v. 95, no. 3, p. 225–243.
- Tyler, IM, Sheppard, S, Pirajno, F and Griffin, TJ 2006, Hart–Carson LIP, Kimberley region, northern Western Australia: Large Igneous Provinces Commission, viewed 10 February 2014, <www.largeigneousprovinces.org/06aug>.
- Vallini, AA, Groves, DI, McNaughton, NJ and Fletcher, IR 2007, Uraniferous diagenetic xenotime in northern Australia and its relationship to unconformity-associated uranium mineralisation: *Mineralium Deposita*, v. 42, p. 51–64.
- Vandenberg, LC, Hendrickx, MA and Crispe, AJ 2001, Structural geology of the Tanami Region: Northern Territory Geological Survey, Record 2001-004, 28p.
- Vandenberg, LC, Hendrickx, MA, Crispe, AJ, Dean, AA, Khan, M and Slater, KR 2014, Stratigraphic drilling report for the Tanami and The Granites 1:250 000 map areas, Northern Territory: Northern Territory Geological Survey, Record 2014-006, 39p.
- Wade, BP, Hand, M, Maidment, DW, Close, DF and Scrimgeour, IR 2008, Origin of metasedimentary and igneous rocks from the Entia Dome, eastern Arunta region, central Australia: a U–Pb LA-ICPMS, SHRIMP and Sm–Nd isotope study: *Australian Journal of Earth Sciences*, v. 55, p. 703–719.
- Weisheit, A, Reno, BL, Beyer, EE, Whelan, JA and McGloin, MV 2016, Multiply reactivated crustal-scale structures and a long-lived counter-clockwise P–T path: New insights into the 1.5 billion year tectonothermal evolution of the eastern Arunta Region, central Australia, *in* Annual Geoscience Exploration Seminar (AGES) Proceedings, Alice Springs, Northern Territory, 15–16 March 2016: Northern Territory Geological Survey, Darwin, Northern Territory, p. 56–82.
- Whelan, JA, Reno, BL, Weisheit, A, Kraus, S, Kositsin, N, Woodhead, JD, Maas, R and Armstrong, RA 2017, The geological evolution of the Arnhem Province: implications for craton-scale correlations, *in* Annual Geoscience Exploration Seminar (AGES) Proceedings, Alice Springs, Northern Territory, 28–29 March 2017: Northern Territory Geological Survey, Darwin, Northern Territory, p. 68–73.
- Whelan, JA, Woodhead, JD and Cliff, J 2014, Zircon LA-ICPMS Hf and SIMS O isotopic data for granitic gneiss of the Billabong Complex, Tanami Region: Northern Territory Geological Survey, Record 2014-002, 8p.
- Wingate, MTD, Bodorkos, S and Bagas, L 2009, 178803: sandstone, drillhole CYDD87, Coyote Mine; Geochronology Record 827: Geological Survey of Western Australia, 5p.
- Wingate, MTD and Lu, Y 2017, Introduction to geochronology information released in 2017: Geological Survey of Western Australia, 5p.
- Worden, K, Carson, C, Scrimgeour, I, Lally, JH and Doyle, N 2008a, A revised Palaeoproterozoic chronostratigraphy for the Pine Creek Orogen, northern Australia: Evidence from SHRIMP U–Pb zircon geochronology: *Precambrian Research*, v. 166, p. 122–144.
- Worden, KE, Carson, CJ, Close, DF, Donnellan, N and Scrimgeour, IR 2008b, Summary of results. Joint NTGS–GA geochronology project: Tanami Region, Arunta Region, Pine Creek Orogen, and Halls Creek Orogen correlatives, January 2005 – March 2007: Northern Territory Geological Survey, Record 2008-003, 180p.
- Worden, KE, Claoué-Long, JC and Scrimgeour, IR 2006a, Summary of results, Joint NTGS–GA geochronology project: Pine Creek Orogen, Tanami Region, Arunta Region and Amadeus Basin, July–December 2004: Northern Territory Geological Survey, Record 2006-006, 63p.
- Worden, KE, Claoué-Long, JC, Scrimgeour, IR and Doyle, N 2006b, Summary of results, Joint NTGS–GA geochronology project: Pine Creek Orogen and Arunta Region, January–June 2004: Northern Territory Geological Survey, Record 2006-005, 39p.
- Worden, KE, Claoué-Long, JC, Scrimgeour, IR and Lally, JH 2004, Summary of results, Joint NTGS–GA geochronology project: August 2003 – December 2003: Northern Territory Geological Survey, Record 2004-004 (digital publication on CD).
- Wygralak, AS, Huston, DL and Mernagh, TP 2017, Gold deposits of the Tanami gold province, *in* Australian ore deposits *edited by* GN Phillips: The Australasian Institute of Mining and Metallurgy, Monograph 32, p. 547–550.
- Zhao, JX and McCulloch, MT 1995, Geochemical and Nd isotopic systematics of granites from the Arunta Inlier, central Australia: implications for Proterozoic crustal evolution: *Precambrian Research*, v. 71, p. 265–299.

Appendices

Appendices 1 and 2 are available with the PDF online as an accompanying digital resource.

The Granites–Tanami Orogen in Western Australia and the Northern Territory preserves a complex record of Paleoproterozoic basin development, deformation and magmatism in the west–central North Australian Craton. The orogen provides an important source of information about the assembly and development of the North Australian Craton, and hosts numerous orogenic gold deposits. This Report provides a compilation of SHRIMP U–Pb zircon geochronology of metasedimentary and granitic rocks in the Granites–Tanami Orogen, carried out as part of collaborative research between the Geological Survey of Western Australia (GSWA), Geoscience Australia (GA) and the Northern Territory Geological Survey (NTGS) in the middle to late 2000s. The geochronological framework for the orogen is assessed within the broader context of the North Australian Craton to evaluate potential geodynamic settings of basin formation, magmatism and deformation.



Further details of geoscience products are available from:

Information Centre
Department of Mines, Industry Regulation and Safety
100 Plain Street
EAST PERTH WA 6004
Phone: (08) 9222 3459

www.dmirs.wa.gov.au/GSWApublications